

---

# **Probing cholesterol homeostasis in models of neurodevelopmental disorders**

---

**Inauguraldissertation**

zur

Erlangung der Würde eines Doktors der Philosophie

vorgelegt der

Philosophisch-Naturwissenschaftlichen Fakultät

der Universität Basel

von

**Charlotte Czernecki**

2023

Originaldokument gespeichert auf dem Dokumentenserver der Universität Basel

<https://edoc.unibas.ch>

Genehmigt von der Philosophisch-Naturwissenschaftlichen Fakultät

auf Auftrag von:

Prof. Dr. Peter Scheiffele

Prof. Dr. Markus Rüegg

Prof. Dr. Frank Pfrieder

Basel, 18. Oktober 2022

---

The Dean of Faculty

Prof. Dr. Marcel Mayor

# Table of Contents

Project Summary .....	6
1. Introduction .....	8
1.1 General Introduction .....	9
1.2 Dissecting neurodevelopmental disorders.....	10
1.2.1 Autism-spectrum disorders .....	11
1.2.2 Overlap between NDD forms .....	16
1.3 Ptchd1, NPC1 and sterol-sensing domain proteins .....	18
1.3.1 Ptchd1 – a neurodevelopmental risk gene .....	18
1.3.2 NPC1 – a cholesterol-related disease gene .....	26
1.3.3 Sterol sensing domain proteins.....	28
1.4 Cholesterol metabolism in neurological disorders .....	31
1.4.1 Cholesterol metabolism in the brain .....	32
1.4.2 Cholesterol implications in diseases .....	37
1.4.3 Tools for probing cellular distribution and dynamics of cholesterol .....	40
1.5 The dissertation project .....	45
2. Results .....	46
2.1 Preface .....	47
2.2 Cell-type specific assessment of cholesterol distribution in models of neurodevelopmental disorders .....	48
2.3 Exploring Ptchd1 localization and potential interactors .....	75
3. Discussion and future directions.....	81
3.1 Conclusions .....	82
3.2 Ptchd1 – cholesterol transporter or sensor?.....	84
3.3 Cell-type specific cholesterol differences .....	89
3.4 Cholesterol alterations in neurodevelopmental disorders.....	92
4. Materials and methods.....	94
4.1 Materials and methods from the manuscript .....	95
4.2 Additional materials and methods .....	99
5. Appendix.....	104
Index of figures.....	105
Index of abbreviations.....	107
6. References .....	111

Acknowledgements .....	132
Curriculum Vitae .....	133



## ***Summary***

## Project Summary

Neurodevelopmental disorders (NDDs) are complex heterogenous brain disorders caused by impaired development or maturation of the central nervous system. NDDs affect about 1% of the population and result from genetic and/or environmental factors. NDDs comprise intellectual disability (ID), autism spectrum disorder (ASD), attention-deficit/hyperactivity disorder (ADHD), amongst others (APA, 2013). ASD is the most studied neurodevelopmental disorder with hundreds of risk genes and several molecular pathways identified as involved in disease pathology. One relatively unexplored pathway which could be implicated in ASD and other NDDs is cholesterol metabolism. Indeed, alterations in cholesterol metabolism have been reported in Fragile X Syndrome (Berry-Kravis, 2015) and Rett's Syndrome (Buchovecky, 2013), two monogenic syndromes where a substantial fraction of individuals meets diagnostic criteria for ASD. Cholesterol is a major lipid in mammalian membranes and is particularly enriched in the brain, where it can affect synaptic activity and plasticity (Korinek et al., 2020, Djelti et al., 2015, Li et al., 2022). However, detecting cholesterol alterations in the brain is technically difficult and complicated by the localized synthesis and transport of cholesterol across cell types and sub-cellular compartments.

In this thesis, I report the development of a ratiometric, genetically-encoded probe that can be applied to monitor cholesterol distribution and levels in a cell-type-specific manner. I validated this probe for in vivo use by probing cholesterol distribution in *NPC1<sup>KO</sup>* mice, a genetic model for a lysosomal storage disorder with cholesterol transport deficits that is characterized by developmental delay and neurodegeneration. I further applied these probes to examining cholesterol distribution in *Ptchd1<sup>KO</sup>* mice. Patched-domain containing 1 (*Ptchd1*) is an X-chromosomal risk gene for both ASD and ID. Alterations in excitatory / inhibitory (E/I) balance and behavior have been reported in *Ptchd1<sup>KO</sup>* mouse models, but the function of Ptchd1 protein remains unknown. Due to the presence of a sterol-sensing domain (SSD), we hypothesized that Ptchd1 could be involved in cholesterol transport or homeostasis similarly to other SSD-containing proteins. We looked for cholesterol-related phenotypes in *Ptchd1*-expressing neuronal populations in a global *Ptchd1<sup>KO</sup>* mouse model, previously established and characterized by our lab (Tora et al., 2017). We did not observe any significant changes in cholesterol levels and distribution using the cholesterol D4H probe or lipidomic analysis. Furthermore, no changes were detected in the peripheral blood of the *Ptchd1<sup>KO</sup>* animals. The lack of cholesterol phenotype in this model seems to indicate that Ptchd1 is not essential for

maintenance of cholesterol homeostasis in mice. I further probed Ptchd1 sub-cellular localization and identified a novel interacting protein. My data suggests that Ptchd1 is localized to early endosomes, interacts with the retromer complex, as well as a the neddylation enzyme Uba3. In sum, this work deepens our understanding of the Ptchd1 protein and the pathophysiology associated with *Ptchd1* mutations, and provides a novel genetically-encoded probe for examining cholesterol homeostasis *in vivo*.

## ***1. Introduction***

## 1.1 General Introduction

The mammalian brain is a complex and multi-faceted organ whose development starts embryonically and expands for years after birth. Normal brain development relies on tightly regulated gene expression programs as well as environmental cues and experience inputs. As such, neurodevelopment can be described as the succession of complex, dynamic and adaptive processes culminating in the establishment of functional neural circuits (Stiles and Jernigan, 2010). A neuronal circuit can be a cluster of neurons involved in the same functional output or alternatively a set of inter-connected brain regions that process more complex and larger amount of information in order to execute higher cognitive functions (Tau and Peterson, 2010). Most neuronal cells are present at birth although maturation and circuit integration occur mostly during the first years of life (Jonhson, 2001) following genetically-defined molecular programs as well as external factors. Adaptation to external factors (environmental or systemic) through neuronal plasticity events is an essential step of circuit maturation which happens during a specific time-window of neurodevelopment and has therefore been termed “critical period” (Dehorter and Del Pino, 2020). While much attention has been devoted to the study of neurons, there is a more recent realization that non-neuronal cells have a major contribution to brain development. Thus, astrocyte-derived factors have emerged as key signals for neuronal synapse formation and microglia-mediated engulfment of neuronal structures has been implicated in synapse pruning (Li and Barres, 2018). Similarly, metabolic processes related to energy and lipid homeostasis have been implicated in brain cell differentiation and maintenance (Guttenplan et al., 2021, Knobloch et al., 2017). Due to the highly complex nature of neurodevelopment, any perturbation of normal developmental processes can induce strong and long-lasting pathogenic effects. The developmental time-window in which the perturbation occurs can greatly affect the pathological effects observed. Indeed, both embryonic and post-natal periods, including the “critical period”, are sensitive to a great number of perturbing factors: genetic mutations and chromosomal disorders, exposure to toxins, medication or pathogenic agents, trauma, and others, which can trigger sequences of molecular, biochemical and/or morphological alterations resulting in abnormal brain function (Suzuki, 2007).

In this thesis, I am focusing on a subset of developmental abnormalities referred to as neurodevelopmental disorders (NDDs). NDDs are defined as life-long, chronic and heterogeneous disorders where perturbations of neurodevelopment induce impairments in cognition, communication, behavior and/or motor skills. Currently, NDDs comprise intellectual disability (ID), communication disorders, autism spectrum disorder (ASD), attention deficit/hyperactivity disorder (ADHD), epilepsy amongst others (APA, 2013). Many NDDs are characterized by overlapping symptoms and genetic risk factors, which complicates diagnosis

– mainly based on clinical behavioral presentation – and treatment (Mullin et al., 2013). Therefore, it becomes essential to better define the cellular, molecular, and metabolic alterations observed in distinct NDDs in order to find effective individualized therapeutic avenues.

In the past decade, preclinical research has enabled linking gene mutations to specific molecular pathways and to unravel their effects on neuronal development and function (Delorme et al., 2013). From these studies, mechanism-based treatments have emerged. In animal models, such work has shown promise for alleviating symptoms in models of monogenic forms of ASD (Ebrahimi-Fakhari and Sahin, 2015). These findings highlight the importance of uncovering the underlying molecular pathways and cellular mechanisms involved NDDs pathology.

During my PhD, I investigated the relatively unstudied role for the cholesterol homeostasis pathway in two animal models of NDDs: *Ptchd1*<sup>KO</sup> and *NPC1*<sup>KO</sup> mice. In order to introduce the context of my dissertation project, I will first discuss NDDs and their pathology, focusing particularly on the most commonly diagnosed ASD. This will be followed by the introduction of the NDD risk genes of interest in this study: *Ptchd1* and *NPC1*. Lastly, I will describe the specific mechanisms of the cholesterol homeostasis pathway in the brain and its relation to neurodevelopmental disorders.

## **1.2 Dissecting neurodevelopmental disorders**

In this section, we will describe in details the most common forms of NDDs, as well as the biological pathways involved in disease pathology. Autism-spectrum disorders (ASD) is the most studied of NDDs and will provide the framework for comparison with other NDD forms such as intellectual disability (ID) and attention deficit/hyperactivity disorder (ADHD). We will discuss the overlapping genetic and biological evidence between these NDDs suggesting that the developmental abnormalities underlying NDD pathology happen along a neurodevelopmental continuum (Morris-Rosendahl and Crocq, 2020). In accordance with this hypothesis, the need for new methods of patient diagnosis and stratification will be discussed.

## 1.2.1 Autism-spectrum disorders

Autism Spectrum Disorder (ASD) are a group of heterogeneous neurodevelopmental disorders which currently included autism, pervasive developmental disorder-not otherwise specified (PDD-NOS) and Asperger's syndrome (AS). The core symptoms of ASD affect two core domains: social communication and interaction and repetitive behaviors/restricted interests (APA, 2013). ASD represents a life-long chronic condition with a high societal burden and costs with few therapeutic options. The estimated prevalence of ASD has steadily increased over the last decades reaching approximately 1.5% in developed countries (Baxter et al., 2015) with 4:1 male to female ratio. The increase of reported ASD cases may be due to improved screening, clinical recognition and diagnosis while the sex ratio may be impacted by alternative symptom presentation and diagnosis bias in females (Beggiato et al., 2017, Dworzynski et al., 2012). The complex etiology and clinical presentation of ASD is highlighted by the identification of many risk factors underlying disease pathology. Mainly, a strong genetic component was found with high disease heritability and hundreds of risk genes identified (Waye and Cheng, 2018). In addition to genetic factors, environmental and systemic factors are known to contribute to ASD pathology (Cheroni et al., 2020). At the biological level, ASD pathology impacts several cellular pathways including chromatin remodeling, transcription regulation and synaptic function (Sestan and Slate, 2018). Deepening the understanding of ASD pathology at the cellular and molecular levels remains essential for the development of effective therapies.

### ***Core and associated symptoms***

Diagnosis of ASD is based on the clinical assessment of ASD core behavioral domains according to the DSM-5 (Diagnostic and Statistical Manual of Mental Disorders) and occurs on average at 4.5 years of age (Lord and Bishop, 2015). However, onset of ASD symptoms can be detected within the first 3 years of life. The core symptoms of ASD are impaired social interactions and communication coupled with restricted interests and/or stereotyped repetitive behaviors. To meet the diagnosis criteria of ASD, a person must exhibit deficits in all social domains (social reciprocity, non-verbal communication, interpersonal relationships) as well as two out of four restricted/repetitive domain impairments (repetitive speech/behavior, insistence on sameness/routine, restricted interests, sensory abnormalities) (**Fig. 1**). Patients with only social interaction/communication deficits are now considered under the social communication disorder (SCD) outside of ASD spectrum. The core ASD symptoms are usually accompanied by several neurological and systemic co-morbidities, which can be more disabling on a daily basis than the core symptoms.

The most common ASD co-morbidities include intellectual disability - ~40% of cases (Christensen et al., 2016) - and attention deficit/hyperactivity - ~30–60% of cases - as well as self-harm/aggression, gastrointestinal problems, immune deficits, anxiety and depression, epilepsy, sleep disturbances, and a range of comorbid medical conditions (Croen et al., 2015, Matson and Cervantes, 2014) (**Fig. 1**). The occurrence of these co-morbidities is higher in ASD patients than in the general population (Elsabbagh et al., 2012), but it remains unclear whether the ASD-associated co-morbidities are consequences of the core symptoms or can actually be their cause. Furthermore, the presence of a unique set of co-morbidities in each ASD individual makes diagnosis and therapeutic intervention difficult. Patient stratification and individualized interventions are necessary for effective treatment of ASD symptomatology. The use of biomarkers could help in patient diagnosis, stratification and targeted interventions. Several putative biomarkers have been proposed for assessing ASD risk, such as biological markers (blood and/or urine metabolic and immune profiles) and neuroimaging markers (MRI, DTI and EEG measurements) (Walsh et al., 2011). The search for pre-symptomatic biomarkers continues for early diagnosis, which would allow for more opportunities of therapeutic intervention.

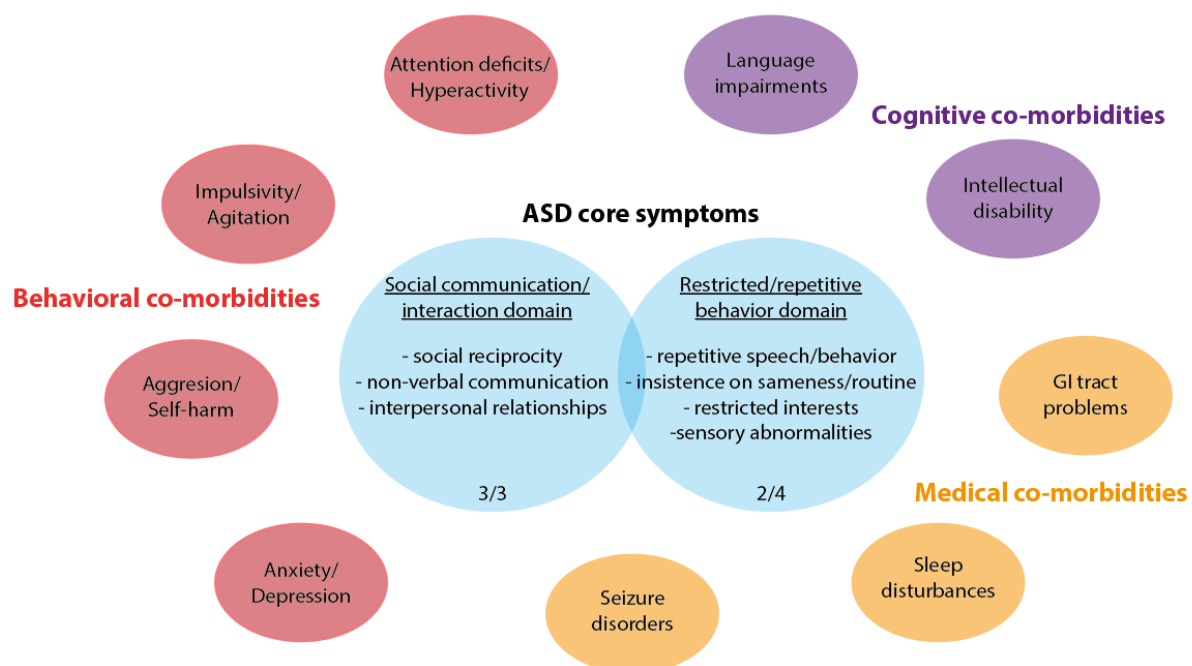


**Figure 1: Representation of the core ASD symptoms and associated co-morbidities.** Adapted from Hewitson, 2013.

*The core symptoms of ASD are defined as impairments in the social communication/interaction and restricted/repetitive behaviors domains, highlighted in blue. The most frequently ASD-associated co-morbidities are reported according to their nature. In red, behavioral symptoms including attention deficit/hyperactivity, impulsivity, self-harm/aggression and anxiety/depression. In purple, cognitive symptoms including language impairment and intellectual disability. In orange, systemic medical symptoms including gastro-intestinal problems, sleep disturbances and seizure disorders.*



### ***Genetic and environmental risk factors***

ASD is considered the most heritable of NDDs with strong evidence highlighting the large contribution of genetic risk factors to ASD etiology. Historically, twin and family studies have estimated heritability between 50% to 95% in Western countries (Hallmayer et al., 2011, Bai et al., 2020). In more details, ASD concordance rate between monozygotic twin ranges from 40% to 90%, while dizygotic twins concordance lowers between 15% and 35% (Ronald and Hoekstra, 2011). The ASD recurrence risk in individuals with autistic siblings is estimated between 3% to 18% (Ozonoff et al., 2011). Further highlighting the genetic contribution to ASD pathology, whole-genome or –exome sequencing studies have identified rare and penetrant genetic variations, including inherited and germline *de novo* mutations as well as copy number variations (CNVs). Syndromic monogenic forms of ASD such as Rett and Fragile X syndromes were also described (Amir et al., 1999, Verkerk et al. 1991), where a highly penetrant mutation in a single gene is underlying ASD phenotypes. However, only a small fraction of the ASD population displays inherited and rare *de novo* mutations or CNVs, although hundreds of ASD risk genes have been identified (SFARI database). It is now believed that genetic risk variants in ASD individuals converge on common genetic pathways where the cumulative effect of multiple common genetic variants (termed polygenic risk) is an important genetic contributor of non-syndromic ASD pathology (de la Torre-Ubieta et al., 2016, Gaugler et al., 2014). Single nucleotide polymorphism (SNP) is a base pair variation commonly found in over 1% of the population in a defined genetic region. The presence of several common SNPs, or polygenic variation, is considered an additive genetic risk contributing up to 50% of ASD cases (Gaugler et al., 2014).

The remaining incidence of ASD cases can be attributed to epigenetic and environmental risk factors. As mentioned previously, neurodevelopment is highly sensitive to external factors at the embryonic stages as well as during the first years of life, particularly during “critical period” of experience-driven neuronal plasticity. Amounting evidence has now identified many environmental factors conferring high ASD risk, most of which are most deleterious when exposure occurs embryonically (Lyall et al., 2017). Fetal exposure to chemicals (endocrine disruptors, heavy metal) and teratogenic medications (anti-depressants, anti-asthmatic and anti-epileptic drugs) during pregnancy is described as a major external risk factor for ASD (Newschaffer et al., 2007). Similarly, maternal hospitalization with infection during pregnancy is associated with increased ASD risk due to maternal immune activation (Lee et al., 2015). Indeed, immune-mediated conditions and autoimmune reactions can potentially influence embryonic neurodevelopment (Zerbo et al., 2016). Other parental factors may influence the risk for ASD in offsprings such as parental age, inter-pregnancy interval, maternal life-style and

diet (Lyll et al., 2017). It is currently believed that environmental factors can lead to epigenetic changes in the parental genomes, which can be transferred across generations (Franklin et al., 2010). In particular, alterations in DNA methylation rates are thought to play a role in ASD pathology (Joubert et al., 2016, Ladd-Acosta and Fallin, 2016).

Taken together, it is clear that ASD etiology is very complex with genetic, epigenetic and environmental risk factors. Furthermore, the burden of ASD can be additive with the combination of different type of risk factors in one individual. It is therefore necessary to know the root of ASD pathology in each patient but even more critical to understand the underlying biological alterations causing the ASD phenotypes in order to find efficient therapeutic interventions.

### ***Molecular pathways and potential therapeutic targets***

Altered brain connectivity is a hallmark of ASD neuropathology with many studies reporting long-range underconnectivity in cortical and subcortical regions accompanied by compensatory short-range overconnectivity (Anderson et al., 2011, Keown et al., 2013). Abnormal connectivity can be due to structural changes such as altered neuronal morphology and aberrant synapse density observed in ASD individuals and animal models (Bourgeron, 2015). However, alterations may also arise from functional rather than structural deficits. Thus, an imbalance of neuronal excitatory and inhibitory function (E/I balance) has been proposed as autism-relevant alteration in neuronal circuits (Nelson and Valakh, 2015). Modifications of the E/I balance occur when the plasticity events of the “critical period” are decreased. ASD was proposed to not only the results embryonic insults altering neurodevelopment *in utero* but also results from an abolition or impairment of the “critical period” plasticity (LeBlanc and Fagiolini, 2011). Dysfunction of somatosensory, visual and auditory information processing due to E/I imbalance may drive the alterations in social interactions and communication in ASD patients (Toro et al., 2010).

The biological pathways implicated in E/I imbalance, abnormal connectivity and altered neuronal morphology observed in ASD are involved in regulation of neuronal and/or synaptic homeostasis through various physiological processes such as chromatin remodeling, metabolism, translation and synaptic function. Indeed many ASD risk genes are directly involved in synaptic function at the pre- and post-synapse: synaptic receptors (NMDA, mGluRs, GABA), scaffolding proteins (SHANKs, Gephyrin) and synaptic adhesion molecules (Neurexins and Neuroligins) (Toro et al., 2010). Other genes regulate synaptic activity by altering neuronal translation and/or transcription, such as the *Fmr1* gene in Fragile X syndrome, *Pten* gene and

*Mecp2* gene in Rett syndrome (Kelleher and Bear, 2008). The **Figure 2** recapitulates the pathways associated with ASD in neurons at both glutamatergic and GABAergic synapses (from Delorme et al., 2013). From the findings in animal models and human patients with ASD syndromic forms, therapeutic strategies have been developed to mitigate the synaptic defects and behavioral ASD phenotypes such as rapamycin (PI3K-mTOR repressor), MPEP or CTEP (mGluR antagonists), clonazepam or arbaclofen (positive allosteric modulator of GABA<sub>A</sub> and GABA<sub>B</sub> receptors, respectively) amongst others (recapitulated in **Fig. 2** from Delorme et al., 2013). Some of these treatments show promise in pre-clinical and clinical studies indicating that symptom alleviation can be achieved outside of the “critical period”. Choice of drug treatment for positive therapeutic impact likely depends on the etiology and genetic mutation identified, symptom severity and the presence of co-morbidities. Therefore, each ASD case is unique and therapy must be tailored to fit the observed ASD phenotypes.

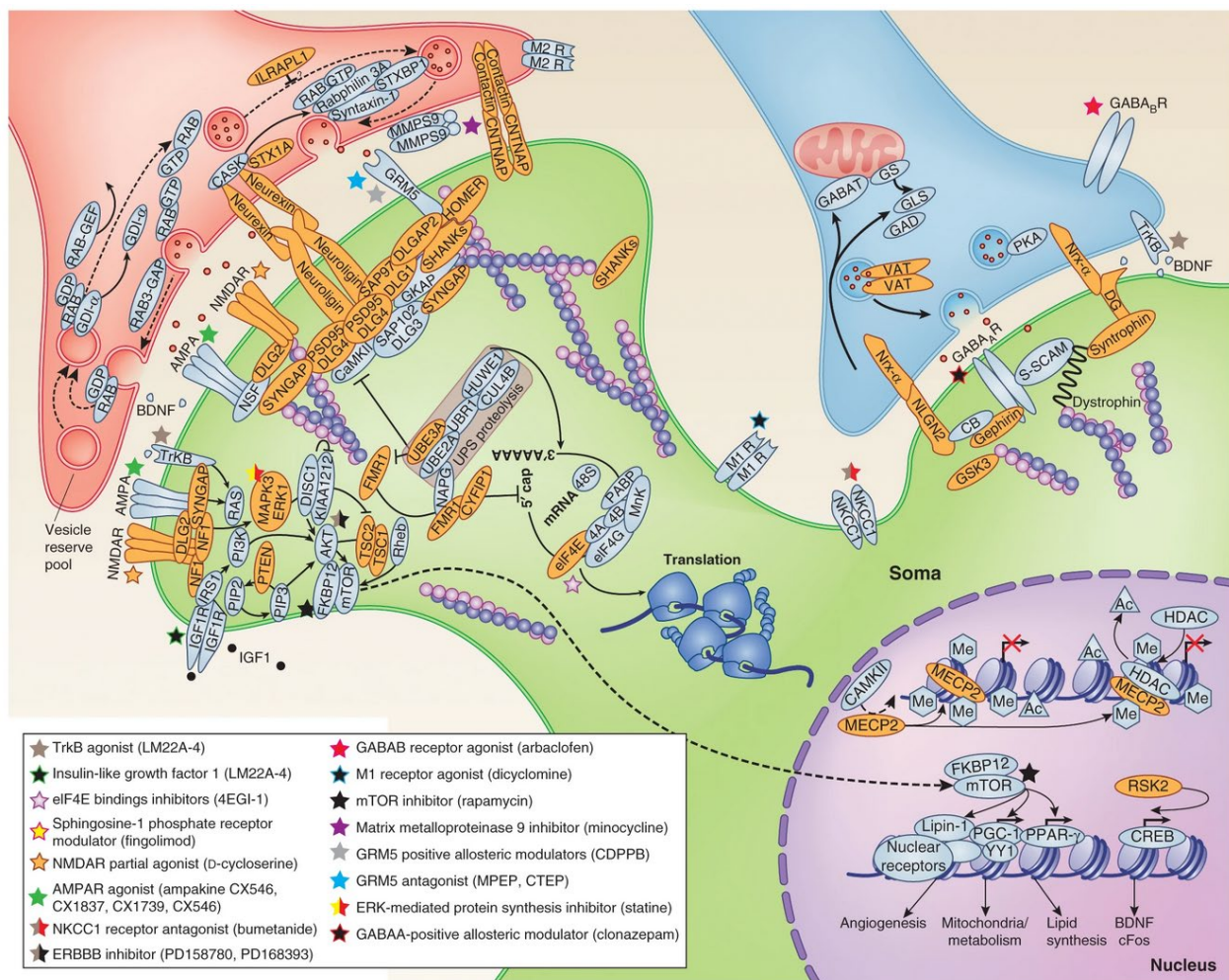


**Figure 2: Schematic representation of pre- and post-synaptic proteins involved in ASD pathophysiology.**

From Delorme et al., 2013.

*Proteins reported to be associated with ASD are in orange. Factors involved in the pathways where ASD-associated proteins are involved are in blue. Pharmacological treatments used to alleviate core symptoms of ASD in animal models and patients are displayed with a star.*

## 1.2.2 Overlap between NDD forms

Due to the complex etiology and heterogeneity in NDD pathology, the actual diagnostic concept characterize each NDD as a distinct disease entity, such as ASD, ID and ADHD. However, the high overlap in NDD pathophysiology and associated co-morbidities tends to demonstrate the need for a more continuous disease spectrum for all NDDs (Thapar et al., 2017). The concept of neurodevelopmental continuum has been proposed, in which all NDDs, including bipolar disorders and schizophrenia, represent the diverse range of outcomes resulting from disrupted or altered brain development (Owen and Donovan, 2017, Morris-Rosendahl and Crocq, 2020, **Fig. 3A**). As mentioned above for ASD patients, each NDD case may be different from its etiology to the implicated cellular and molecular pathways in disease pathology, thus it can be argued that each case falls somewhere within the neuronal developmental continuum depending on their phenotypic profile and degree of overlap in associated NDD co-morbidities. Patient stratification and grouping would therefore rely on pathway- or proteome-based classification along the continuum and across current diagnostic boundaries, which some studies have already suggested as a valuable alternative stratification concept (Mullin et al., 2013, Ismail and Shapiro, 2019). Indeed, patient stratification is essential to identify NDD population subsets that may respond and benefit from specific mechanism-based treatments.

Taking ASD as a framework for this continuum concept, studies have demonstrated the high co-morbidity rate of ASD with other NDDs, such as ID, ADHD, epilepsy and anxiety amongst others (**Fig. 3B**), and vice-versa other NDDs can display high rate of ASD or ASD-like features (Lai et al., 2014, Rosen et al., 2018). All NDDs also share the distinct male-to-female diagnostic bias (DSM-5, APA, 2013). From recent studies, ASD, ID and ADHD have been shown to share specific generic risk alleles with each other, and with other NDD such as schizophrenia (Owen et al., 2011, Sing et al., 2017). Moreover, evidence revealed overlapping risk factors, both genetic and environmental, and implicated cellular pathways in NDD pathology (Mullin et al., 2013). The concept of neurodevelopmental continuum is based on a neurodevelopmental gradient hypothesis where disorders are graded according to the severity of the observed impairments. Grading would be dependent on pathological contributing features such as age of onset, degree of cognitive alterations and persistence of functional impairments (Owen and Donovan, 2017). In concordance with this hypothesis, burden of CNVs was shown to be positively correlated with NDD severity, e.g. greater in ID than ASD, and greater in ASD with ID than without (Girirajan et al., 2011). Similarly, burden of large and rare CNVs implicated in NDDs is higher in patients with global developmental delay, ASD or congenital malformations than in schizophrenia (Kirov et al., 2014). Moreover, increased rates

of *de novo* variants were found in most NDDs and when comparing the relative *de novo* variants enrichment across NDDs, the rates decreased in frequency when placed again the gradient described in **Figure 3A**, from ID to ASD to schizophrenia in accordance with the neurodevelopmental continuum and gradient hypothesis (Morris-Rosendahl and Crocq, 2020). At the gene and pathway levels, it appears that NDDs share implicated genetic and functional causes. Indeed, genes affected by loss-of-function *de novo* mutations were enriched in patients diagnosed with ID, ASD and schizophrenia (Fromer et al., 2014, Iossifov et al., 2014). These genes preferentially encode functionally related biological processes, including synaptic plasticity and chromatin remodeling. These findings suggests that the neurodevelopmental continuum concept has value for the redefinition of NDD classification and diagnosis.

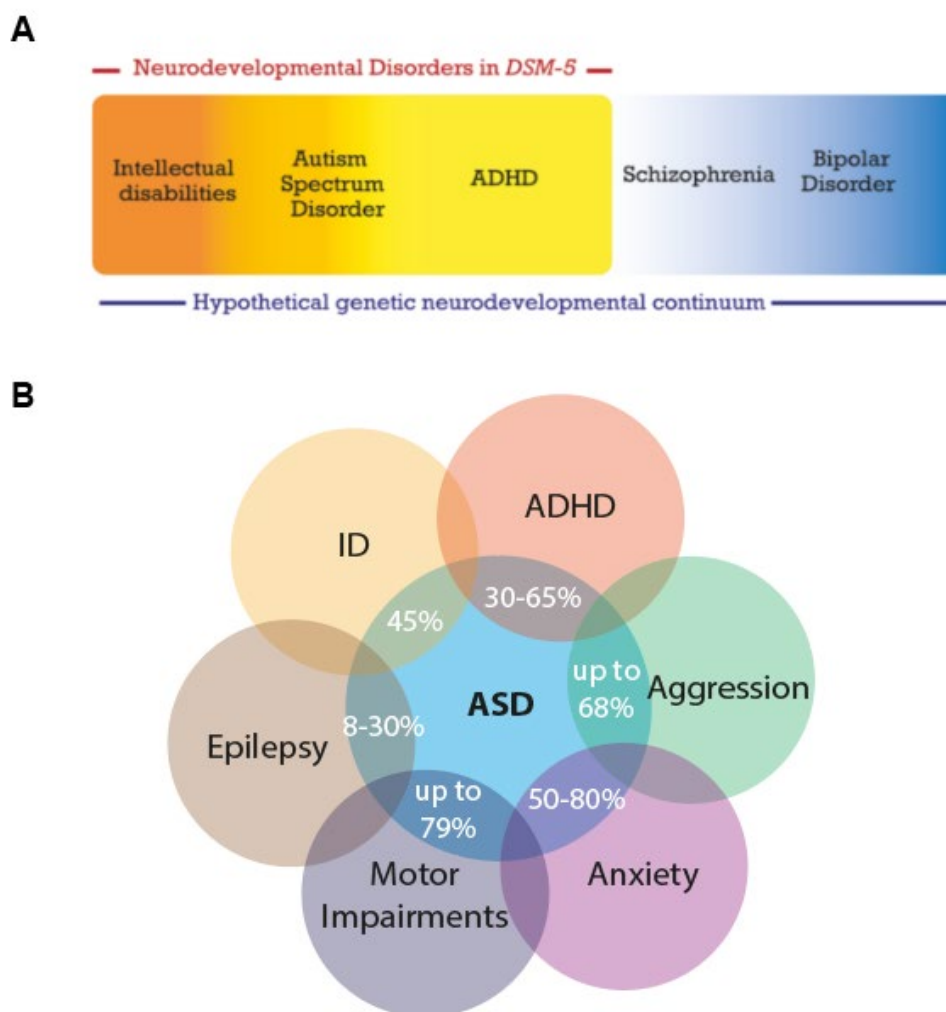


**Figure 3: Neurodevelopmental continuum hypothesis and ASD-associated NDD co-morbidity rates.**

(A) Illustration of the neurodevelopmental continuum and gradient hypothesis for the classification of NDD, adapted from Morris-Rosendahl and Crocq, 2020. (B) Rate of ASD-associated NDD co-morbidities. ID: intellectual disability, ADHD: attention deficit/hyperactivity disorder (Pastore et al., 2022, Morris-Rosendahl and Crocq, 2020).

The technological advances in genomic studies has enabled the identification of hundreds of

NDD genetic risk factors. The individual study of monogenic NDD forms has provided invaluable insights on the cellular pathophysiological underlying neurological alterations, and remains a rational and instrumental approach for the identification of new therapeutic targets and the development of mechanism-based treatments. However, despite their high heritability, NDDs are more often multi-factorial in their etiology. Therefore, flexible patient stratification and grouping strategies are needed for efficient and individualized treatments. The neurodevelopmental continuum and underlying gradient hypothesis, along with genetic and pathway-based characterization, may provide a new diagnostic approach and stratification method, allowing fruitful therapeutic interventions in across current diagnostic boundaries (Mullin et al., 2013, Morris-Rosendahl and Crocq, 2020).

### **1.3 Ptchd1, NPC1 and sterol-sensing domain proteins**

One relatively unexplored biological pathway that may participate in NDD pathology is lipid metabolism. Particularly, cholesterol homeostasis plays an important role in neuronal development and function. Cholesterol alterations have been linked to several NDDs such as Smith-Lemli-Opitz syndrome, Niemann-Pick disease type C and Fragile X syndrome. Before introducing the mechanisms of brain cholesterol homeostasis and its relation to neurological diseases, we will discuss the monogenic mouse models used in this work to assess the role of cholesterol homeostasis in NDD pathology. In this project, we focused on two NDD risk genes, which encode proteins containing a sterol-sensing domain (SSD) and therefore may relate to cholesterol homeostasis: *Ptchd1* and *NPC1*.

#### **1.3.1 Ptchd1 – a neurodevelopmental risk gene**

The X-chromosomal *Ptchd1* gene encodes a putative 12-pass transmembrane protein from the Patched-related protein family (**Fig. 4**). Within its sequence, Ptchd1 protein contains a sterol-sensing domain (SSD) and SSD-like regions similarly to Patched-1 (Ptch1), Dispatched-1 (Disp1) and NPC intracellular cholesterol transporter 1 (NPC1). As both Ptch1 and NPC1 display a cholesterol transporter activity, we hypothesized that Ptchd1 may have a similar biological function. In this section, I will discuss how the *Ptchd1* gene was first identified as a NDD risk gene, the phenotypes associated with *Ptchd1* pathology and finally the proposed biological function of Ptchd1.

### ***Ptchd1, an ASD/ID risk gene and its associated phenotypes***

*Ptchd1* was first reported as an ASD risk gene by the identification of a 167Kb deletion in the Xp22.11 genomic region, which encompasses the first exon of *Ptchd1* (resulting in a null allele) and exons of the *Ptchd1 antisense non-coding RNA (Ptchd1-AS)* (Marshall et al., 2008). Given the X-linked inheritance patterns, the microdeletion was transmitted from an unaffected mother to male ASD proband. Several studies confirmed this initial finding and identified other CNVs (44 inherited and 2 *de novo* deletions) in the *Ptchd1* and *Ptchd1-AS* genomic regions in ASD and ID individuals (Pinto et al., 2010, Noor et al., 2010, Whibley et al., 2010). To date, approximately 70 rare genomic variants were identified ([www.PTCHD1-base.com](http://www.PTCHD1-base.com)), including microdeletions and single-nucleotide variants (SNVs). The identified SNVs in the *Ptchd1* coding region consisted of 18 inherited missense variants, 4 truncating variants (including 1 *de novo* variant) and 1 inherited non-sense mutation (Chaudhry et al., 2015, Firth et al., 2009, Noor et al., 2010, Halewa et al., 2021, Karaca et al., 2015, Rohtus et al., 2020, Torrico et al., 2015). In total, both CNVs and SNVs variants have been reported in 69 unrelated probands (67 males) with NDDs. These deleterious variants were almost exclusively transmitted from the maternal side to males diagnosed with ASD, ID and other developmental delays (Pastore et al., 2022). It has been proposed that disruption of the *Ptchd1-AS* region is more causally related to ASD, while *Ptchd1* region disruptions relate more to ID phenotypes (Ross et al., 2020). However, SNVs in the *Ptchd1* coding region, without any variants in *Ptchd1-AS* region, have been identified in ASD individuals. Thus, it is reasonable to conclude that *Ptchd1* and *Ptchd1-AS* are both individual, penetrant and heritable risk genes for ASD and ID, and can therefore be referred to as NDD risk genes.

A cohort of 23 individuals with loss-of-function SNVs or CNVs disrupting the *Ptchd1* gene was assessed by Chaudhry et al. to define the clinical presentation of individuals with *Ptchd1* mutations and understand the underlying genotype-phenotype relationship. From this relatively small cohort, most cases did not present growth abnormalities with only 9% displaying early growth retardation. Minor facial dysmorphic features (open-mouth posture and secondary orofacial hypotonia) were reported in 48% of cases. Relative or absolute macro- and microcephaly was observed in 18% and 13% of cases respectively. At the cognitive level, 78% of subjects show a global developmental delay in early childhood. Furthermore, formal diagnosis of ID was made for 39% of patients while 35% received an ASD diagnosis and 9% have ASD-like features but no formal diagnosis. Behavioral co-morbidities such as mood disorders and aggression were reported in 18% of cases. Medical co-morbidities were also observed such as hypo- and hypertonia (26% and 9% respectively), balance and gait abnormalities (22%) and vision problems (35%). Taken together, it is clear that *Ptchd1*



mutations in human patients are linked to NDD diagnosis and pathology. Several *Ptchd1*<sup>KO</sup> mouse models have been created in order to uncover cellular phenotypes and the underlying mechanisms involved in *Ptchd1* physiopathology.

### ***Ptchd1* KO mouse models and their phenotypes**

The association between *Ptchd1* mutations and abnormal neurodevelopment is evident from the genetic studies and clinical assessment of patients. However, the pathological mechanisms remain poorly understood. Several *Ptchd1*<sup>KO</sup> (*Ptchd1*<sup>-/-</sup>) mouse models have been used to assess the effects of *Ptchd1* at the behavioral and cellular levels. Due to the variation in observed CNVs and SNVs in the *Ptchd1* gene, many different KO models have been generated with exon-specific deletions:  $\Delta$ ex1/y (Murakami et al., 2019),  $\Delta$ ex2/y (Tora et al., 2017),  $\Delta$ ex3/y (Ko et al., 2019). Most groups achieved *Ptchd1*<sup>KO</sup> by targeting the exon 2 for conditional deletion (*Ptchd1* <sup>$\Delta$ ex2/y</sup>), which results in a transcript with a premature truncation before the final nine transmembrane domains. Notably, *Ptchd1* transcript levels are not altered in *Ptchd1* <sup>$\Delta$ ex2/y</sup> mice, potentially due to shorter transcript expression, while protein expression is abolished (Tora et al., 2017). In male *Ptchd1*<sup>KO</sup> mice, generated by any of the exon-specific deletions, many behavioral phenotypes reminiscent of the clinical presentation of ASD and ADHD were reported. The phenotypes described below are mainly described in *Ptchd1* <sup>$\Delta$ ex1/y</sup> and *Ptchd1* <sup>$\Delta$ ex2/y</sup> mice.

*Ptchd1*<sup>KO</sup> mice display hyperactivity in the open-field test (OFT) (Tora et al., 2017, Murakami et al., 2019, Ko et al., 2019), global elevated locomotor activity (Wells et al., 2016, Ung et al., 2018) as well as reduced habituation to novel environments (Murakami et al., 2019). Increase in impulsivity was also observed in a cliff avoidance test (CAT) (Murakami et al., 2019). These phenotypes are ADHD-like behaviors and interestingly, treatment of *Ptchd1*<sup>KO</sup> mice with Atomoxetine (an norepinephrine reuptake inhibitor used to treat ADHD patients) was shown to alleviate both hyperactivity and impulsivity phenotypes in the OFT and CAT (Murakami et al., 2019). Motor dysfunctions were reported in *Ptchd1*<sup>KO</sup> mice including altered gait, hypotonia and impaired motor coordination (Wells et al., 2016, Ung et al., 2018). *Ptchd1*<sup>KO</sup> mice also exhibit sleep disturbances and heightened aggression, but no defects in sensorimotor gating functions were observed in the prepulse inhibition test of acoustic startle response (Wells et al., 2016). Mild stereotypic behaviors were also reported in *Ptchd1*<sup>KO</sup> mice such as increased jumping and rearing in the home-cage and OFT settings (Tora et al., 2017, Ung et al., 2018).

At the cognitive level, *Ptchd1*<sup>KO</sup> mice display impairments in learning and memory. Diminished short-term working memory was observed in the Y-maze test (Ung et al., 2018, Murakami et



al., 2019) while reduced recognition memory was reported in the novel-object recognition test (Tora et al., 2017, Ung et al., 2018, Murakami et al., 2019). In a conditional knock-down of *Ptchd1* in the anterodorsal thalamus, alteration in long-term memory was also reported in a contextual fear conditioning paradigm (Roy et al., 2021). Other learning impairments were observed in *Ptchd1*<sup>KO</sup> mice including diminished latency to cross in the inhibitory avoidance task and decreased freezing in contextual and cued conditioning paradigms (Wells et al., 2016, Ung et al., 2018). The learning impairments may partially result from deficits in sensory filtering. Indeed, *Ptchd1*<sup>KO</sup> mice display cognitive impairments in the presence of visual distractor indicating sensory-related attention deficits (Wells et al., 2016). Similarly, *Ptchd1*<sup>KO</sup> mice show decreased discrimination abilities of auditory stimuli when background noise levels are high, with or without preceding visual cues (Nakajima et al., 2019). A conditional KO of *Ptchd1* in the somatostatin interneurons of the thalamic reticular nucleus (TRN) recapitulated the hyperactivity, attention deficits and sleep disturbances phenotypes suggesting that *Ptchd1* expression in the TRN somatostatin interneurons is essential for these specific functions (Wells et al., 2016).

Metabolic alterations were also found in *Ptchd1*<sup>KO</sup> mice, specifically in the kynurenine pathway (Murakami et al., 2019). The kynurenine pathway metabolizes tryptophan to produce the nicotinamide adenine dinucleotide (NAD) co-enzyme, which is involved in redox reactions of metabolism and energy production. Several metabolites are dysregulated in the serum and frontal cortex of *Ptchd1*<sup>KO</sup> mice. Again, administration of Atomoxetine (ADHD treatment) to *Ptchd1*<sup>KO</sup> ameliorated both serum and frontal cortex concentrations of the altered kynurenine metabolites suggesting a link between kynurenine pathway, tryptophan metabolism and ADHD-like phenotypes.

Surprisingly, no deficits in social interactions were found in *Ptchd1*<sup>KO</sup> mice although *Ptchd1* has been linked to ASD in several genetic studies. However, a possible explanation to this lack of social abnormalities was given by Ko et al. in a preliminary study. Although exon 1 or exon 2 deletion result in *Ptchd1* protein loss-of-function, the transcripts levels remain unaltered due to the expression of the shorter alternatively-spliced isoform to compensate for the loss of the full-length functional isoform. Despite the fact that protein expression from the short transcript has yet to be established, the remaining transcript and potential protein expression could be masking further phenotypes. Indeed, when using a exon-3 truncating mutation which completely abolishes *Ptchd1* transcript expression (both full-length and short), *Ptchd1*<sup>Δex3/y</sup> mice exhibit learning and memory impairments in contextual fear conditioning, similar to other learning impairments observed in *Ptchd1*<sup>Δex1/y</sup> and *Ptchd1*<sup>Δex2/y</sup> mice, but also showed social abnormalities. The following social deficits were reported: reduced male-female interaction in

the three chamber social assay, reduced ultrasonic vocalization during social interaction and decreased sniffing time in the social odor cue reactivity test (Ko et al., 2019).

Taken together, all *Ptchd1*<sup>KO</sup> mouse models recapitulate several ASD and ADHD behaviors seen in patients. The cognitive impairments observed in *Ptchd1*<sup>KO</sup> mice can also be linked to ID phenotypes. Investigations into the biological function of the Ptchd1 protein are therefore essential to better understand the underlying pathways leading to NDD pathology and the discovery of potential therapeutic targets.

### ***Biological function of Ptchd1 protein***

The first step to characterize the role of the *Ptchd1* gene and protein is to assess its expression pattern. Studies have shown that Ptchd1 is a lowly expressed transcript in the brain and other peripheral organs in both human and mice (Noor et al., 2010). In the brain, Ptchd1 expression levels vary across development. At birth, Ptchd1 expression is mostly restricted to the thalamic reticular nucleus (TRN) but expression decreases in this region throughout adolescence and adulthood. At later developmental stages, Ptchd1 transcript can be detected in several brain regions including cortex, striatum and thalamus but is highest in the cerebellum and dentate gyrus of the hippocampus, specifically in granule cells (Tora et al., 2017, Wells et al., 2016, Roy et al., 2021). *In vitro* evidence suggests that Ptchd1 transcript expression may be regulated by neuronal activity. Indeed, Ptchd1 mRNA expression was increased three-fold following neuronal depolarization by potassium chloride for 6h in primary mouse cortical neurons (Kim et al., 2010). Similarly, a two-fold increase in Ptchd1 mRNA expression was reported after depolarization in human induced pluripotent stem cell (iPSC)-derived cortical neurons (Ross et al., 2020). This transcriptional regulation of *Ptchd1* by neuronal activity seem to indicate a potential neuronal function of Ptchd1, which may relate to long-term potentiation at the post-synaptic site.

At the protein level, Ptchd1 is a predicted 12-pass transmembrane protein with SSD and SSD-like (SSDL) regions and a carboxyterminal PDZ-binding motif (ITTV), with high sequence similarity to the Patched receptor (Ptch1) and NPC intracellular cholesterol transporter (NPC1) (**Fig. 4**). Studies have investigated the subcellular localization of Ptchd1 with debatable results. Due to its low expression levels, no commercial antibodies are able to detect Ptchd1 in immunohistochemical applications. Therefore, visualization of Ptchd1 has relied on the fusion of Ptchd1 to green fluorescent protein reporter (GFP) at either its N- or C-terminus and expressing it in cell lines or primary neuronal cultures. Ptchd1-GFP fusion protein was localized at the plasma membrane of various cell lines *in vitro* (Noor et al., 2010), and at the membrane

of dendritic spines in transiently expressing primary hippocampal cultures co-localizing with the post-synaptic density protein Psd95 (Ung et al., 2018). However, GFP-Ptchd1 did not exhibit the same membrane and spine localization but was found ubiquitously distributed across the cell cytoplasm. The variation in localization was attributed to impaired N-terminus processing by the authors, as Ptchd1 has 10 predicted site for N-linked glycosylation. It is important to note that those results need to be confirmed *in vivo*, preferentially with a smaller fluorescent reporter or tag, before the statement that Ptchd1 protein is located at post-synapses can be reliably made. However, through its PDZ-binding motif, interaction between Ptchd1 and Psd95 was demonstrated *in vitro* (Tora et al., 2017, Ung et al., 2018), which could also point to a post-synaptic localization of Ptchd1. Other potential interactors of Ptchd1 at the carboxyterminal segment include components of the retromer complex such as Vps35, Vps26b and Snx27 (Tora et al., 2017) (**Fig. 4**), which suggests a potential recycling of Ptchd1 from endosomes back to the plasma membrane.

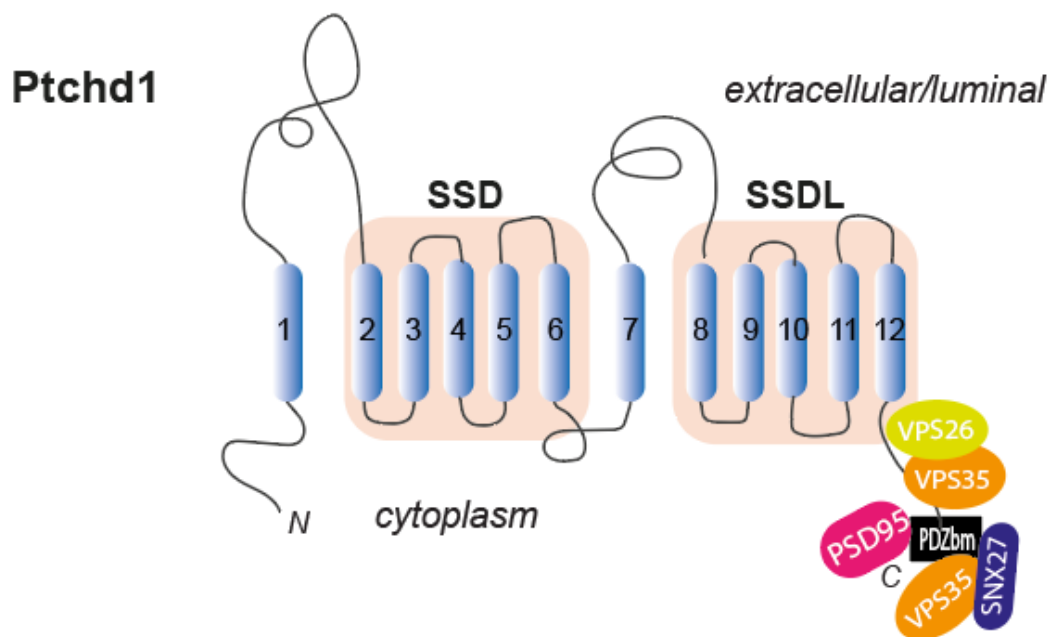


**Figure 4: Ptchd1 protein structure and potential interactors.**

*Hypothetical structure topology of Ptchd1. The two predicted sterol-sensing domain (SSD) and sterol-sensing domain-like (SSDL) regions are highlighted in orange, transmembrane domains in blue (numbered from 1-12), and the PDZ binding-motif (PDZbm) in black. Potential carboxyterminal interactors reported by Tora et al. (2017) are represented at their putative binding sites. PDZbm-dependent binding proteins include the post-synaptic density protein 5 (Psd95) and sorting nexin-27 (Snx27), while the vacuolar protein sorting-associated protein 35 and 26 (Vps35 and Vps26) can bind along the carboxyterminal segment as well.*

Due to its sequence similarity to Ptch1 (21.62% identity, Clustal Omega multiple sequence alignment), Ptchd1 has been hypothesized to be involved in the Hedgehog (Hh) signaling pathway like Ptch1. Ptch1 is a transmembrane receptor that acts as a repressor of the G-protein coupled receptor Smoothed (Smo) inhibiting downstream effectors of the Hh signaling pathway. Repression of Smo by Ptch1 is mediated indirectly by the cholesterol transporter activity of Ptch1, which maintains a local low cholesterol concentration around Smo restricting into a negative protein conformation. Binding of Hh ligand to Ptch1 triggers endocytosis of Ptch1, which enables cholesterol membrane replenishment and activation of Smo, ultimately resulting in activation of the GLI transcription factor family (Hu et al., 2019). Over-expression of Ptchd1 in a Hh-responsive cell line (10T1/2) was reported to inhibit GLI-dependent transcription *in vitro*, similarly to Ptch1 used as a control, suggesting that Ptchd1 is also involved in the Hh signaling pathway (Noor et al., 2010). However, this finding was not recapitulated in other studies. Indeed, Ptchd1 expression was not sufficient to rescue the canonical sonic hedgehog pathway in absence of Ptch1 and exogenously expressed Ptchd1 does not induce repression of GLI-dependent transcription in mouse embryonic fibroblasts derived from *Ptch1*<sup>KO</sup> mice (Ung et al., 2018). Furthermore, Ptchd1 does not bind Hh *in vitro* and proliferation of Hh-dependent neuronal population was not impaired in *Ptchd1*<sup>KO</sup> mice (Tora et al., 2017). Given the larger evidence, it is reasonable to conclude that although Ptchd1 may be active in a similar fashion to Ptch1, it is not part of the Hh signaling pathway.

In order to unravel the neurophysiological mechanisms underlying the phenotypes observed in *Ptchd1*<sup>KO</sup> mice, many electrophysiological have been performed and have revealed interesting changes. As mentioned previously, deletion of *Ptchd1* in the somatostatin interneurons of the TRN region recapitulated the ADHD-like behavioral phenotypes seen in the global KO mice. The TRN is comprised of GABAergic neurons and provides the major source of inhibition to other thalamic regions such as the thalamic relay nuclei (Fogerson and Huguenard, 2016). Electrophysiological whole-cell patch clamp recordings of the TRN somatostatin cells showed a significant decrease in repetitive bursting in absence of Ptchd1. Additionally, TRN somatostatin interneurons also displayed reduced burst firing rate during sleep leading to decreased sleep spindles and fragmented sleep patterns (Wells et al., 2016). The bursting reduction observed in those cells was induced by a decrease in small conductance calcium-activated potassium (SK) ion channels currents resulting in reduced hyperpolarization. A two-fold reduction of basal intracellular calcium concentration was observed, which together with the decreased hyperpolarization, may impair the recruitment of other calcium-dependent channels and affect overall excitability of the somatostatin interneurons of the TRN. Interestingly, TRN perturbations have been linked to sleep disturbances and attention deficits in disease including schizophrenia (Young and Wimmer, 2017), which can be due to reduced thalamic inhibition

and subsequent inability to suppress background sensory stimuli (Halassa et al., 2014). Pharmacological increase of the SK currents with 1-EBIO in the somatostatin interneurons lacking *Ptchd1* rescued the reduced hyperpolarization in those cells and the sensory-evoked thalamic inhibition, thereby alleviating the ADHD-like behavioral phenotypes in these mice. Further evidence of thalamic dysregulation was observed in the auditory subnetwork of the TRN (audTRN). audTRN neurons displayed reduced sound-evoked firing rates resulting in the inability to discriminate between auditory stimuli when background noise levels were high. These impairments were rescued by 1-EBIO treatment when no visual cues were provided before stimulus presentation, suggesting a deficit in executive control of sensory filtering potentially mediated by the pre-frontal cortex (PFC). Synergic treatment with 1-EBIO and modafinil (cognitive enhancer) completely restored the discrimination phenotypes in *Ptchd1*<sup>KO</sup> mice, with and without visual cues. Knock-down of *Ptchd1* in the anterodorsal thalamus induced a neuronal decrease of action potential half-width and the corresponding increase in firing frequency (Roy et al., 2021). A lack of synaptic strengthening (stable AMPA/NMDA ratio) in the fear-conditioning paradigm was also observed in those mice, which was due to reduced voltage-gated P-type calcium channels (Ca<sub>v</sub>2.1 and Ca<sub>v</sub>2.2) current amplitude leading to neuronal hyperexcitability and could be rescued by pharmacological inhibition (Roy et al., 2019).

In addition to thalamic impairments, electrophysiological phenotypes were observed in the hippocampus of *Ptchd1*<sup>KO</sup> mice, which could explain the memory impairments seen in this model. Although no differences were observed in the glutamatergic dendritic spine density and morphology, dentate granule cells of *Ptchd1*<sup>KO</sup> mice exhibited a reduced excitation/inhibition ratio accompanied by an increase in the basal frequency of spontaneous excitatory and inhibitory potentials (sEPSC and sIPSC) but no changes in AMPA/NMDA ratio and paired-pulse ratio upon stimulation of the Schaffer collateral axons (Tora et al., 2017). To elucidate the observed electrophysiological changes in the hippocampus, RNA sequencing was performed on hippocampal samples from *Ptchd1*<sup>KO</sup> mice (Ung et al., 2018). This study revealed significant enrichment of up-regulated genes encoding synaptic proteins including both pre-synaptic (e.g. *Syt1*, *Bsn*, *Vamp3*) and post-synaptic proteins (e.g. *Psd95*, *Camk2a*, *Syngap1* and *Shank1-3*). Up-regulation of genes involved in neuronal activity-dependent transcription (*Npas4* and *Egr1*) and neurodevelopment, such as axogenesis and dendritogenesis, was also observed. Taken together, these findings suggest that *Ptchd1*<sup>KO</sup> mice have altered synaptic structure and function. However, despite all the observed cellular and behavioral phenotypes observed in the *Ptchd1*<sup>KO</sup> mouse models, no clear biological role of the *Ptchd1* protein was defined.

### **1.3.2 NPC1 – a cholesterol-related disease gene**

As mentioned previously, NPC1 is 13-pass transmembrane protein with a sterol-sensing domain, which functions as lysosomal cholesterol transporter with an essential role in cholesterol homeostasis, especially in neuronal cells. After endocytosis-mediated intake of exogenous cholesterol in the cell, unesterified cholesterol is stored in late endosomes/lysosomes where NPC1, in collaboration with the NPC2 protein, is responsible for its egress and subsequent transfer to the intended intracellular membrane. Disruption of cholesterol exit from lysosome results in a lysosomal lipid storage disorder with severe neurological and systemic symptoms known as Niemann-Pick disease type C (NPC). In this section, I will introduce the clinical phenotypes observed in NPC patients and the underlying genetic etiology. The biological role of NPC1 will then be discussed.

#### ***NPC clinical presentation and genetics***

Niemann-Pick disease type C (NPC) is an autosomal recessive neurovisceral lipid storage disorder, characterized by unesterified cholesterol accumulation in late endosomes/lysosomes (LE/LY) compartments of all organs. Mutations in the *NPC1* and *NPC2* genes account for respectively 95% and 5% of all NPC cases (Vanier, 2010). Defective NPC1 and/or NPC2 proteins cause impaired cholesterol egress from LE/LY resulting in altered intracellular cholesterol trafficking and overall cholesterol homeostasis, which is the cellular disease hallmark (Vanier, 2010, Wheeler and Sillence, 2020). NPC is a clinically heterogenous disorder with symptoms including psychiatric conditions, neurological defects and multi-organ systemic dysfunction (Vanier, 2010, Berry-Kravis, 2021). Disease severity correlates with the level of NPC1 protein dysfunction, as total loss-of-function results in neonatal death while minimal impairment induces adult-onset milder forms. NPC patient average life-span ranges from 10 to 25 years (Vanier and Millat, 2003, Wraith et al., 2009). The severity level is assessed by the level of neurological involvement, which vary with age of onset. Neurological symptoms include developmental delay, motor coordination deficits and cerebellar ataxia, language and learning impairments, seizure disorders and progressive cognitive decline (Vanier, 2010, Maresca et al., 2021, Berry-Kravis, 2021). According to the age of onset and disease severity, NPC can be classified as a NDD when diagnosis occurs in infancy, while adult-onset will have the characteristics of a neurodegenerative disease. Diagnosis is confirmed biologically by observation of filipin-stained cholesterol accumulation in patient-derived fibroblasts and by blood measurements of disease-related metabolites (Papandreou and Gissen, 2016).

The clinical heterogeneity of NPC is reflected in its genetic heterogeneity, with at least 420 pathogenic *NPC1* variants identified (Geberhiwot et al., 2018). The most frequent mutation, I1061T, accounts for 10% to 25% of cases depending on the population (Millat et al., 1999). Homozygotes for this mutation present with juvenile-onset severe forms while heterozygotes display the milder adult-onset forms. At the protein level, the I1061T mutation induces a misfolded but functional protein, which is excessively targeted for ER degradation due to its misfolding (Gelsthorpe et al., 2008). The second most frequent *NPC1* mutation, P1007A, causes less severe disease phenotypes, with homozygotes presenting milder adult-onset forms (Ribeiro et al., 2001). Specific populations display unique recurrent mutations in the *NPC1* gene due to the founder's effect (Berry-Kravis, 2021). The correlation between genotype-induced *NPC1* impairment and disease severity suggests that missense or frameshift mutations that completely abolish *NPC1* protein function are likely to result in the most severe infantile- or juvenile-onset NPC forms, especially in homozygotes (Berry-Kravis, 2021). Indeed, missense mutations in the SSD result in *NPC1* loss-of-function and subsequently give rise to the severe disease phenotype (Millat et al., 2001). The NPC phenotypes and genetic evidence highlight the importance of the *NPC1* protein in cellular cholesterol homeostasis and for normal brain and systemic function.

### ***Biological function of Npc1 protein***

As mentioned previously, *NPC1* collaborates with *NPC2* to mediate the LE/LY egress of free cholesterol. Endocytosed lipoproteins are transported to the LE/LY where unesterified cholesterol is hydrolyzed into free cholesterol. *NPC1*, as a direct cholesterol transporter via its sterol-sensing domain, mediates the cholesterol lysosomal exit (Berry-Kravis, 2021). Free cholesterol is then intracellularly trafficked to the plasma membrane for its intended use or to the ER for potential degradation. *NPC1* is primarily localized to late endosomes and has been shown to transiently interact with lysosomes and the trans-Golgi network (Neufeld et al., 1999, Higgins et al., 1999). Interrogations remain on the global function of *NPC1*, which may not simply be restricted to cholesterol transport. It has been posited that *NPC1* could regulate or mediate the transport of other lysosomal cargo, such as glycolipids. Indeed, glycolipid accumulation is the main phenotype observed in *NPC1*-deficient neuronal cells, cholesterol imbalance being much lower in comparison (Walkley and Vanier, 2009). In addition to glycolipids, brain accumulation of other lipid species was reported such as sphingosine (Davidson et al., 2009). It has been proposed that sphingosine accumulation and storage could act as the trigger for the pathogenic effects of NPC, since sphingosine was shown to disrupt lysosomal calcium homeostasis (Lloyd-Evans et al., 2008, Lloyd-Evans and Platt, 2010). Therefore, the current hypothesis is that *NPC1* is a cholesterol transporter but could also act as

a transporter of other lipid species via its SSD. This remains to be proven experimentally *in vivo*. Cholesterol accumulation in absence of NPC1 can also affect lipid homeostasis by the dysregulation of several key enzymes, thus NPC1 deficiency could therefore trigger a more global intracellular lipid homeostasis and trafficking disorder (Walkley and Vanier, 2009, Salviooli et al., 2004). LE/LY cholesterol accumulation in NPC also induces impaired trafficking of several LE proteins, including Rab9 and mannose-6-phosphate receptors, involved in LE/LY system function (Ganley and Pfeffer, 2006). These findings also implicate alterations in the vesicular trafficking pathway as part of the NPC pathophysiology (Vanier, 2010).

### 1.3.3 Sterol sensing domain proteins

The link between Ptchd1 and NPC1 protein is the presence of a structural sterol-sensing domain, which is found in other proteins such as Hmgcr, Scap, Disp1 and Ptch1. The SSD-containing proteins are membrane proteins involved in cholesterol homeostasis, and possess a conserved SSD core essential for their sterol-dependent functions. As inferred from its denomination, the SSD allows membrane proteins to “sense” the presence of sterol substrates, namely cholesterol, by direct interaction and may modulate protein activity depending on sterol levels (Kuwabara and Labouesse, 2002). **Figure 5** depicts the cellular localisation and proposed roles of identified SSD proteins (adapted from Wu et al., 2022). From structural and mechanistic characterization, SSD-containing proteins can be divided into two groups: cholesterol sensors (or modulators) and cholesterol transporters (Wu et al., 2022). The following sections will describe the biological function of each category.

#### ***Cholesterol sensors***

SSD-containing proteins classified as cholesterol sensors or modulators are relatively small and highly mobile membrane proteins, implicated in cholesterol synthesis and metabolism (Wu et al., 2022). The 7-dehydrocholesterol reductase enzyme (7dhcr) as well as the E3 ubiquitin ligases March6 and Rnf145 were proposed to contain a SSD but without any structural evidence to corroborate it and contrary prediction models (Tunyasuvunakool et al., 2021). Therefore, we will only focus on the two proteins in which the presence of a SSD was experimentally demonstrated, namely 3-Hydroxy-3-methylglutaryl-CoA reductase (Hmgr), the rate-limiting cholesterol synthesis enzyme, and sterol regulatory element-binding protein (SREBP)-cleavage activating protein (Scap), a cholesterol synthesis regulatory protein (Kuwabara and Labouesse, 2002). The SSD of these two proteins encompasses the transmembrane (TM) helices TM2 to TM6 and mediates the sterol-dependent binding of the ER-retaining insulin-induced gene 1 and 2 proteins (Insig1 and Insig2) (Hua et al., 1996,



Nohturfft et al., 1998). As exemplified in **Figure 5** (adapted from Wu et al., 2022), Scap and Scap-bound SREBP transcription factor are sequestered in the ER membrane by binding to Insig proteins via Scap SSD when cellular cholesterol levels are high, resulting in minimal expression of cholesterol synthesis and uptake genes such as *Hmgcr*. Decrease in cholesterol levels triggers the dissociation of Scap-SREBP protein complex from Insig and its subsequent trafficking to the Golgi, where proteolytic cleavages of SREBP liberates its N-terminal transcription factor domain inducing nuclear entry and transcription upregulation of cholesterol synthesis and uptake genes (Brown et al., 2018). *Hmgcr* expression is therefore controlled by the SREBP pathway but the presence of a SSD within *Hmgcr* structure also point to another sterol-dependent direct regulation of *Hmgcr* protein. Indeed, the ER-localized *Hmgcr* protein also binds to Insig proteins in the high cholesterol context, similarly to Scap (Wu et al., 2022). The binding of *Hmgcr* to Insig triggers the recruitment of E3 ubiquitin ligases (March6 and Rnf145 amongst others) and ubiquitination of *Hmgcr* targeting it for proteasomal degradation (Sever et al., 2003, Zelcer et al., 2014, Menzies et al., 2018, Jiang et al., 2018). This ER-associated degradation mechanism is an additional post-translational regulation layer of the cholesterol synthesis pathway (Goldstein and Brown, 1990, DeBose-Boyd, 2008), also mediated by the presence of the structural sterol-sensing domain.

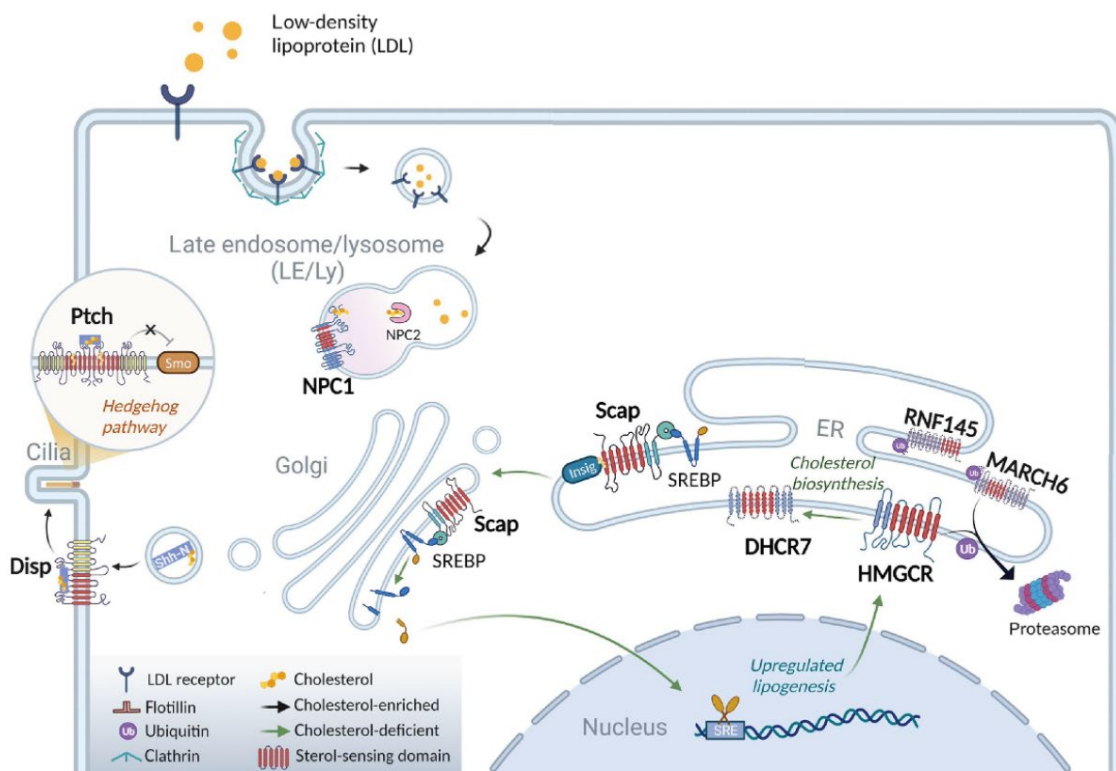


**Figure 5: SSD-containing proteins and their cellular functions.**

Adapted from Wu et al., 2022

*The biological role of many SSD-containing proteins is related to the cholesterol homeostasis pathway.*

SSDs are represented in red in the protein structure, and putative SSDs are shown with broken lines for 7DHCR, MARCH6 and RNF145 due to lack of structural evidence. The function of all SSD-containing proteins displayed on this cellular map is discussed throughout the introduction and will not be repeated here. DHCR7: 7-dehydrocholesterol reductase; Disp: Dispatched; HMGCR: hydroxy-3-methylglutaryl-CoA reductase; NPC1: Niemann-Pick disease type C 1; Ptch: Patched; Scap: SREBP-cleavage activating protein; RNF145: RING finger protein 145; MARCH6: E3 ubiquitin-protein ligase; Smo: Smoothened; SREBP: sterol regulatory element-binding protein; SRE: sterol regulatory element.

### **Cholesterol transporters**

The SSD-containing proteins classified as cholesterol transporter are bigger and mobile proteins, still implicated in cholesterol homeostasis but also cellular signaling (Wu et al., 2022). SSD-containing cholesterol transporters regroup the NPC1, Patched (Ptch1) and Dispatched (Disp1) proteins, and their respective homologs. The conserved core structure of these transporters comprises 12 TMs that organize in two repeats, namely SSD and SSDL (SSD-like), which exhibit C2 pseudosymmetry around an axis perpendicular to the membrane (Gong et al., 2018, Gong et al., 2016, Qi et al., 2018). A large extracellular or luminal loop is found between the TM1 and TM2 of each domain, which is also similar across the SSD and SSDL. Interestingly, the conserved TM core of SSD cholesterol transporter proteins share high similarity with the TM core structure of the bacterial multidrug-resistance transporters in the resistance/nodulation/division (RND) family (Murakami et al., 2002). At the functional level, NPC1 is involved in cholesterol homeostasis pathway as a lysosomal cholesterol transporter, while Ptch1 and Disp1 are part of the Hh signaling pathway (Kuwabara and Labouesse, 2002, Wu et al., 2022). Despite their different biological functions, the mechanistic activity and subsequent function of SSD-containing cholesterol transporters are mediated by the SSD-induced cholesterol transport (Wu et al., 2022). Although they are structurally similar, SSDL remains nearly rigid in all contexts while the SSD display substantial flexibility in its conformation, which partially underlies its sterol transporter activity (Wu et al., 2022). The transport path within the SSD of these cholesterol transporter has been elucidated for Ptch1 and NPC1. Structural evidence suggests that cholesterol transport occurs from the an SSD shoulder site (SSD cavity) and tunnels through the membrane to the extracellular upper site, but the exact mechanistic aspects differ between Ptch1 and NPC1 (Gong et al., 2018, Zhang et al., 2018, Gong et al., 2016, Qi et al., 2018). In Ptch1, the cholesterol transport activity may be coupled to Na<sup>+</sup> transmembrane gradient as it is required for Ptch1 function (Myers et al., 2017). The essential role of SSD for cholesterol transport activity was further determined by the identification of key amino acid residues (Gong et al., 2018, Zhang et al., 2018) and pathogenic mutations in this domain, which abolished cholesterol transport for both NPC1 and Ptch1 (Qian et al., 2020, Zhang et al., 2018). Given the high sequence and putative structure similarity of the patched-related Ptchd1 protein to both Ptch1 and NPC1, it has been proposed that Ptchd1 also exert its biological function through SSD-mediated cholesterol transport.

Despite their size and functional differences, all SSD-containing proteins share structural similarities in their SSD and other extracellular or luminal domain (Wu et al., 2022). In conclusion, the SSD is an essential domain for the function of all SSD-containing proteins. The SSD directly interacts with cholesterol for sensing or transport purposes and subsequently underlies protein function and regulation.

## 1.4 Cholesterol metabolism in neurological disorders

Cholesterol is an essential lipid component of mammalian membranes and is also involved in cellular signaling as a precursor of numerous signaling molecules such as steroid hormones. Cholesterol plays an important role in the CNS, both during development and throughout life (Martin et al., 2014). The brain is the most cholesterol-rich organ of the body with 23% of total cholesterol content found in this organ that represents only 2% of the total body mass (Dietschy and Turley, 2004). Cholesterol homeostasis in the body relies mainly on dietary cholesterol uptake, *de novo* synthesis and lipo-protein-mediated transport in the blood circulatory system. However, due to the low permeability of the blood-brain barrier (BBB) to cholesterol-loaded lipoproteins, brain cells are cut-off from peripheral cholesterol homeostasis and rely almost exclusively on *de novo* synthesis, but do excrete cholesterol in the form of 24-hydroxycholesterol (24-OHC) back to the peripheral blood circulation to be metabolized by the liver. Brain cholesterol homeostasis involves high levels of inter-cellular cholesterol exchange, particularly between neuronal and glial cells (Pfrieger and Ungerer, 2011). In all cells, cholesterol homeostasis is a tightly regulated pathway with an intricate feedback mechanism to balance cholesterol synthesis, import and export. Alterations in cellular cholesterol levels can trigger a number of pathogenic effects, especially in the brain. Indeed, high brain cholesterol levels have been implicated in aging-related cognitive decline and several neurodegenerative disorders such as Alzheimer's and Parkinson's diseases (Kadish et al., 2009, Li et al., 2022). On the other end, low brain cholesterol levels during development were linked to neurodevelopmental disorders (Kanungo et al., 2013, Esposito et al., 2021). In this section, I will describe in details the mechanisms of cholesterol homeostasis in the brain. I will then discuss the link between cholesterol homeostasis and neurological disorders, with a particular focus on NDDs. Lastly, I will introduce the technical methods for investigation of cholesterol levels in the brain.

### 1.4.1 Cholesterol metabolism in the brain

In the presence of an intact BBB, the brain is isolated from the peripheral cholesterol homeostasis pathway. Therefore, it relies on *de novo* synthesis and an intricate exchange of cholesterol between different cell-types. The following part will detail how cholesterol homeostasis is maintained in the brain as well as the function of cholesterol in various cell populations.

#### ***Neuron-astrocyte cholesterol exchange***

In the brain, neurons and astrocytes are the main players in cholesterol homeostasis. Indeed, astrocytes are the primary source of cholesterol synthesis while neurons are responsible for cholesterol excretion due to their unique expression of the cytochrome P450 oxidase Cyp46a1 enzyme, which converts cholesterol into 24-OHC. Mammalian cells can synthesize cholesterol from the acetyl coenzyme A precursor through a complex series of reaction catalyzed by more than 20 enzymes and requiring energy and molecular oxygen (Gaylor, 2002). A feedback mechanism regulates the rate of cholesterol synthesis through cholesterol-sensing transcription factors in membranes, namely the sterol regulatory element-binding proteins (SREBPs) who control the transcription of genes encoding cholesterol synthesis enzymes and lipoprotein receptors (Brown and Goldstein, 1999). Cholesterol synthesis rates are highest during the second week of postnatal development with variation across brain regions. During this developmental period, neuronal *de novo* cholesterol synthesis is required for cell survival and neurite outgrowth (Fünfschilling et al., 2012). However, adult neurons have significantly decreased levels of cholesterol synthesis and rely mainly on astrocyte-derived cholesterol import (Pfrieger and Ungerer, 2011). In astrocytes, newly generated cholesterol is loaded onto ApoE vesicles and secreted for neuronal up-take, through the ATP binding cassette transporter (Abca1)-mediated lipidation and secretion. Neuronal cells receive unesterified cholesterol by the low-density lipoprotein receptor-related protein 1 (Lrp1)-mediated endocytosis into the endosomal/lysosomal system. The lysosomal cholesterol transporters NPC1 and NPC2 are then responsible for cholesterol exit from this cellular compartment to reach its final intended destination in other cellular membranes, in particular the plasma membrane of dendrites and axons. Excess of cholesterol can be either stored intracellularly in lipid droplets after esterification or eliminated by conversion into the 24-OHC metabolite, which is secreted out of neuronal cells into the bloodstream by the Abca1 transporter (Pfrieger and Ungerer, 2011). The **Figure 6A** illustrates the mechanisms of intracellular cholesterol metabolism while **Figure 6B** demonstrate the cholesterol homeostasis collaboration between neurons and astrocytes and other brain cell populations (adapted from Martin et al., 2014). Loss-of-function of any

component of this cholesterol homeostasis pathway results in a wide-range of cholesterol-related neurological disorders (Martin et al., 2014). However, neuronal *de novo* cholesterol synthesis is required during development and may impact adult neuronal processes but is not essential for synaptic functions (Fünfschilling et al., 2012). Lrp1 expression in neuronal cell is indeed required for correct synaptic functions (Liu et al., 2010), highlighting the crucial intake of astrocyte-derived cholesterol for proper neuronal activity.

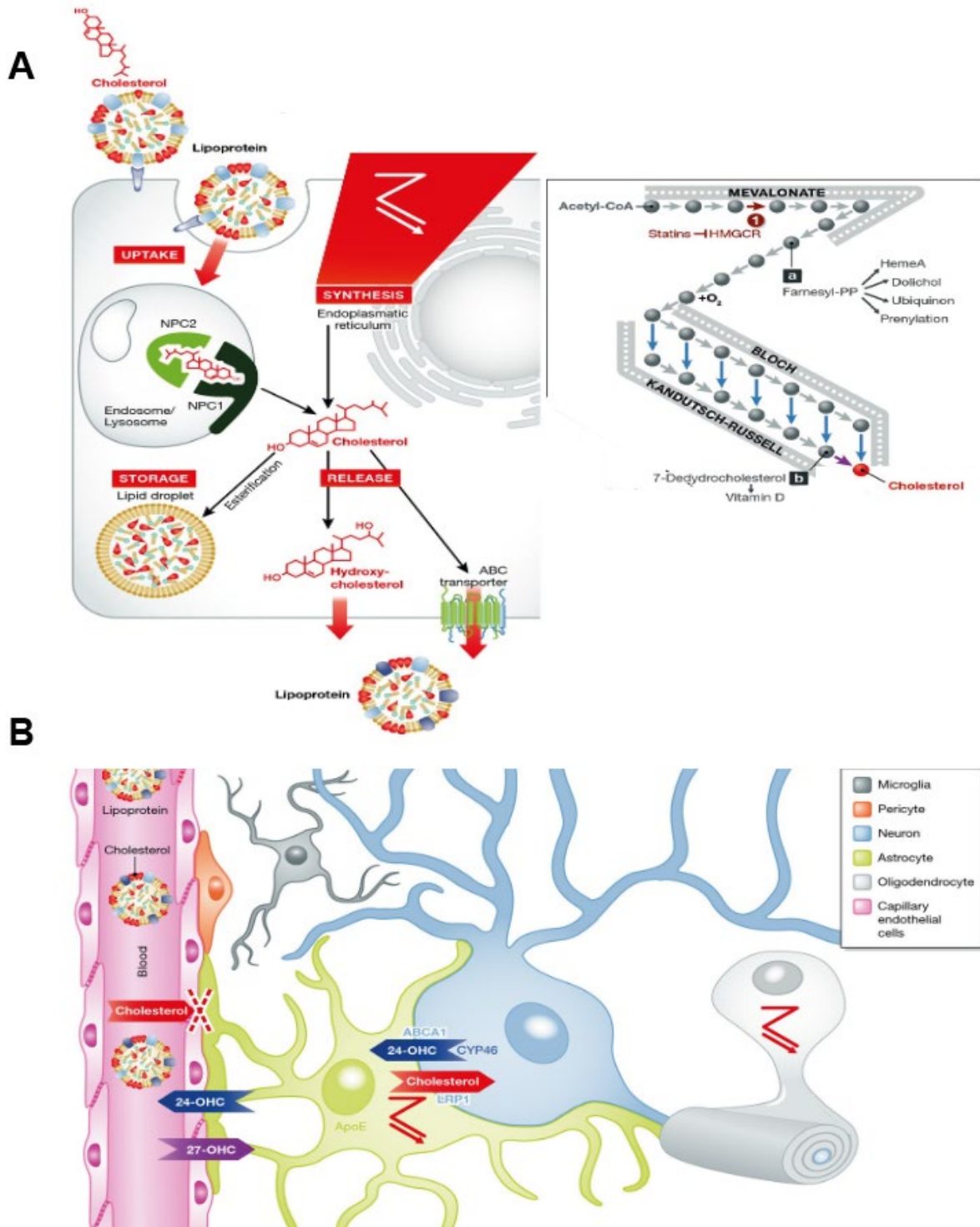


Figure 6: Cholesterol metabolism and transport in the brain.

Adapted from Martin et al., 2014

**(A)** Schematic representation of cellular cholesterol metabolism from uptake to excretion, with a simplified summary diagram of the cholesterol synthesis enzymatic chain reactions on the left. *Hmgcr*: hydroxy-3-methylglutaryl-CoA reductase; *NPC1/2*: NPC intracellular cholesterol transporter 1/2. **(B)** Illustration of the brain cholesterol homeostasis with an emphasis on the interplay between different cell populations. Cellular cholesterol synthesis is indicated by the zagged pathway symbol. Neurons may import cholesterol from astrocyte-derived APOE vesicles via lipoprotein uptake (*Lrp1*) and reject surplus cholesterol in the form of 24-OHC, which is excreted via *Abca1* and which enters the blood circulation.

### **Essential roles of neuronal cholesterol**

Both neuronal and glial cells have a very high cholesterol content due to their extensive membrane surfaces. In neurons, synapses have large membrane amounts in both post-synaptic spines and pre-synaptic vesicles, which are enriched in cholesterol (40%mol) compared to the other neuronal membranes (Takamori et al., 2006). Cholesterol is not uniformly distributed within cellular membranes and a “cholesterol” gradient can be defined across cellular compartments. Indeed, the plasma membrane displays the highest cholesterol levels (30%mol), particularly in the cytoplasmic inner leaflet (Mondal et al., 2009), the endosomal/lysosomal system has slightly lower levels (30-20%mol) while other intracellular membranes have significantly lower cholesterol concentrations (Golgi apparatus: 15%, mitochondria: 8% , ER: 2%, nucleus: 1-2%). Moreover, the plasma membrane contains microdomains enriched in cholesterol termed lipid rafts. These cholesterol-rich domains are thought to be dynamic membrane platforms enriched at synaptic sites, where many receptors and signaling proteins converge for correct functioning and signal responsiveness (Lingwood and Simons, 2010). Ample evidence was uncovered which supports the notion that cholesterol is a major regulator of neuronal activity and synaptic transmission, potentially through its enrichment at lipid rafts.

At the pre-synapse, cholesterol is considered an organizer of synaptic vesicles (SVs) and is necessary for efficient SVs exocytosis and subsequent neurotransmitter release at the synaptic cleft. As a major SVs component, cholesterol mediates the intrinsic negative curvature of membranes necessary for the fusion process. Cholesterol also interacts with the SV protein synaptophysin (Thiele et al., 2000) and clusters the SNAREs protein family at fusion-competent sites in lipid rafts, which are necessary for correct SNARE function (van der Bogaart et al., 2013). Cholesterol depletion consequently results in a dose-dependent decrease of the rate and kinetics of SVs fusion (Thiele et al., 2000). This is accompanied by impairment in SVs exocytosis (Linetti et al., 2010) and pre-synaptic plasticity events (Kudinov et al., 2006), as well as a significant reduction of calcium-evoked neurotransmitter release from synaptosomes (Chamberlain et al., 2001). Reversely, cholesterol supplementation is able to increase pre-synaptic transmitter release *in vitro* (Mauch et al., 2001, Göritz et al., 2005).

Post-synaptically, cholesterol is necessary for synaptic organization by the partitioning of several ion channels and receptors in lipid rafts. The most telling example is the NMDA receptor localization at post-synaptic lipid rafts, which may facilitate their oligomerization and subsequent functioning (Allen et al., 2007). Cholesterol supplementation or depletion affects NMDA-induced long-term depression (LTD), improving it (Martin et al., 2014) or impairing it (Frank et al., 2008) *in vivo* respectively, which in turn affected memory formation and consolidation. Studies have also identified 24-OHC, the cholesterol excreted metabolite, as a potent allosteric NMDA receptor modulator able to restore long-term potentiation (LTP) and the related cognitive deficits in rodents treated with NMDA receptor blockers (Paul et al., 2013). The AMPA receptors can also be found to cluster in lipid rafts and *in vivo* cholesterol depletion triggers AMPA receptor accumulation at the cell surface due to decreased lateral mobility and impaired endocytosis (Martin et al., 2014). The subsequent altered internalization of AMPA receptors causes learning and memory impairments. Acetylcholine receptors (AChR) are also localized to lipid rafts and their organization are regulated by cholesterol levels due to the presence of cholesterol-binding motifs in their sequence (Sharp et al., 2019, Baier et al., 2011), unlike both NMDA and AMPA receptors where cholesterol interaction and regulation may be indirect. Cholesterol levels control the internalization rate, clustering properties and ion channel kinetics of AChR (Barrantes, 2007), which may impact short-term memory formation (Pfeiffer et al., 2020). *In vitro* and *in vivo* evidence suggests that astrocyte-derived ApoE particles, amongst others astrocytic substances, are necessary for the formation, maturation and maintenance of synapses (Shan et al., 2021). Furthermore, it has been shown that ApoE vesicles contain vectored miRNAs, which extensively bind to the 3'UTR of cholesterol synthesis genes in neurons. Consequently, cholesterol synthesis is decreased in neuronal cells leading to acetyl coenzyme A accumulation in the nucleus, which triggers histone acetylation and transcription of immediate early genes and genes involved in memory formation. Therefore, astrocytes do not only provide cholesterol and other metabolic substances to neurons but actively regulate in neuronal function. To conclude, these findings highlight the importance of cholesterol homeostasis as a potent regulator of neuronal activity and synaptic function.

### ***Microglia, oligodendrocytes and myelin***

As illustrated in **Figure 6B**, other brain cells play a part in CNS cholesterol homeostasis including microglia and oligodendrocytes. Microglia are the brain innate immune cells (macrophages), which are in close proximity to neurons in order to serve support and clearance functions. Aside from removal of cellular debris, microglial cells are regulators of synaptic function and plasticity as well as adult neurogenesis (Parkhurst et al., 2013, Wang et

al., 2020). Microglia are also responsible for the non-enzymatic phagocytosis-mediated clearance of cholesterol (Cantuti-Castelvetri et al., 2018) while also require exogenous cholesterol for cell survival and maintenance of their phagocytic activity (Bohlen et al., 2017). Microglial exogenous cholesterol up-take is performed by the Triggering receptor expressed on myeloid cells 2 (Trem2), a lipid receptor mediating the endocytosis of cholesterol-loaded ApoE vesicles (Yeh et al., 2016). Trem2 is also responsible for demyelination-induced cholesterol clearance, by sensing lipid components of myelin and promoting myelin debris removal through lipid transport and catabolism (Poliani et al., 2015). Loss-of-function of Trem2 has been linked to learning and memory impairments as well as Alzheimer's disease pathology (Kim et al., 2017, Qin et al., 2021). Taken together, microglial cells rely on cholesterol for phagocytic activity but also dynamically react to cholesterol homeostasis alterations via Trem2 lipid-sensing capabilities and subsequent protective microglial responses.

Oligodendrocytes also play an important part in brain cholesterol homeostasis by producing cholesterol-rich myelin for axonal sheathing, thereby regulating neuronal function. Cholesterol is a major structural component of myelin but is also required for myelin growth and subsequent axonal enwrapping (Mathews and Appel, 2016). Remarkably, myelin is comprised of approximately 70% lipids – mainly cholesterol, and 30% proteins, and it is estimated that up to 70% of total brain cholesterol is in myelin (Björkhem and Meaney, 2004). Myelination of axons, which is the repetitive wrapping of oligodendrocytic plasma membranes around an axon, is essential for rapid impulse transmission along the axonal length. High cholesterol concentration in myelin induces a reduction in ion permeability (high resistance and low conductance) enabling the downward current propagation along the axon rather than diffusion across the membrane (Snipes and Suter, 1998). To produce the large cholesterol amounts for myelination, oligodendrocytes display increased levels of *de novo* cholesterol synthesis during myelination, which are maintained by a positive feedback mechanism (Voskuhl et al., 2019, Mathews and Appel, 2016). Cholesterol activates the PI3K/Akt/mTOR signaling pathway, potentially through its interaction with other myelin proteins in myelin-specific rafts signaling platforms (Saher et al., 2005), leading to the activation of SREBP transcription factor and subsequently increasing cholesterol synthesis gene expression (Mathews et al., 2014). Under specific circumstances, such as myelin diseases or chronic demyelination, neuron-derived cholesterol may participate to the remyelination process by promoting oligodendrocyte progenitor cells proliferation (Berghoff et al., 2021). Surprisingly, astrocyte-derived cholesterol cannot serve as an alternative cholesterol source for remyelination (Itoh et al., 2018). These results suggest that oligodendrocytes do not only rely on *de novo* cholesterol synthesis but also on cholesterol exchanges with other cell type including neuronal cells, highlighting once again the importance of inter-cellular cholesterol transfers and brain cholesterol homeostasis.



## 1.4.2 Cholesterol implications in diseases

Brain cholesterol homeostasis is a complex and inter-connected balance between *de novo* synthesis, lipoprotein-mediated cholesterol transfer and cholesterol turnover at the inter- and intra-cellular levels. Due to the pleiotropic effects of cholesterol on neuronal activity and synaptic functions, alterations in cholesterol homeostasis results in a wide-range of neurological disorders. Ample evidence has now demonstrated the impact of impaired cholesterol metabolism in the context of neurodegenerative diseases, particularly in Alzheimer's disease (Varma et al., 2021). Changes in cholesterol homeostasis are also observed in other pathologies, such as stroke, head trauma and aging (Martin et al., 2014). Indeed, age-dependent loss of cholesterol was observed in the human brain (Porter and Herman, 2011, Svennerholm et al., 1991), which may participate to the cognitive decline and memory impairments observed in normal aging. In this section, I will focus on the reported alterations of cholesterol homeostasis in the context of neurodevelopmental disorders, particularly ASD and ID. The Niemann-Pick disease type C would be a valid example of cholesterol-related NDD pathology, but has been thoroughly discussed in a previous introduction section and will therefore not be mentioned here.

### **SLOS**

The Smith-Lemli-Opitz syndrome (SLOS) is a rare autosomal recessive NDD that perfectly illustrates the importance of cholesterol homeostasis for normal neurodevelopment and brain function. Originally described as a multiple malformation syndrome (Smith et al., 1964), SLOS patients exhibit a wide-range of systemic and neurological phenotypes due to impaired function of the 7-dehydrocholesterol reductase enzyme (*7dhcr*) induced by mutations in the corresponding gene (De Barber et al., 2011). *7dhcr* is the last enzyme in the Kandutsch-Russell cholesterol synthesis pathway, catalyzing the 7-dehydrocholesterol to cholesterol reaction. Disease severity correlates with the degree of enzymatic function impairment, with complete loss resulting in fetal or newborn death due to multiple organ failure and malformations. Milder cases display numerous systemic symptoms such as facial and cranial malformations, genital abnormalities, limb malformations, gastrointestinal problems, liver disease and cardiac defects (Nowaczyk and Irons, 2012). At the behavioral level, SLOS patients frequently exhibit NDD-associated symptoms and co-morbidities. Namely, global developmental delay, language impairment, self-harm and repetitive stereotyped movements, sleep disturbances, sensory alterations and irritability are frequently reported in SLOS individuals, which are consistent with ASD and ID phenotypes (Diaz-Stransky and Tierney, 2012, Ryan et al., 1998). Indeed, most SLOS patients are diagnosed with intellectual disability

(moderate to severe) and also meet the criteria for ASD diagnosis (Sikora et al., 2006). The reduction in brain cholesterol levels is described as the cause of SLOS pathology. Decreases down to 2% of normal plasma cholesterol concentration were observed in severe SLOS cases along with low cholesterol amount in all organs and especially in the brain (Cunniff et al., 1997). Milder cases may have normal plasma cholesterol concentration due to dietary intake and remaining synthesis ability, but peripheral cholesterol cannot compensate for cholesterol loss in the brain given the BBB impermeability to lipoproteins. Moreover, dietary cholesterol supplementation does not rescue developmental and behavioral phenotypes (Sikora et al., 2006). The neurological symptoms in SLOS are likely caused by the reduced cholesterol levels in neuronal cells since, as described above, cholesterol largely impacts neuronal activity and synaptic functions. Low cholesterol concentration in membranes can also affect the sonic hedgehog signaling pathway essential for developmental processes, thereby accounting for some of the teratogenic and malformation defects observed in this disorder (Cooper et al., 1998, Koide et al., 2006). Accumulation of the 7dhr substrate and/or its oxidized metabolites may also play a role in SLOS pathophysiology (De Barber et al., 2011). To conclude, SLOS is neurodevelopmental disorder in which the neurological and systemic effects are causally related to cholesterol metabolism alterations, resulting in ASD and/or ID diagnoses therefore linking ASD and ID pathology to cholesterol homeostasis. Similarly, mutations in other enzymes of the cholesterol synthesis pathway also results in severe cholesterol alterations and NDD phenotypes such as developmental delay, ID and/or ASD, as observed in desmosterolosis (Dhcr24 deficiency), Squalene synthase deficiency, Lanosterol synthase deficiency and lathosterolosis (sterol C5-desaturase deficiency) disorders (Coman et al., 2020).

### ***Fragile X and Rett syndromes***

The association between cholesterol homeostasis and NDD pathology was made stronger by recent findings of cholesterol level alterations in patients with monogenic forms of ASD and ID, in which no cholesterol synthesis enzymes are mutated or impaired. Namely, cholesterol metabolism has been implicated in the pathophysiology of the Fragile X and Rett syndromes. Fragile X syndrome (FXS) is the most common inherited form of ID and leading genetic cause of ASD (Crawford et al., 2001). FXS is caused by the presence of over 200 repeats of a CGG expansion mutation in the promoter of the fragile X mental retardation 1 (*Fmr1*) gene resulting in hypermethylation and transcriptional silencing of this gene, which subsequently leads to decreased expression of the encoded fragile X mental retardation 1 protein (Fmrp) (Hagerman et al., 2017). Fmrp is a RNA-binding protein responsible for the regulation of translation, trafficking and stability of hundreds of target mRNAs (Penagarikano et al., 2007). In the brain, Fmrp acts as a negative regulator of many proteins involved in neuronal functions and synaptic

plasticity, such as the group I metabotropic glutamatergic receptors (mGluRs) and NMDA receptors (Darnell et al., 2011). Interestingly, *Fmrp* regulated targets also include cholesterol and lipid homeostasis mRNAs, such as several lipoproteins receptors (e.g. *Lrp1*), SREBPs and *Scap* transcription regulators (Darnell et al., 2011). Correspondingly, alterations in cholesterol and cholesterol-related metabolites plasma levels were reported in cohorts of FXS individuals, including a significant reduction of cholesterol, high- and low-density lipoprotein (HDL, LDL) concentrations (Berry-Kravis et al., 2015, Lisik et al., 2016). The observed plasma hypocholesterolemia seems to correlate with reduction of cholesterol levels in platelet lipid rafts of FXS patients (Toupin et al., 2022). Abnormal cholesterol distribution in membranes and disruption of lipid rafts in the brain may underlie the neurological impairments of FXS pathology, which remains a hypothesis to investigate although some lipid rafts alterations have already been reported in a FXS mouse model (Kalinowska et al., 2015). Interestingly, lovastatin treatment was shown to rescue some neurological and behavioural phenotypes in FXS mouse model (Muscas et al., 2019), and show promise in human clinical trials (Thurman et al., 2020, Champigny et al., 2021). Symptom alleviation following cholesterol-modulating drug treatment further highlights the importance of cholesterol homeostasis in the pathology of FXS.

Rett syndrome (RS) is a X-linked neurodevelopmental disorder, historically classified as part of the autism spectrum (ASD), characterized by impaired motor control and locomotor activity, cognitive deficits, language impairments, stereotyped movements, seizure disorders and intellectual disability (Kyle et al., 2018). RS is caused by mutations in the methyl CpG binding protein 2 gene (*Mecp2*) resulting in the encoded homonym *Mecp2* protein loss-of-function. *Mecp2* is a methyl DNA-binding protein implicated in gene repression by methylation-induced chromatin remodeling and transcription regulation in association with several co-factors (Chahrour et al., 2008, Castro et al., 2013). Similarly to FXS, the link between RS and cholesterol metabolism is not readily apparent, but RS patients were shown to possess elevated plasma cholesterol, HDL and LDL levels (Sticozzi et al., 2013). Moreover, dysregulation of cholesterol synthesis enzyme expression, including *Hmgcr* and *Sqle* (squalene epoxidase), was detected in the brain of RS mouse models resulting in decreased brain cholesterol synthesis (Buchovecky et al., 2013, Lopez et al., 2017, Pacheco et al., 2018, Lutjohann et al., 2018). Interestingly, RS mouse models also displayed increased blood cholesterol levels and lovastatin treatment or a suppressing mutation in the *Sqle* gene both significantly rescued the peripheral cholesterol profile, improved motor behaviours and overall life-span of *Mecp2*-null mice (Buchovecky et al., 2013). However, beneficial impact of lovastatin in RS needs to be further evaluated, as another study has failed to replicate the rescue phenotypes mentioned above (Villani et al., 2016). Taken together, these findings suggest that *Mecp2*, like *Fmrp*, may be involved in the regulation of cholesterol metabolism proteins at the

transcriptional levels and highlight the clear role of cholesterol homeostasis in NDD pathology.

As demonstrated in the three monogenic NDD forms mentioned above, alterations in cholesterol metabolism and homeostasis may be directly/indirectly implicated and underlie the neurological impairments observed in disease pathology. Notably, cholesterol homeostasis dysregulation has also been linked to non-syndromic form of ASD (Luo et al., 2020) suggesting that dyslipidemia and cholesterol-related phenotypes may be a useful biomarker and molecular research avenue for therapies in a large subset of ASD/ID patients. In addition to ASD and ID, cholesterol homeostasis may be involved in the pathology of other types of NDDs. Indeed, plasma/serum cholesterol levels have been linked to the severity of cognitive defects in schizophrenia as well as depression, impulsivity and violent behaviors (Maas et al., 2020, Krakowski and Czobor, 2011, You et al., 2013, Tomson-Johanson and Harro, 2018). It remains unclear if peripheral cholesterol levels simply reflect similarly altered CNS cholesterol levels or could directly affect brain cholesterol homeostasis due to impaired BBB function, but it can be used as a NDD biomarker. As a significant regulator of neuronal activity and synaptic function from early development throughout adulthood, it is not surprising that cholesterol homeostasis may underlie some of the pathogenic effects observed in several NDDs.

### **1.4.3 Tools for probing cellular distribution and dynamics of cholesterol**

There is an intricate interplay between brain cells contributing to overall CNS cholesterol homeostasis, as well as differences in intracellular cholesterol metabolism between cell types and across brain regions. Thus, it is essential to further define and assess cholesterol levels and distribution at the cellular level in a cell-type specific manner. This section will focus on the currently available methods for cholesterol detection in the brain, ranging from the conventional use of filipin to the newly developed D4H cholesterol sensors, and their applicability for cell-type specific study of brain cholesterol homeostasis.

#### ***Conventional cholesterol detection methods***

Multiple techniques can be used to quantify and visualize cholesterol *in vitro* and *in vivo*. Routinely, cholesterol levels can be quantified using the classical chemical modified Abell-Kendall method, fluorometric enzymatic assay based on the cholesterol esterase and oxidase enzymatic reactions, as well as gas or liquid chromatography and mass spectrometry (Li et al., 2019). The amount of cholesterol and other lipid species can also be determined in many

tissues by advanced mass-spectrometry techniques, which are referred to as lipidomic analysis (Giles et al., 2018). Although the depth of detection has greatly increased, lipidomic analysis has one major drawback for brain cholesterol determination in disease models. Given the large amount of myelin-associated cholesterol in the brain, any alterations in cholesterol levels from other cellular pools may be masked by over-represented myelin-associated cholesterol. Furthermore, the lack of cell-type specificity in lipidomic analysis prevents the dissection of cell-type specific cholesterol phenotypes, which as evidenced by the major differences in cholesterol metabolism between cell types is a major disadvantage. One possible alternative to circumvent this issue would be to isolate the cell population of interest by cell-sorting flow cytometry but this may lead to loss of material, particularly from axons and dendrites of neuronal cells, and biased lipidomic analysis. Therefore, albeit necessary for overall cholesterol content quantification in brain regions, current quantitative methods do not allow for the cell-type specificity needed in order to understand the cellular cholesterol homeostasis alterations in particular disease contexts.

Regarding cholesterol visualization in cells, filipin has been the most widely used tool for several decades (Butler et al., 1987). Filipin is an antibiotic and antifungal substance of the polyenes family, constituted of four macrolides with filipin III being the most abundant (Bolard, 1986). The antibiotic activity of filipin is based on the induction of structural disorders in sterol-containing membranes. Membrane permeation after filipin exposure leads to leakage of cellular component and eventually cell death. As a fluorescent polyene macrolide derived from *Streptomyces filipinensis*, filipin is used to visualize free cholesterol in cells and tissues. Although its spectroscopic properties are not advantageous (rapid bleaching, in brain sections high auto-fluorescence and light scattering of the short wavelength emitted light), filipin staining is still a prominent tool for probing cholesterol in biological membranes. Due to its cytotoxic effects, filipin can only be applied on fixed samples, which only enables visualization of steady-state cholesterol pools with no dynamic information. It is also worth mentioning that some studies have shown that not all sterol-containing membrane are labeled by filipin (Pelletier and Vitale, 1994, Steer et al., 1984, Severs and Simmons, 1983), which may question whether filipin staining correctly reflects cellular cholesterol distribution (Gimpl and Gehrig-Burger, 2007). To conclude, filipin can be a useful tool for visualization of cholesterol in the brain but present major disadvantages such as sub-optimal spectroscopic properties, required fixation and its potential artefacts, and lack of cell-type specificity. In order to bypass the limitations of filipin and assess cholesterol distribution at the cellular level, many studies have used fluorescent cholesterol analogs (FCA) such as dehydroergosterol, NDB-cholesterol and BODIPY-cholesterol. Due to their cholesterol mimicking properties and good spatial/temporal resolution, FCA were applied to study cholesterol distribution and trafficking in vitro and in vivo

and have yielded valuable insights into cellular cholesterol metabolism (Gimpl and Gehrig-Burger, 2007, Sezgin et al., 2016, Wüstner et al., 2016). However, FCA also presents several drawbacks for applications in the brain. Indeed, although FCA may reflect how cholesterol can be trafficked and distributed within cells, visualization still relies on exogenous application of cholesterol-like molecules, which may trigger hypercholesterolemia-related and/or artificial phenotypes. Furthermore, FCA delivery into the brain would not be technically easily achievable and will definitely lack cell-type specificity.

To summarize, many conventional methods are available for cholesterol quantification and visualization but all come with drawbacks for cell-type specific assessment of cholesterol distribution in the brain. Recently, perfringolysin O-derived cholesterol biosensors have been developed, which may provide the wanted tool for such a study.

### ***Perfringolysin O-derived D4H cholesterol probes***

Cholesterol-dependent cytolysins are produced by several bacteria as a defense mechanism against foreign organisms. Cytolysins are a large family of toxins that bind to cholesterol-containing membranes via a cholesterol-binding domain, spontaneously oligomerize to form aqueous pores and induce cytotoxicity (Tweten et al., 2001). Cholesterol alone is sufficient to induce cytolysin-binding to membranes in absence of any other lipid. *Clostridium Perfringens*, a Gram positive anaerobe bacteria, produces Perfringolysin O (PFO), a cytolysin that binds to cholesterol-containing membranes through its D4 cholesterol-binding domain. As expected, D4 domain alone was sufficient for cholesterol-dependent membrane binding (Rossjohn et al., 1997). Many transformations of the PFO toxin were applied for its use as a cholesterol reporter, such as non-toxic PFO (Das et al., 2013) and biotinylated PFO segment (Iwamoto et al., 1997), but we will focus on D4 domain mutations for the context of this work.

D4 is a 13KDa protein domain and the smallest PFO segment sufficient for cholesterol-binding without cytotoxicity (Ramachandran et al., 2002, Shimada et al., 2002, Heuck et al., 2007). D4 is located at the carboxyterminal part of PFO and organizes as a separate  $\beta$ -sandwich domain composed of two four-stranded  $\beta$ -sheets (**Fig. 7**). Cholesterol interaction by D4 is done only through the tips of the  $\beta$ -sheets, the rest of the domain does not enter into contact with cholesterol (Ramachandran et al., 2002). Visualization of the D4 probe is achieved by its fusion with fluorophores (GFP, mCherry) at either the amino- or carboxy-terminal ends. One major advantage of the D4 cholesterol sensor is that its small size (even with fluorophore fusion) allows for genetically-encoded expression via plasmid or viral vectors. Binding of D4 to membranes is dependent on the membrane cholesterol concentration but also sphingomyelin

content, which limits probe accessibility. The cholesterol concentration threshold for D4 binding is believed to be over 30%mol (Maekawa and Fairn, 2015) and therefore limits the use of D4 for intracellular membrane cholesterol distribution assessment. To circumvent this issue, D4-derived cholesterol probes have been developed through the introduction of several mutations, which resulted in varying cholesterol thresholds (Maekawa and Fairn, 2015, Liu et al., 2017).

One study identified the D434S mutation in the D4 domain as a cholesterol threshold-lowering mutation (Johnson et al., 2012), decreasing D4<sup>D434S</sup> binding (termed D4H, for D4 with Higher affinity) to 20%mol cholesterol-containing membranes. *In vitro*, cytosolically-expressed D4H was able to bind the inner leaflet of the plasma membrane (PM) while native D4 was not (Maekawa and Fairn, 2015), highlighting the necessary cholesterol threshold decrease for recognition and binding to inner PM. However, intracellular organelle membranes have even lower cholesterol levels, which prevents the use of D4H for cholesterol visualization, except in some lysosomal/endosomal (LY/E) vesicles that may be over 20%mol cholesterol-containing membranes. Therefore, additional mutagenesis of the D4 domain was performed to further decrease the cholesterol-binding threshold of the probe. Three other key amino acid residues were identified as determinant for D4H cholesterol affinity: Y415, Q433 and A463 (Liu et al., 2017). Liu et al. developed four new D4 mutants with different cholesterol thresholds: D434A (similar to D4H) 20%mol, D434/A463W 10%mol, Y415A/D434W/A463W (YDA) 3-2%mol and Y415A/Q433W/D434W/A463W (YQDA) 2-1%mol. Like the native D4, these mutants bind to cholesterol-containing membrane independently of the surrounding phospholipidic composition (Liu et al., 2017).

Given the wide range of sensitivity of these sensors, their combined use will prove very useful to study the cholesterol distribution in all membranes *in vitro* and *in vivo* (Maekawa, 2017), with D4H and D434/A463W for assessing PM and LY/E compartments whereas YDA and YQDA can evaluate the remaining intracellular organelle membrane (ER, mitochondria, etc.). Indeed, the fluorophore-fused D4-derived cholesterol sensors possess many of the needed properties for cell-type specific assessment of cholesterol distribution *in vitro* and *in vivo*: variable cholesterol sensitivity, possible genetic-encoding and therefore cell-specific expression, possible live imaging or detergent-free staining for endogenous cholesterol visualization. Many studies have made use of these cholesterol sensors for visualization of cholesterol distribution and trafficking under various physiological and pathogenic conditions, mainly *in vitro* (Wilhem et al., 2019, Lasic et al., 2019, Lim et al., 2019, Weiss et al., 2019, Koponen et al., 2019, Koponen et al., 2020). But relatively small number of *in vivo* and live imaging studies have been performed (Marek et al., 2020). However, some disadvantages also need to be taken into account such as endogenous fluorescence independently of cholesterol-binding, probe

aggregation when over-expressed resulting in possible artefacts, expression levels variability between cell preventing intercellular cholesterol levels comparisons. Moreover, not all cellular pools of cholesterol are accessible to probe binding. Regardless, D4H probes represent an important part of the experimental tool-kit to assess cholesterol transport and homeostasis.

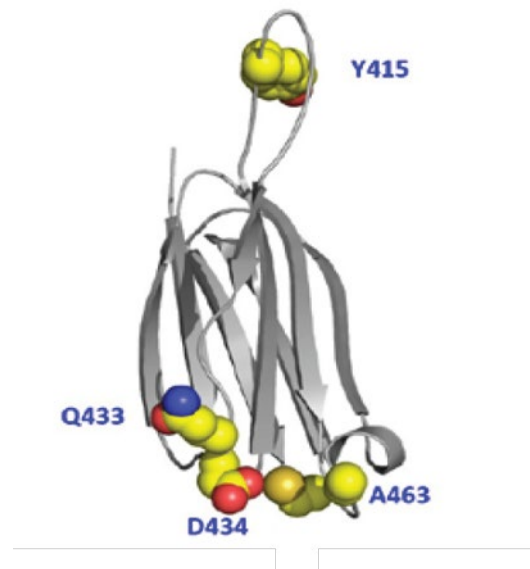


**Figure 7: PFO cholesterol-binding D4 domain structure and mutations.**  
From Maekawa, 2017

*Secondary structure organization of the isolated PFO-derived D4 domain. The amino acid residues, displayed as spheres on the structure (yellow: carbon, red: oxygen, blue: nitrogen), were targeted by mutagenesis for D4 cholesterol-binding threshold lowering (Liu et al., 2017). The one-letter code and respective amino acid position are indicated in blue. Y: tyrosine, Q: glutamine, D: aspartic acid, A: alanine.*



## 1.5 The dissertation project

Neurodevelopmental disorders, particularly ASD, are a group of heterogeneous and overlapping disorders with complex etiologies and a high societal burden. Many genetic and environmental risk factors have been identified leading to the implication of several cellular pathways in disease pathology, including synaptic function and transcription regulation (Delorme et al., 2013). The relatively unstudied cholesterol metabolism and homeostasis pathway has gathered interest in this field due to the reported cholesterol alterations in several monogenic and non-syndromic NDD forms (Martin et al., 2014). The main goal of this study was to evaluate the role of cholesterol homeostasis in NDD pathophysiology using two mouse models of monogenic forms of NDD: *Npc1*<sup>KO</sup> and *Ptchd1*<sup>KO</sup>. NPC1 and Ptchd1 are both transmembrane proteins containing a sterol-sensing domain (SSD) in their structure. NPC1 is a known lysosomal cholesterol transporter and its loss-of-function results in the Niemann-Pick type C disease, a NDD with known cholesterol accumulation phenotypes. However, relatively little is known about the cell-type specific effects of *Npc1*<sup>KO</sup> on cholesterol distribution in the brain. Ptchd1 has no defined biological function although it was proposed to act as in a similar manner to the Ptch1 cholesterol transporter. The secondary objective of this study was to define the biological role of *Ptchd1* and the pathological mechanisms induced by Ptchd1 loss-of-function.

In order to achieve these overarching goals, we define specific experimental aims, listed below:

- Adoption of D4H sensors for *in vivo* application,
- Examination of cell type-specific cholesterol distribution in brain regions of the *Npc1*<sup>KO</sup> and *Ptchd1*<sup>KO</sup> NDD mouse models,
- Examination of Ptchd1 protein sub-cellular localization and interacting partners.

The results are presented here in the form of a manuscript with additional data. The following discussion will be centered on remaining questions and future experimental directions:

- The challenges of uncovering the biological function of Ptchd1 and its downstream cellular pathway,
- The implications of whole-brain cholesterol distribution differences between cells and cell-types, and potential experimental methods,
- The importance of cholesterol homeostasis alterations in NDD pathophysiology and potential therapeutic interventions.

## ***2. Results***

## 2.1 Preface

The following result chapter represents the work of my PhD. First, the most advanced results, which were carried out in close collaboration with several people, are presented in a manuscript form. Individual contributions will be highlighted below. Supplementary experiments that were not included in the manuscript will be summarized in additional result sections and/or put into perspective in the discussion section.

This project was supervised by Prof. Dr. Peter Scheiffele who was involved in writing the manuscript. My PhD work was supported by the Fellowship for Excellence PhD Program, the CANDY initiative and AIMS2-TRIALS consortium.

### **Cell type-specific assessment of cholesterol distribution in models of neurodevelopmental disorders**

Charlotte Czernecki<sup>1</sup>, Shirley Dixit<sup>1</sup>, Sabrina Innocenti<sup>1</sup>, Caroline Bornmann<sup>1</sup>, Isabelle Riezman<sup>2</sup>, Howard Riezman<sup>2</sup>, Peter Scheiffele<sup>1</sup>

<sup>1</sup>Biozentrum of the University of Basel, Switzerland

<sup>2</sup>Department of Biochemistry and National Centre for Competence in Research in Chemical Biology, Sciences II, University of Geneva, Switzerland

*In preparation*

In this study, I performed some in vitro experiments in the HEK293T cell line as well as in vivo stereotaxic injections in both the *NPC1*<sup>KO</sup> and *Ptchd1*<sup>KO</sup> mouse lines. Following the in vivo injections, I performed the cutting, staining and imaging of some brain samples. Shirley Dixit also performed some in vivo stereotaxic injections, and subsequent cutting, staining and imaging in collaboration with Sabrina Innocenti. All image analyses and quantification was performed by myself.

Caroline Bornmann did all virus production and some in vitro experiments in HEK293T cells.

I performed sample collection and preparation of plasma and cerebellum in collaboration with Sabrina Innocenti, for plasma and lipidomic analyses. Lipidomic analysis was performed by Isabelle Riezman.

## **2.2 Cell-type specific assessment of cholesterol distribution in models of neurodevelopmental disorders**

### **ABSTRACT**

Most nervous system disorders manifest through alterations in neuronal signaling based on abnormalities in neuronal excitability, survival, and synaptic transmission. However, such neuronal phenotypes are frequently accompanied – or even caused – by metabolic dysfunctions in neuronal or non-neuronal cells. The tight packing and highly heterogeneous properties of neural, glial and vascular cell types pose significant challenges to dissecting metabolic aspects of neurodevelopmental disorders. Cholesterol and lipid homeostasis has recently emerged as key parameter associated with sub-sets of neurodevelopmental disorders. However, tools for tracking and visualizing endogenous cholesterol distribution in the brain have limited capability of resolving cell type-specific differences. We here develop tools for genetically-encoded sensors that report on cholesterol distribution in the mouse brain with cellular resolution. We apply these probes to examine sub-cellular cholesterol accumulation in two genetic mouse models of neurodevelopmental disorders, *NPC1* and *Ptchd1* knock-out mice. While both genes encode proteins with sterol-sensing domains that have been implicated in cholesterol transport, we uncover highly selective and cell type-specific phenotypes in cholesterol homeostasis. The tools established in this work should accelerate probing sub-cellular cholesterol distribution in complex tissues like the mammalian brain and enable capturing cell type-specific alterations in cholesterol flow between cells in models of brain disorders.

### **INTRODUCTION**

Neurodevelopmental conditions, including autism, are highly heterogeneous in their severity, phenotypic characteristics, and underlying mechanisms. This heterogeneity arises from diverse genetic, metabolic, and environmental factors that contribute to the etiology of the conditions. Consequently, therapies will need to be tailored specifically to the afflicted individuals, highlighting the importance of gaining deep insights into the origin and pathophysiology of these complex disorders (Sahin and Sur, 2015; van Karnebeek et al., 2016; Basilico et al., 2020). Previous work identified alterations in specific synaptic neurotransmitter receptor systems, neuromodulators, intracellular signaling pathways, and transcriptional regulators that arise from autism-associated mutations and that resemble candidate targets for interventions (Bhakar et al., 2012; Won et al., 2013; Sahin and Sur, 2015; Thomson et al., 2017; Asiminas et

al., 2019; Nakanishi et al., 2019; Hornberg et al., 2020). Lipid homeostasis is an additional, but comparably less deeply explored, process that – when perturbed - increases likelihood of neurodevelopmental conditions, including autism. There is a high incidence of autistic spectrum features in individuals with Smith-Lemli-Opitz syndrome (SLOS) with more than half of individuals meeting diagnostic criteria for autism (Tierney et al., 2001; Sikora et al., 2006). SLOS arises from loss-of-function mutations in the 7-dehydrocholesterol reductase (7dhcr), an enzyme that catalyzes the conversion of 7-dehydrocholesterol to cholesterol. Metabolically, SLOS is characterized by cholesterol insufficiency and accumulation of its dehydrocholesterol precursors. Notably, alterations in cholesterol homeostasis are more widely associated with neurodevelopmental disorders. Population-level differences in blood lipid profiles (LDL, total cholesterol, and triglycerides) were reported between individuals with ASD and matched controls (Tierney et al., 2006; Luo et al., 2020). Moreover, cholesterol alterations have been implicated in Fragile X Syndrome (Berry-Kravis et al., 2015) and Rett's Syndrome (Buchovecky et al., 2013), two monogenic syndromes where a substantial fraction of individuals meets diagnostic criteria for autism. Finally, neurodevelopmental assessment of children with Niemann-Pick Disease, a lysosomal storage disorder associated with elevation of cellular cholesterol levels, reported a high incidence of developmental delay in these children. Thus, defects in cholesterol homeostasis were hypothesized to play an important role in a sub-group of neurodevelopmental conditions and to contribute to the etiology of autism (Gillberg et al., 2017).

While blood lipid profiles are routinely analyzed in clinical practice, detecting altered cholesterol homeostasis in the brain is complicated by the localized synthesis and transport of cholesterol across sub-cellular compartments and cell types. The high cholesterol levels in the brain are achieved largely through local *de novo* synthesis (Pfrieger and Ungerer, 2011). Neuronal cells exhibit very low level of cholesterol synthesis. Instead, cholesterol synthesized in astrocytes is released in form of lipoprotein particles which are internalized by neurons through receptor-mediated endocytosis (Herz and Bock, 2002). Considering that lipoproteins are only poorly transported across the blood-brain barrier, measurement of peripheral cholesterol provides little information about brain cholesterol levels. Moreover, measurements in brain extracts are difficult to interpret with respect to cholesterol distribution across neuronal, astrocytic, microglial cells, and oligodendrocyte-derived myelin membranes. Thus, new approaches are needed to probe cholesterol homeostasis in the brain.

The development of genetically-encoded cholesterol sensors provided a major advance in probing cellular distribution and dynamics of cholesterol. These probes are based on domain 4 (D4) of the bacterial toxin perfringolysin O which binds to accessible pools of cholesterol in

cellular membranes (Das et al., 2013; Maekawa and Fairn, 2014). D4H derivatives exhibit a range of minimum cholesterol concentrations required for binding, such as derivatives D4H and YDA that are recruited to membranes containing 20%mol and 2%mol cholesterol, respectively (Maekawa, 2017). These probes provided important insights into cholesterol dynamics associated with synaptic plasticity in neuronal *in vitro* systems (Brachet et al., 2015; Mitroi et al., 2019). Here, we extended the use of such probes to the mouse brain. We generated a set of ratiometric cholesterol sensors to probe cholesterol distribution in a cell type-specific manner. We then demonstrate the utility of these probes for the quantitative assessment of cell type-specific alterations of cholesterol distribution in mouse models of neurodevelopmental disorders.

## RESULTS

### Alterations in regulators of sterol metabolism are associated with neurodevelopmental conditions

Genes involved in lipid regulation are enriched amongst deleterious variants that segregate with ASD in the population (David et al., 2016; Luo et al., 2020). To extend these observations specifically to cholesterol homeostasis, we used the GeneTrek tool (Leblond et al., 2021) to search for neurodevelopmental disorders associated with mutations in genes controlling cholesterol metabolism (89 genes, KEGG pathways hsa04979 and hsa00900; Table S1). We also searched for NDD-association of genes predicted to contain sterol-sensing domains (SSD) (13 genes, Table S1) (Kuwabara and Labouesse, 2002; Wu et al., 2022), a membrane domain contained in proteins involved in cholesterol biosynthesis (e.g. HMG-CoA reductase and 7-dehydrocholesterol reductase enzymes), intracellular cholesterol transport (NPC1), and cholesterol efflux involved in cell signaling (Patched-1, *Ptch1*). Notably, 20 of the 89 genes involved in sterol metabolism were classified as associated with epilepsy or neurodevelopmental disorders (**Fig. 1A**). When focusing on SSD proteins, four of the 13 genes are defined as risk genes: *NPC1*, *NPC1L1*, *Ptch1*, and *Ptchd1*. *NPC1*, *NPC1L1* and *Ptch1* encode proteins with cholesterol transporter functions. For *Ptchd1*, knock-out in mice results in behavioral and electrophysiological alterations (Wells et al., 2016; Tora et al., 2017; Ung et al., 2017). Moreover, loss of *Ptchd1* impairs cholesterol-dependent  $\mu$ -opioid receptor trafficking and function (Maza et al., 2022). This close association of NDD and cholesterol metabolism genes warrants further investigation to elucidate alterations in brain cholesterol homeostasis in NDD models.

## Adaptation of cholesterol sensors for in vivo applications

To investigate cholesterol distribution in the mouse brain, we adapted fluorescent D4H sensors for in vivo assessment of cell type-specific cholesterol levels. We combined the mCherry-fused sensors D4H and YDA with an equimolar eGFP normalizer through a T2A linker (**Fig. 1B**; D4H: eGFP-2A-mCherry-D4H and YDA: eGFP-2A-mCherry-YDA). To monitor overall membrane distribution (independently from cholesterol content) we created an analogous probe containing a myristoylation and palmitoylation site for membrane targeting Myr/Palm-mCherry-2A-eGFP (Myr/P). In transiently transfected HEK293T cells identified by cytoplasmic eGFP expression, the probes exhibited varying degrees of plasma membrane enrichment. D4H signal was highly concentrated at the plasma membrane (PM) with few (presumptive) endosomal structures marked. By contrast, the YDA signal was more widely distributed across intracellular membranes. The Myr/P signal was similar to the YDA pattern with the exception of a higher accumulation in perinuclear membranes. Line histograms of fluorescence intensity (see methods for details) confirmed the strong plasma membrane enrichment of mCherry-D4H whereas the eGFP signal derived from the T2A cleavage was abundant in the cytoplasm (**Fig. 1E**). By comparison, the YDA and Myr/P probes exhibit reduced plasma membrane enrichment due to their association with intracellular structures.

We then used stereotaxic injection of recombinant adeno-associated viruses (AAV9 capsid) to deliver the probes under control of the neuron-specific human synapsin promoter into the dentate gyrus of C57Bl6/J mice (**Fig. 2A**). 7-9 days following injection, probes were imaged in sections from perfusion fixed mice. Interestingly, D4H and YDA probes strongly labeled dendrites of dentate granule cells with only little probe signal detected in the granule cell somata (**Fig. 2B**). By contrast, cell somata located in the hilus (which mostly represent GABAergic interneurons) were strongly D4H and YDA-positive. Comparison to the eGFP normalizer as well as the Myr/P probe revealed that this was not a consequence of higher sensor expression in the hilar cells but rather a high abundance of cellular membranes within somata of these cells (**Fig. 2B**). In dentate granule cells, D4H signal was highly enriched in the plasma membrane with a small number of punctate somatic structures marked. Similar to the *in vitro* conditions, YDA and Myr/P signals exhibited less plasma membrane enrichment due to the increased association with intracellular structures (**Fig. 2C**). These experiments demonstrate the suitability of D4H-derived cholesterol sensors for analysis of neuronal cholesterol distribution in the mouse hippocampus.

### Visualization of neuron-specific cholesterol distribution in *NPC1*<sup>KO</sup> hippocampus

Considering that mutations in the SSD protein NPC1 are associated with neurodevelopmental disorders and alterations in cholesterol transport, we then used *NPC1*<sup>KO</sup> mice to validate the suitability of the probes to quantitatively capture alterations in cholesterol distribution *in vivo*. We expressed the D4H sensor in neurons of the dentate gyrus of 4 week old wild-type and *NPC1*<sup>KO</sup> (-/-) mice (**Fig. 3A**). *NPC1*<sup>KO</sup> mice displayed a strong accumulation of the D4H-positive puncta in neuronal somata. These puncta resemble cholesterol accumulation in lysosomes, a hallmark of Niemann-Pick Disease pathology. Increased puncta density as compared to control littermates was not due to alterations in sensor expression level or cell size as confirmed by comparable eGFP signal intensity and area (**Fig. 3B**). While a small number of D4H probe-positive puncta are observed in littermate control animals, there was a substantial increase in mean puncta density and size in dentate granule cell neurons of the *NPC1*<sup>KO</sup> mice (**Fig. 3B**, see methods for details on the quantification). Moreover, the frequency distribution of D4H puncta density and size was strongly shifted towards higher densities and areas, with a trend towards increased probe intensity observed for these structures (**Fig. 3C**).

### Normal intracellular cholesterol distribution in *Ptchd1*<sup>KO</sup> mice

*Ptchd1* knock-out mice represent a second NDD-model carrying a mutation in a sterol-sensing domain protein. In the mouse brain, *Ptchd1* mRNA is most highly expressed in neurons of the thalamic reticular nucleus, cerebellar granule cells, and in dentate granule cells of the hippocampus (Noor et al., 2010; Wells et al., 2016; Tora et al., 2017). To test whether loss of *Ptchd1* results in alterations in neuronal cholesterol distribution, we delivered the ratiometric D4H probes into the dentate gyrus of 4 week old male mice and compared membrane enrichment and intracellular structures between *Ptchd1*<sup>-/-</sup> mutant and littermate control animals. We detected no significant difference between genotypes in D4H probe recruitment to the plasma membrane or intracellular structures (**Fig. 4A-D**). This suggests that loss of *Ptchd1* from dentate granule cells is not associated with detectable changes in cholesterol levels or distribution in these cells.

Considering that *Ptchd1* is also expressed in non-neuronal tissues (Noor et al., 2010) and alterations in blood cholesterol levels have been reported in ASD patients (Tierney et al., 2006; Luo et al., 2020), we performed blood sampling from 6 day and 30 day old *Ptchd1*<sup>-/-</sup> and littermate control animals and quantified cholesterol, LDL, HDL, and triglycerides levels. Notably, we did not observe significant genotype differences in any of these parameters at both ages (**Fig. 4E**). Finally, no significant changes in overall lipid composition, including fatty acid chain length or saturation were observed using mass-spectrometry-based lipidomic analysis of



*Ptchd*<sup>-/-</sup> mutant brain samples (Fig. S1 and Supplementary Table 2). Taken together, these results suggest that deletion of the sterol-sensing domain protein Ptchd1 does not significantly alter cholesterol level and lipid metabolism in the mouse brain.

### **Selective targeting of sensors reveals cell type-specific differences in cholesterol distribution**

A major advantage of molecularly-encoded sensors is the ability to target them to genetically-defined cell populations. Considering the segregation of brain cholesterol synthesis and cholesterol turn-over between astrocytes and neuronal cells, respectively, we modified the AAV vectors for cell type-specific expression. Thus, we expressed the ratiometric D4H probe selectively in astrocytes of the dentate gyrus using a minimal GFAP promoter (*GfaABC1D*) (**Fig.5A**) (Lee et al., 2008). Cholesterol distribution in astrocytes *in vivo* differed from neuronal cells, with a significant accumulation of probe-positive structures in the astrocytic cytoplasm in wild-type mice (**Fig. 5B**). Interestingly, these astrocytic cholesterol-containing structures were not enlarged in *Npc1*<sup>KO</sup> mice, highlighting neuron-specific alterations in intracellular cholesterol distribution (**Fig.5c**). To further expand the range of cell populations that can be targeted with ratiometric D4H probes in mice, we further generated viral vectors for cre-recombinase dependent expression. We validated those vectors by selective expression in parvalbumin-positive interneurons in the mouse dentate gyrus (**Fig. S2**). In combination, these versatile tools should prove highly valuable to complement lipidomic and molecular studies providing cell type and sub-cellular resolution for assessment of cholesterol distribution *in vivo*.

## **DISCUSSION**

In recent years, mounting evidence has linked lipid – and more particularly cholesterol – metabolism alterations to neurodevelopmental disorders. Neuronal cholesterol is tightly balanced as both, increased or decreased levels are associated with disease states. As a key component of cellular membrane and membrane microdomains, cholesterol modulates ion channel function, signaling receptors, and synaptic vesicle release (Pfrieger, 2003; van den Bogaart et al., 2013; Ikonen and Zhou, 2021). For example, cholesterol is required for function of multiple GPCRs (Oates and Watts, 2011; Duncan et al., 2020), including the high-affinity state of the oxytocin receptor, a receptor centrally involved in the regulation of social behaviours (Gimpl and Fahrenholz, 2001). Consequently, disrupted cholesterol homeostasis has severe impact on brain function (Martin et al., 2014). A deeper understanding of cell type-specific alterations in cholesterol homeostasis associated with disease states might open up new therapeutic avenues, particularly, as cholesterol-modulating drugs are available.

D4-derived cholesterol sensors have been employed to map distribution of pools of cholesterol in cultured cells (Maekawa, 2017; Mitroi et al., 2019) and in *C.elegans* (Cadena Del Castillo et al., 2021). Here, we adapted those probes for cell type-specific use in the rodent brain. Combining ratiometric D4H- and YDA-based sensors with a cholesterol-independent membrane probe allows for normalization to probe expression and differences in intracellular membrane content across cell types. We demonstrate the utility of these probes to capture cholesterol distribution across brain cell types and to visualize cell type-specific cholesterol trafficking defects in the *NPC1<sup>KO</sup>* model. Interestingly, we observed highly divergent cholesterol distribution phenotypes in *NPC1<sup>KO</sup>* astrocytes and granule cells in the mouse dentate gyrus. While loss of NPC1 resulted in major intracellular trafficking defects in granule neurons, the probe-accessible pools in hippocampal astrocytes were unaltered. This observation is consistent with the proposal that anatomically-defined phenotypes can be rescued by neuron-specific re-expression of NPC1 protein (Lopez et al., 2011). The cre-recombinase-dependent sensors developed here should facilitate the dissection of cholesterol trafficking defects in additional cell types in the *NPC1<sup>KO</sup>* model, like microglia, where impaired lysosomal lipid trafficking, enhanced phagocytic uptake, and impaired myelin turnover have recently been reported (Colombo et al., 2021).

In contrast to *NPC1<sup>KO</sup>* mice, we did not detect significant alterations in the D4H-accessible cholesterol pool in *Ptchd1<sup>KO</sup>* animals. Moreover, overall sterol levels, lipid composition or acyl chain saturation in *Ptchd1* mutants were unchanged. This suggests that Ptchd1 protein is unlikely to have a major cholesterol transport function in mice. While NPC1 and Ptchd1 share sterol-sensing domains, they differ in key amino acid residues linked to transport function in the RND permease protein family. NPC1 and the sonic hedgehog receptor Ptch1, two SSD proteins with cholesterol transport function contain GxxxDD and GxxxE/D motifs in transmembrane domains 4 and 10, respectively (Gong et al., 2018; Zhang et al., 2018). Notably, in Ptchd1, these motifs are not conserved, similar to Scap another SSD protein (**Fig. S3**). Scap is involved in cholesterol biosynthesis regulation where it acts as cholesterol sensor (Brown et al., 2018). Notably, a recent study linked Ptchd1 and plasma membrane cholesterol to  $\mu$ -opioid receptor trafficking (Maza et al., 2022). Thus, it might be of interest to further investigate sterol-sensing and cholesterol-dependent trafficking functions of Ptchd1 in the future.

A subset of individuals with autism have characteristic dyslipidemia including cholesterol alterations, which can be identified by analysis of blood samples (Tierney et al., 2006; Luo et al., 2020). Initial trials in individuals with Fragile X have not supported therapeutic benefits from treatment with cholesterol lowering drugs. The approach developed in our work should enable

probing brain cholesterol distribution on a cellular level in models of brain disorders. Such an analysis should provide valuable information on forms of ASD, where a modification of cholesterol levels may hold promise for therapeutic intervention. Finally, alterations in cholesterol homeostasis are more widely implicated in brain pathology, including Alzheimer's Disease (Li et al., 2022). Thus, the virally-delivered probes developed in our work should accelerate capturing cell type-specific cholesterol distribution in the mammalian brain and enable tracking alterations in cholesterol flow across cell types in a wide-array of brain disorders.

**Acknowledgements.** We are grateful to all our collaborators for insightful comments on the manuscript, and for their advice. This work received funding from AIMS-2-TRIALS which are supported by the Innovative Medicines Initiatives from the European Commission. The results leading to this publication has received funding from the Innovative Medicines Initiative 2 Joint Undertaking under grant agreement No 777394. This Joint Undertaking receives support from the European Union's Horizon 2020 research and innovation programme and EFPIA and AUTISM SPEAKS, Autistica, SFARI. Moreover, the work has received funding from the European Union's Horizon 2020 research and innovation programme under grant agreement No 847818 (CANDY). The funders had no role in the design of the study; in the collection, analyses, or interpretation of data; in the writing of the manuscript, or in the decision to publish the results.

**Conflict of interest.** The authors have no competing financial interests in relation to the work described.

**Figure 1**

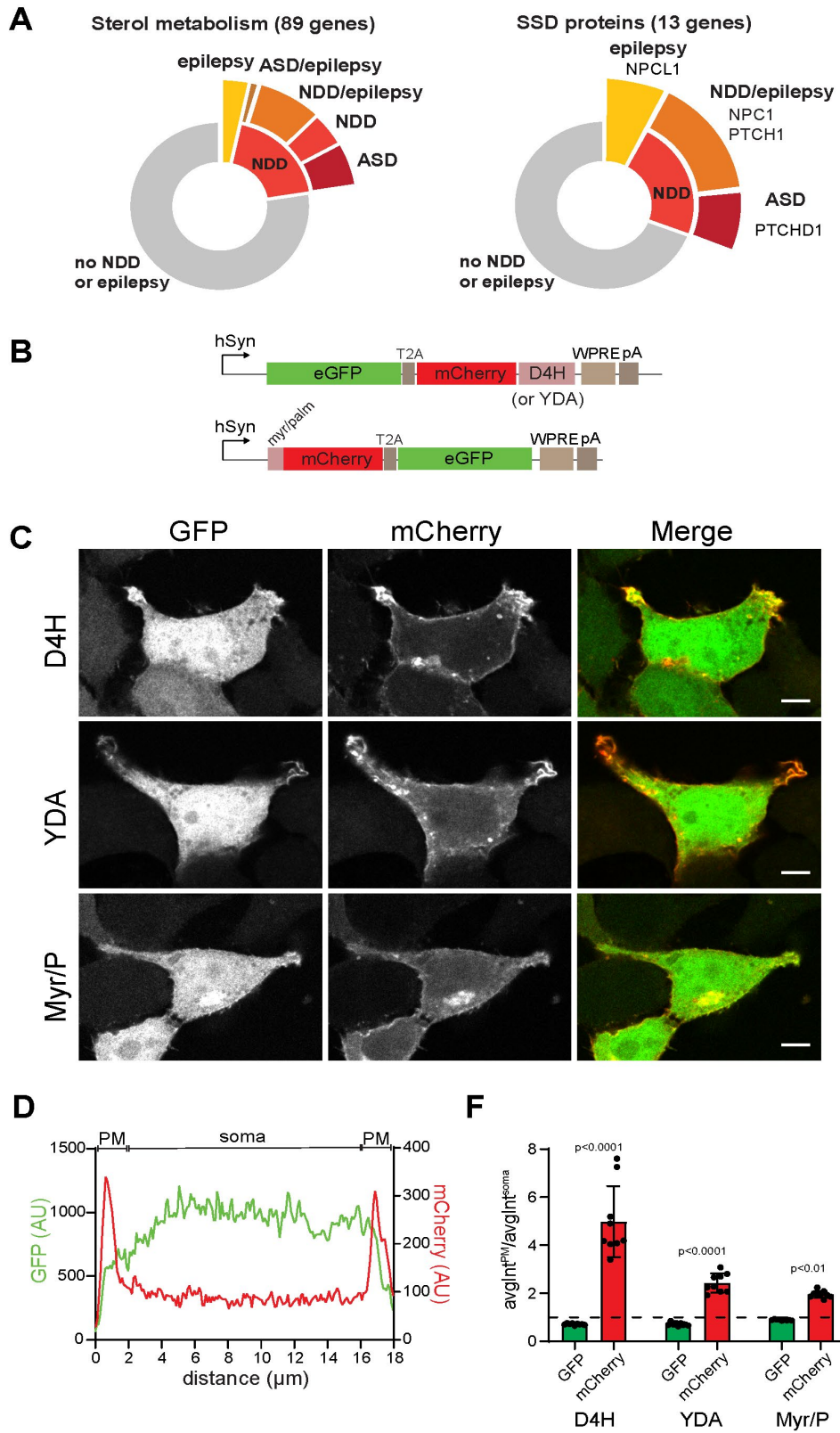


**Figure 1 : Adaptation of perfringolysin O-derived cholesterol probes for analysis of cholesterol distribution**

**(A)** Pie chart results from GeneTrek analysis of curated gene lists of sterol metabolism and sterol-sensing domain (SSD) proteins (89 and 13 genes respectively). GeneTrek is used to explore association of human genes with several neurodevelopmental disorders (NDD) including autism-spectrum disorders (ASD), intellectual disability (ID) and others. Some sterol metabolism genes as well as SSD proteins genes are neurodevelopmental disorders candidate genes including *NPC1*, *Ptch1* and *Ptchd1*. **(B)** Plasmid design of ratiometric D4H cholesterol probes under human synapsin promoter control. **(C)** Confocal images of HEK293T cells at 63X magnification, transfected with 200ng of Syn-eGFP-2A-mCherry\_D4H, Syn-eGFP-2A-mCherry\_YDA or Syn-Myr\_mCherry-2A-eGFP plasmids. Scale bar: 5 $\mu$ m. **(D)** Intensity line histogram of eGFP (green) and mCherry (red) signals across one HEK293T cell transfected with 200ng of Syn-eGFP-2A-mCherry\_D4H plasmid. Line width: 10 pixels. **(E)** Plasma membrane (PM) enrichment ratios of eGFP (green) and mCherry (red) for each cholesterol probe (D4H, YDA or Myr\_P) plasmid in HEK293T cells. PM enrichment is calculated from average peak maximum intensity (from two consecutive pixels) at PM divided by average soma intensity ( $\text{avgIntPM}/\text{avgIntsoma}$ ). Mean  $\pm$  SD, N=3 independent experiments, n=3 coverslips per condition (avg. 18 cells per coverslip), Ordinary two-way ANOVA with Tukey's multiple comparisons tests, with individual variances computed for each comparison.

**Figure 2**

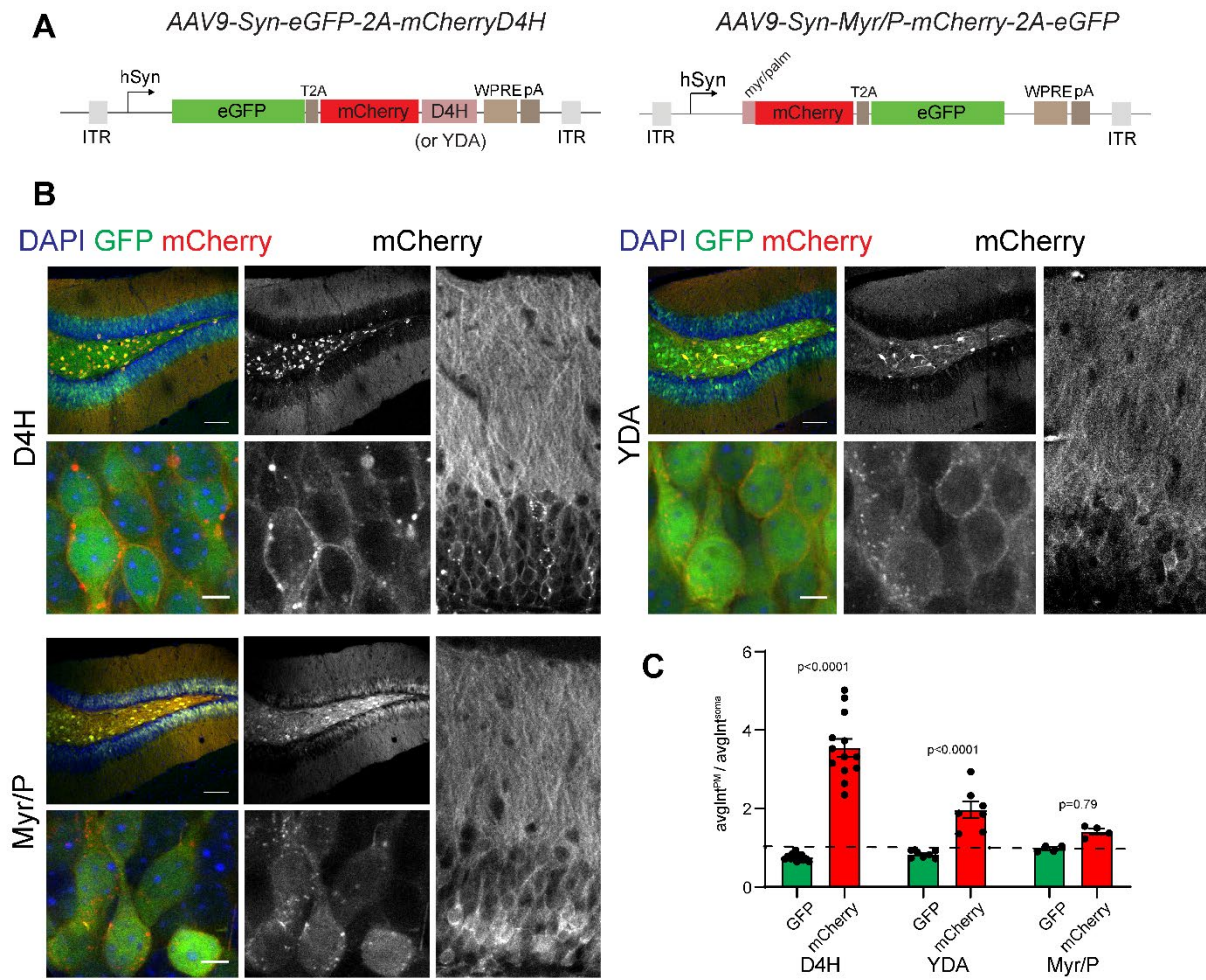


## Figure 2: Application of ratiometric D4H cholesterol probes in mice

**(A)** Virus design of ratiometric D4H cholesterol probes under human synapsin promoter control for neuronal expression. **(B)** Confocal images of 50 $\mu$ m coronal brain sections of injected P27-32 wild-type mice (C57B6/J background). Upper left panel: 10X magnification view of DG, scale bar: 100 $\mu$ m. Lower left panel: 63X magnification of granule cells (GC), scale bar: 10 $\mu$ m. Right panel: 20X magnification view of granule cell layer (GCL) and corresponding dendrites. **(C)** Plasma membrane (PM) enrichment ratios of eGFP (green) and mCherry (red) for each cholesterol probe (D4H, YDA or Myr\_P) virus in DG granule cells. PM enrichment is calculated from average peak maximum intensity (from two consecutive pixels) at PM divided by average soma intensity ( $\text{avgIntPM}/\text{avgIntsoma}$ ). Mean  $\pm$  SD, n=4-13 mice per condition (avg. 22 cells per mouse), Ordinary two-way ANOVA with Tukey's multiple comparisons tests, with individual variances computed for each comparison



**Figure 3**

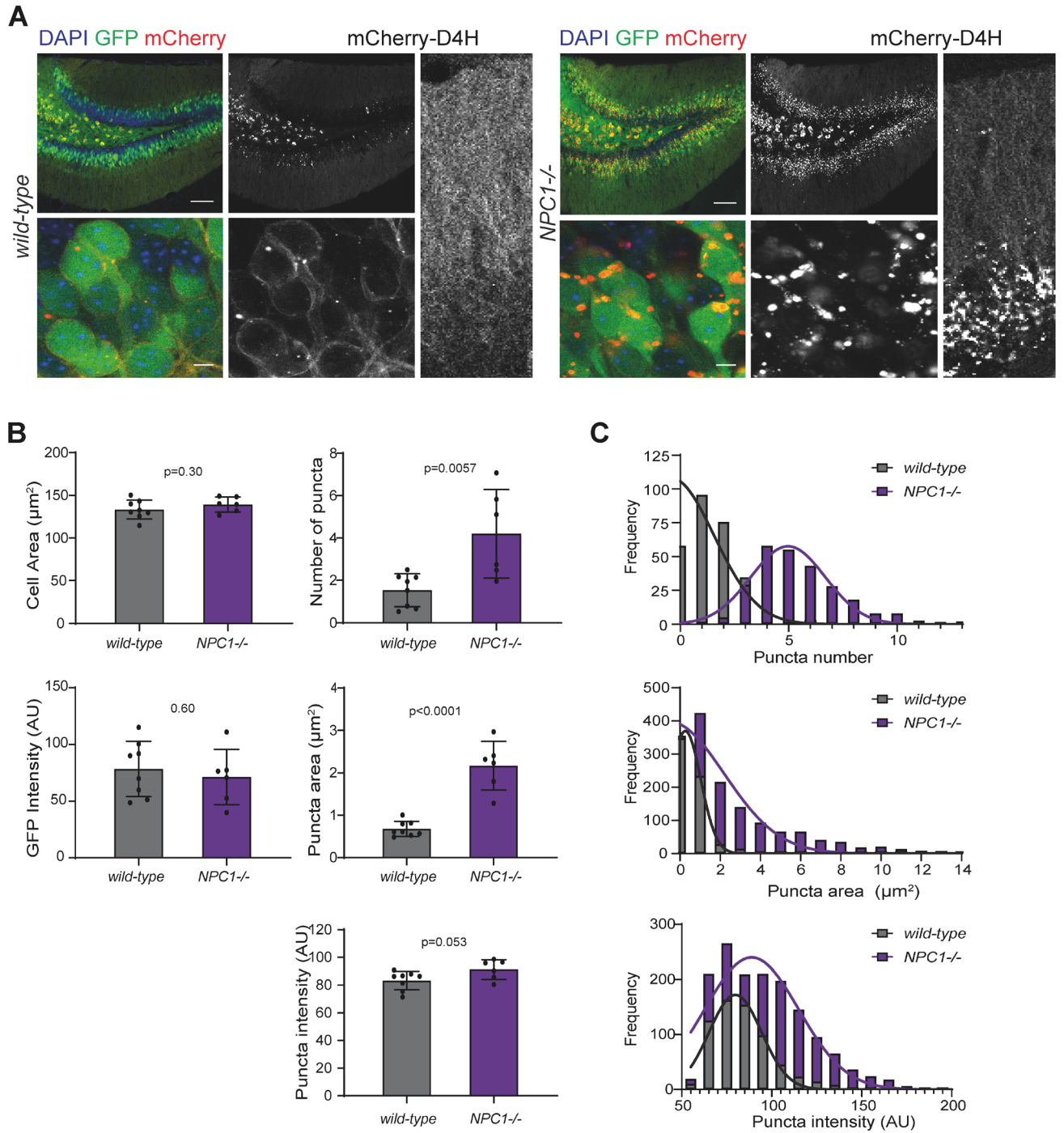




### Figure 3: Neuronal cholesterol distribution in *Npc1<sup>KO</sup>* mice

**(A)** Confocal images of 50 $\mu$ m coronal brain sections of injected P27-32 wild-type or knock-out (-/-) *NPC1* mice (BALB/c background). Upper left panel: 10X magnification view of DG, scale bar: 100 $\mu$ m. Lower left panel: 63X magnification of granule cells (GC), scale bar: 10 $\mu$ m. Right panel: 20X magnification view of granule cell layer (GCL) and corresponding dendrites. **(B)** Analysis of mCherry puncta in DG granule cells from *NPC1* wild-type and -/- mice. Each cell was manually traced and mCherry puncta (with an intensity threshold of 55 to exclude background noise) were computed in the defined cells. Subsequently, puncta smaller than 2 pixels (puncta area < 0.04  $\mu$ m<sup>2</sup>) were excluded from the analysis. Left graphs display whole cell parameters (cell area and eGFP intensity), right graphs display puncta parameters (avg puncta number per cell, avg puncta area and avg puncta intensity). Mean  $\pm$  SD, n=6-8 mice per condition (avg. 162 cells per mouse), unpaired Student's t-test. **(C)** Frequency distribution of puncta analysis parameters (number per cell, area and intensity) with Gaussian fit.

# Figure 4

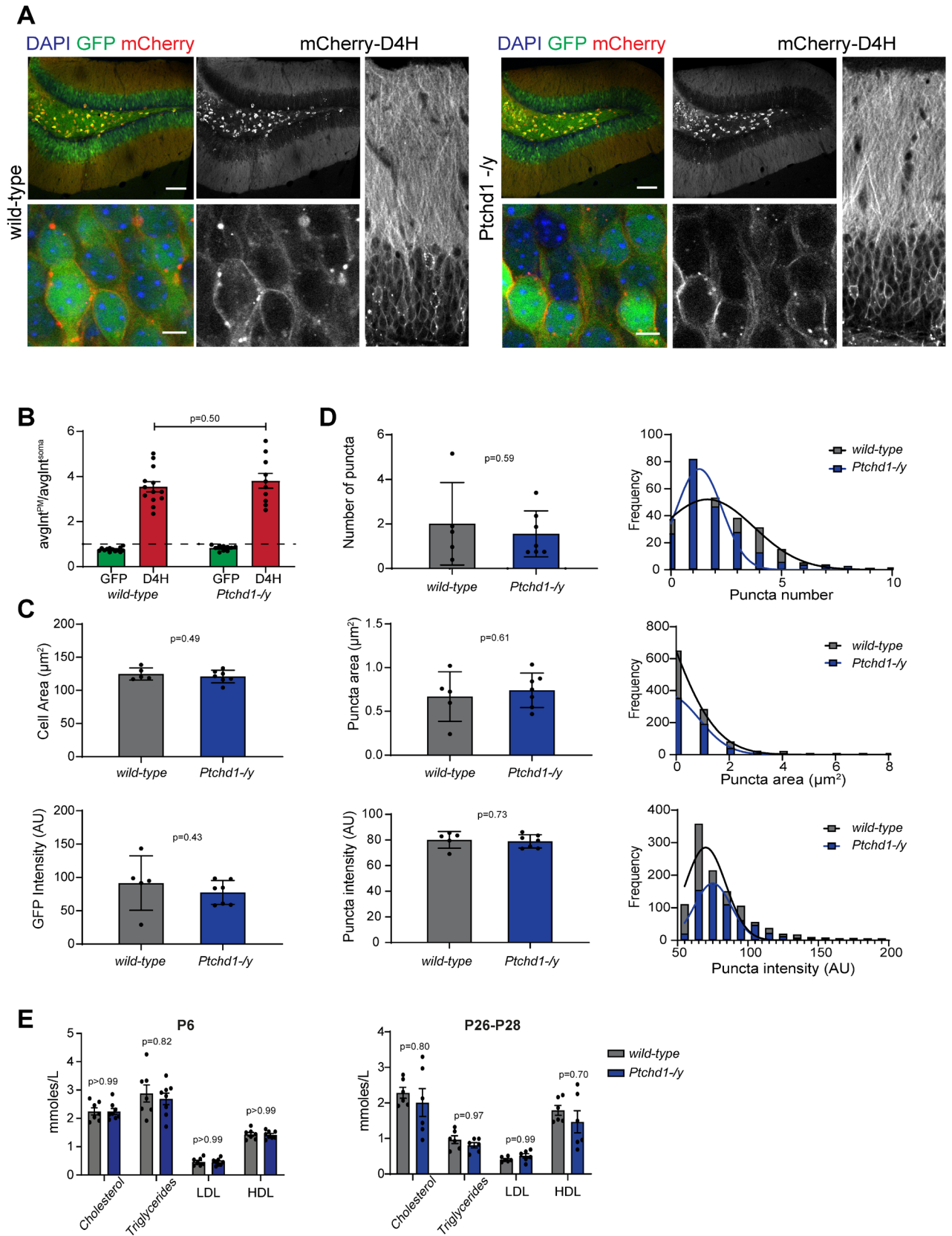


#### Figure 4: Neuronal cholesterol distribution in *Ptchd1*<sup>KO</sup> mice

**(A)** Confocal images of 50µm coronal brain sections of injected P27-32 wild-type or knock-out (-/y) *Ptchd1* mice (C57B6/J background). Upper left panel: 10X magnification view of DG, scale bar: 100µm. Lower left panel: 63X magnification of granule cells (GC), scale bar: 10µm. Right panel: 20X magnification view of granule cell layer (GCL) and corresponding dendrites. **(B)** Plasma membrane (PM) enrichment ratios of eGFP (green) and mCherry (red) in DG granule cells of injected wild-type and -/y *Ptchd1* mice. PM enrichment is calculated from average peak maximum intensity (from two consecutive pixels) at PM divided by average soma intensity (avgIntPM/avgIntsoma). Mean ± SD, n=10-13 mice per condition (avg. 45 cells per mouse), multiple unpaired Student's t-test with Holm-Sidak method for statistical significance determination. **(C)** Analysis of mCherry puncta in DG granule cells from *Ptchd1* wild-type and -/y mice. Each cell was manually traced and mCherry puncta (with an intensity threshold of 55 to exclude background noise) were computed in the defined cells. Subsequently, puncta smaller than 2 pixels (puncta area < 0.04 µm<sup>2</sup>) were excluded from the analysis. Left graphs display whole cell parameters (cell area and eGFP intensity), right graphs display puncta parameters (avg puncta number per cell, avg puncta area and avg puncta intensity). Mean ± SD, n=5-7 mice per condition (avg. 166 cells per mouse), unpaired Student's t-test. **(D)** Frequency distribution of puncta analysis parameters (number per cell, area and intensity) with Gaussian fit. **(E)** Plasma concentration of cholesterol-related metabolites from P6 or P30 *Ptchd1* wild-type and -/y mice using a Cobas c111 analyzer. LDL: low density lipoprotein, HDL: high density lipoprotein. Mean ± SD, n=7-8 mice, Ordinary two-way ANOVA with Tukey's multiple comparisons tests, with individual variances computed for each comparison.

## Figure 5

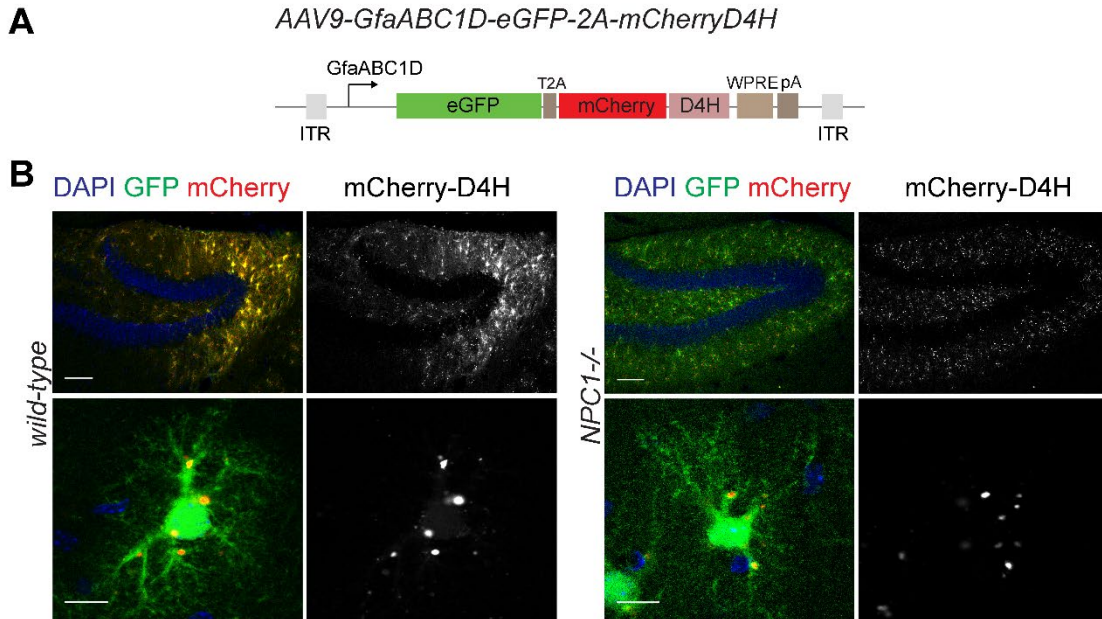


**Figure 5: Adaptation of D4H probes for probing astrocyte-specific cholesterol distribution**

**(A)** Virus design of ratiometric D4H cholesterol probe under astrocyte-specific GfaABC1D promoter control. **(B)** Confocal images of 50µm coronal brain sections of injected P27-32 wild-type or knock-out (-/-) *NPC1* mice (BALB/c background). Upper left panel: 10X magnification view of DG, scale bar: 100µm. Lower left panel: 63X magnification of astrocyte, scale bar: 10µm. Right panel: 20X magnification view of granule cell layer (GCL) and corresponding dendrites.

## Figure supplement 1

A

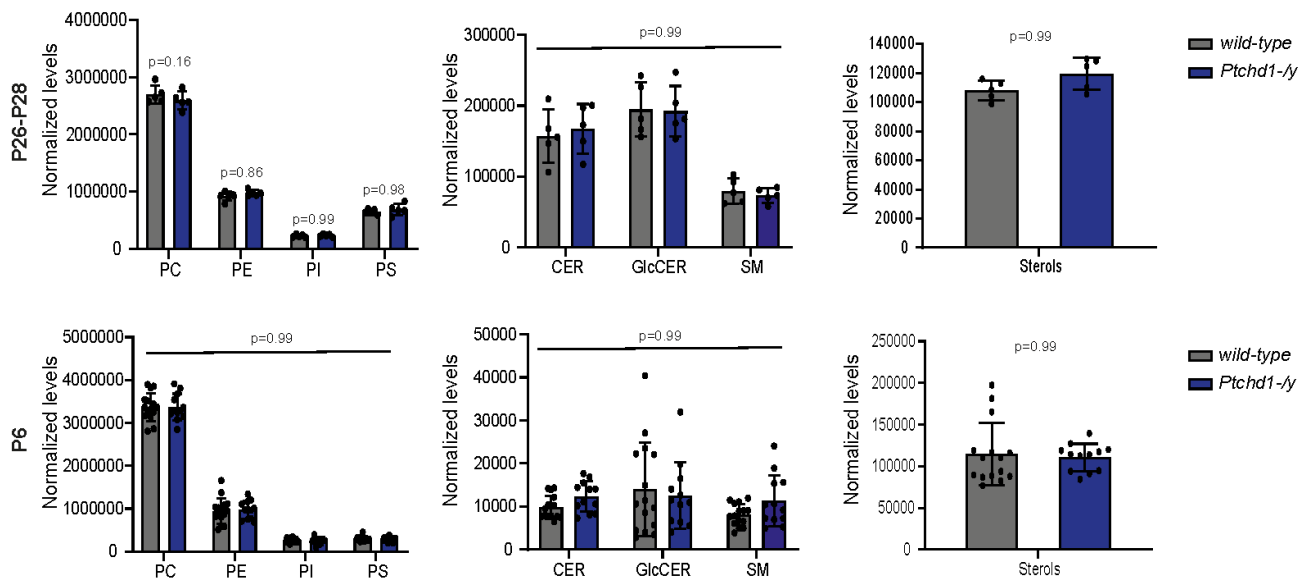


**Figure supplement 1 – related to Figure 4: Summary of lipidomic comparison of wild-type and *Ptchd1*<sup>KO</sup> tissue**

**(A)** Normalized lipids levels in cerebellar tissue of P26-28 *Ptchd1* wild-type or *-/-* mice (n=5) by lipidomics. **(B)** Normalized lipids levels in cerebellar tissue of P6 *Ptchd1* wild-type or *-/-* mice (n=15-12) by lipidomics. PC: phosphatidylcholine, PE: phosphatidylethanolamine, PI: phosphatidylinositol, PS: phosphatidylserine, CER: ceramide, GlcCER: glucosylceramide, SM: sphingomyelin. Mean  $\pm$  SD, Ordinary two-way ANOVA with Tukey's multiple comparisons tests, with individual variances computed for each comparison.



## Figure supplement 2

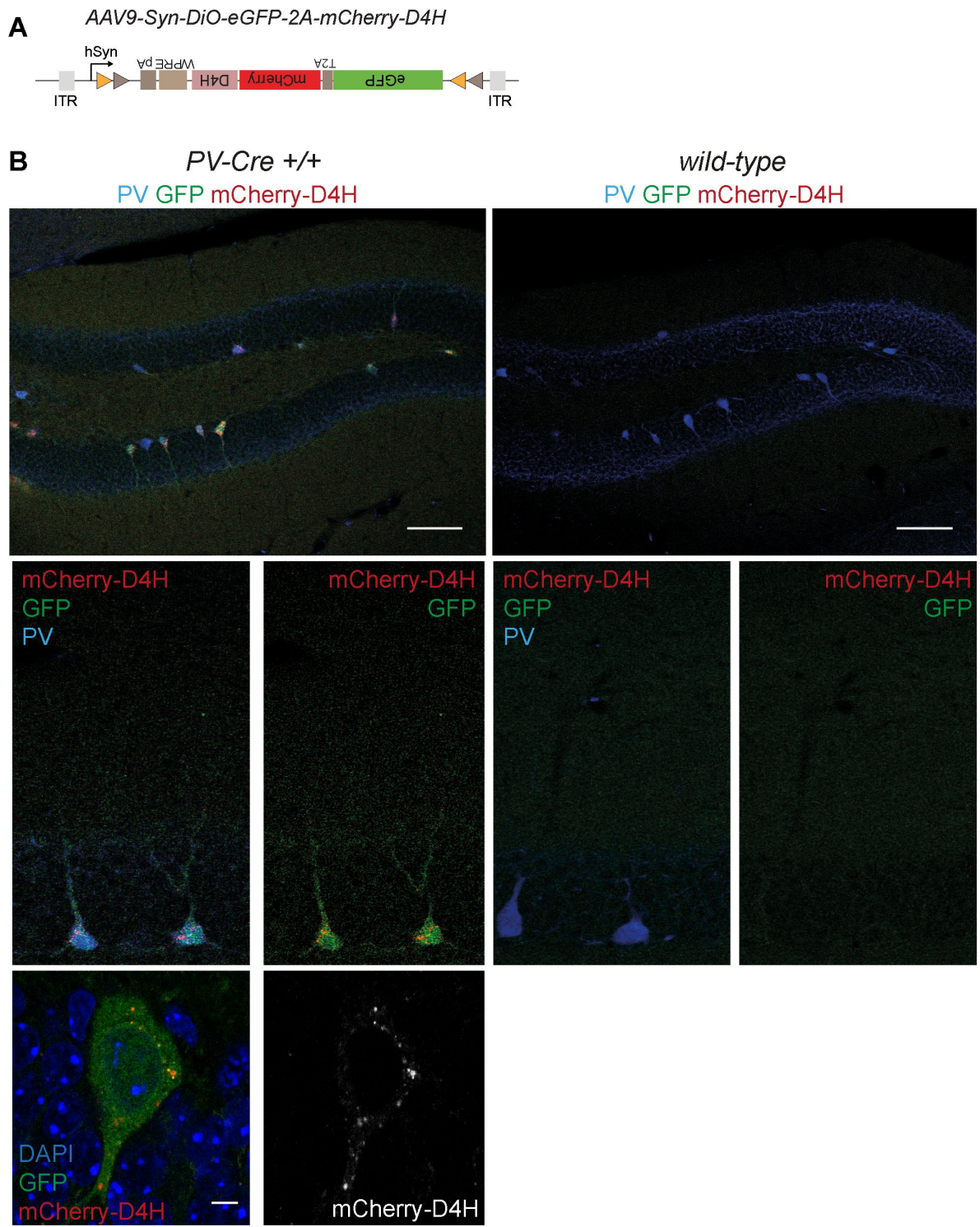


**Figure supplement 2 – related to Figure 5: AAV vectors for cell-type specific visualization of cholesterol distribution**

**(A)** Virus design of ratiometric D4H cholesterol probe with DiO configuration for cre-dependent expression in specific neuronal population. **B.** Confocal images of 50 $\mu$ m coronal brain sections of injected P27-32 wild-type or knock-out (-/-) parvalbumin (PV)-Cre mice (C57B6/J background). Upper left panel: 10X magnification view of DG, scale bar: 100 $\mu$ m. Lower left panel: 63X magnification of granule cells (GC), scale bar: 10 $\mu$ m. Right panel: 20X magnification view of granule cell layer (GCL) and corresponding dendrites.

## Figure supplement 3

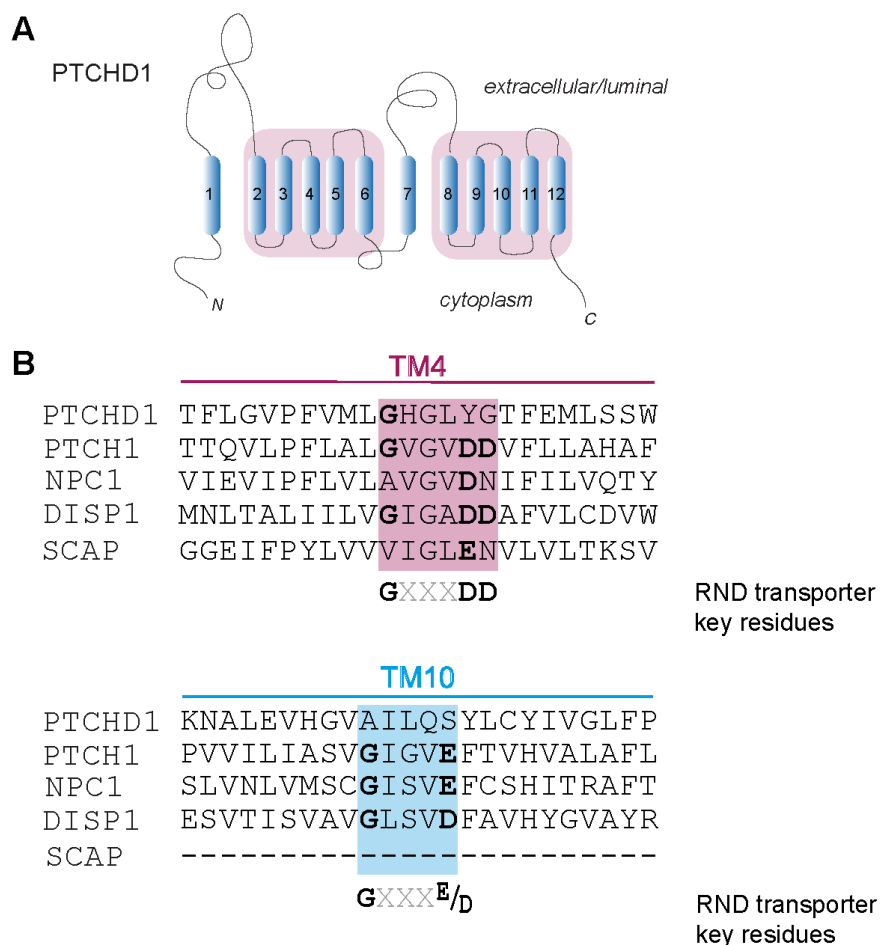


### Figure supplement 3: Key amino acid residues of RND transporter family are not conserved in PTCHD1.

**(A)** Hypothetical topology of Ptchd1. The two predicted sterol-sensing domains are highlighted in orange, transmembrane domains in blue (numbered from 1-12). **(B)** Alignment of amino acid sequences (mouse proteins) in transmembrane domains 4 and 10 which play key roles in cholesterol transport by Ptch1. Critical amino acid residues contributing to transport function in bacterial RND transporters as well as Ptch1 are highlighted (GxxxDD and GxxxD/E motif) (Gong et al., 2018; Zhang et al., 2018). NPC1 and Disp1 which also exhibit cholesterol transport activity share the conserved motifs. By contrast, Scap lacks cholesterol transporter activity also lacks these motifs. Note that Scap contains only one SSD and, thus, only 8 transmembrane domains.



**Table S1 – List of genes involved in cholesterol metabolism and sterol-sensing domain proteins**

CHOLESTEROL PATHWAY							
Uniprot ID	entrezgene	name	symbol	alias	taxid	HGNC	KEGG
O95477	19	ATP binding cassette subfamily A member 1	ABCA1	ABC1, HDLDT1	9606	HGNC:29	hsa04979
P02647	335	apolipoprotein A1	APOA1		9606	HGNC:600	hsa04979
P06858	4023	lipoprotein lipase	LPL	LIPD	9606	HGNC:6677	hsa04979
P04180	3931	lecithin-cholesterol acyltransferase	LCAT		9606	HGNC:6522	hsa04979
Q9Y5X9	9388	lipase G, endothelial type	LIPG		9606	HGNC:6623	hsa04979
P55058	5360	phospholipid transfer protein	PLTP		9606	HGNC:9093	hsa04979
P11597	1071	cholesteryl ester transfer protein	CETP		9606	HGNC:1869	hsa04979
P11150	3990	lipase C, hepatic type	LIPC		9606	HGNC:6619	hsa04979
P08519	4018	lipoprotein(a)	LPA	LP	9606	HGNC:6667	hsa04979
P16671	948	CD36 molecule	CD36		9606	HGNC:1663	hsa04979
P01130	3949	low density lipoprotein receptor	LDLR		9606	HGNC:6547	hsa04979
Q6PIU2	57552	neutral cholesterol ester hydrolase 1	NCEH1	AADACL1	9606	HGNC:29260	hsa04979
P35610	8435	sterol O-acyltransferase 2	SOAT2	SOAT, STAT	9606	HGNC:11177	hsa04979
O75908	6646	sterol O-acyltransferase 1	SOAT1		9606	HGNC:11178	hsa04979
P02654	341	apolipoprotein C1	APOC1		9606	HGNC:607	hsa04979
P02655	344	apolipoprotein C2	APOC2		9606	HGNC:609	hsa04979
P02749	350	apolipoprotein H	APOH	B2G1	9606	HGNC:616	hsa04979
Q9Y5C1	27329	angiotensinogen like 3	ANGPTL3	ANGPT5	9606	HGNC:491	hsa04979
Q9BY76	51129	angiotensinogen like 4	ANGPTL4		9606	HGNC:16039	hsa04979
Q6LXH0	55908	angiotensinogen like 8	ANGPTL8	C19orf80	9606	HGNC:24933	hsa04979
Q8WTV0	949	scavenger receptor class B member 1	SCARB1	CD36L1	9606	HGNC:1664	hsa04979
Q99523	6272	sortilin 1	SORT1		9606	HGNC:11186	hsa04979
P04114	338	apolipoprotein B	APOB		9606	HGNC:603	hsa04979
Q8NBP7	255738	proprotein convertase subtilisin/kexin type 9	PCSK9	HCHOLA3	9606	HGNC:20001	hsa04979
Q5SW96	26119	low density lipoprotein receptor adaptor protein 1	LDLRAP1		9606	HGNC:18640	hsa04979
Q8WY64	29116	myosin regulatory light chain interacting protein	MYLIP		9606	HGNC:21155	hsa04979
P02649	348	apolipoprotein E	APOE	AD2	9606	HGNC:613	hsa04979
Q07954	4035	LDL receptor related protein 1	LRP1	APR, A2MR	9606	HGNC:6692	hsa04979
P98164	4036	LDL receptor related protein 2	LRP2		9606	HGNC:6694	hsa04979
P30533	4043	LDL receptor related protein associated protein 1	LRPAP1	A2MRAP, RAP	9606	HGNC:6701	hsa04979
P38571	3988	lipase A, lysosomal acid type	LIPA		9606	HGNC:6617	hsa04979
Q14849	10948	star related lipid transfer domain containing 3	STARD3		9606	HGNC:17579	hsa04979
P21796	7416	voltage dependent anion channel 1	VDAC1		9606	HGNC:12669	hsa04979
P45880	7417	voltage dependent anion channel 2	VDAC2		9606	HGNC:12672	hsa04979
Q9Y277	7419	voltage dependent anion channel 3	VDAC3		9606	HGNC:12674	hsa04979
P30536	706	translocator protein	TSPO	BZRP	9606	HGNC:1158	hsa04979
Q02318	1593	cytochrome P450 family 27 subfamily A member 1	CYP27A1	CYP27	9606	HGNC:2605	hsa04979
Q9P0L0	9218	VAMP associated protein A	VAPA		9606	HGNC:12648	hsa04979
O95292	9217	VAMP associated protein B and C	VAPB		9606	HGNC:12649	hsa04979
O15118	4864	NPC intracellular cholesterol transporter 1	NPC1		9606	HGNC:7897	hsa04979
P49675	6770	steroidogenic acute regulatory protein	STAR		9606	HGNC:11359	hsa04979
P22680	1581	cytochrome P450 family 7 subfamily A member 1	CYP7A1	CYP7	9606	HGNC:2651	hsa04979
O95342	8647	ATP binding cassette subfamily B member 11	ABCB11	BSEP, PFIC2	9606	HGNC:42	hsa04979
Q9H222	64240	ATP binding cassette subfamily G member 5	ABCG5		9606	HGNC:13886	hsa04979
Q9H221	64241	ATP binding cassette subfamily G member 8	ABCG8		9606	HGNC:13887	hsa04979
P02652	336	apolipoprotein A2	APOA2		9606	HGNC:601	hsa04979
P02656	345	apolipoprotein C3	APOC3		9606	HGNC:610	hsa04979
P06727	337	apolipoprotein A4	APOA4		9606	HGNC:602	hsa04979
Q9BWD1	39	acetyl-CoA acyltransferase 2	ACAT2		9606	HGNC:94	hsa00900
P24752	38	acetyl-CoA acyltransferase 1	ACAT1	ACAT	9606	HGNC:93	hsa00900
Q01581	3157	3-hydroxy-3-methylglutaryl-CoA synthase 1	HMGCS1	HMGCS	9606	HGNC:5007	hsa00900
P54868	3158	3-hydroxy-3-methylglutaryl-CoA synthase 2	HMGCS2		9606	HGNC:5008	hsa00900
P04035	3156	3-hydroxy-3-methylglutaryl-CoA reductase	HMGCR		9606	HGNC:5006	hsa00900
Q03426	4598	mevalonate kinase	MVK		9606	HGNC:7530	hsa00900
Q15126	10654	phosphomevalonate kinase	PMVK		9606	HGNC:9141	hsa00900
P53602	4597	mevalonate diphosphate decarboxylase	MVD		9606	HGNC:7529	hsa00900
Q13907	3422	isopentenyl-diphosphate delta isomerase 1	ID1		9606	HGNC:5387	hsa00900
Q9BXS1	91734	isopentenyl-diphosphate delta isomerase 2	ID2		9606	HGNC:23487	hsa00900
P14324	2224	farnesyl diphosphate synthase	FDPS		9606	HGNC:3631	hsa00900
O954749	9453	geranylgeranyl diphosphate synthase 1	GGPS1		9606	HGNC:4249	hsa00900
Q5T2R2	23590	decaprenyl diphosphate synthase subunit 1	PDSS1	TPRT	9606	HGNC:17759	hsa00900
Q86YH6	57107	decaprenyl diphosphate synthase subunit 2	PDSS2	C4orf210	9606	HGNC:23041	hsa00900
Q86SQ9	79947	dehydrodolichyl diphosphate synthase subunit	DHDDS		9606	HGNC:20603	hsa00900
Q96E22	116150	NUS1 dehydrodolichyl diphosphate synthase subunit	NUS1	C6orf68	9606	HGNC:21042	hsa00900
P49354	2339	farnesyltransferase, CAAX box, alpha	FNTA		9606	HGNC:3782	hsa00900
P49356	2342	farnesyltransferase, CAAX box, beta	FNTB		9606	HGNC:3785	hsa00900
Q9Y256	9986	Ras converting CAAX endopeptidase 1	RCE1	RCE1A, RCE1B	9606	HGNC:13721	hsa00900
O75844	10269	zinc metalloproteinase STE24	ZMPSTE24		9606	HGNC:12877	hsa00900
O60725	23463	isoprenylcysteine carboxyl methyltransferase	ICMT		9606	HGNC:5350	hsa00900
Q9UHG3	51449	prenylcysteine oxidase 1	PCYOX1		9606	HGNC:20588	hsa00900
P37268	2222	Farnesyl-Diphosphate Farnesyltransferase 1	FDFT1		9606	HGNC:3629	hsa00100
Q14534	6713	squalene epoxidase	SQLE		9606	HGNC:11279	hsa00100
P48449	4047	lanosterol synthase	LSS		9606	HGNC:6708	hsa00100
Q16850	1595	Cytochrome P450 Family 51 Subfamily A Member 1	CYP51A1	CYP51	9606	HGNC:2649	hsa00100
Q15800	6307	methylsterol monooxygenase 1	MSMO1	SC4MOL	9606	HGNC:10545	hsa00100
Q15738	50814	NAD(P) Dependent Steroid Hydrogenase-Like	NSDHL		9606	HGNC:13398	hsa00100
O75845	6309	sterol-C5-desaturase	SC5D	SC5DL	9606	HGNC:10547	hsa00100
Q9UBM7	1717	7-dehydrocholesterol reductase	DHCR7	SLOS	9606	HGNC:2860	hsa00100

STEROL-SENSING DOMAIN PROTEINS						
UNIPROT ID	entrezgene	name	symbol	alias	taxid	HGNC
Q96F81	84976	dispatched RND transporter family member 1	DISP1	DISPA	9606	HGNC:19711
A7MBM2	85455	dispatched RND transporter family member 2	DISP2	C15orf36, DISP2, Hst16908, LINC009	9606	HGNC:19712
Q9P2K9	57540	dispatched RND transporter family member 3	DISP3	PTCHD2, KIAA1337	9606	HGNC:29251
F1T0I3	57540	dispatched RND transporter family member 3	DISP3	PTCHD2, KIAA1337	9606	HGNC:29251
A0A024RAP2	3156	3-hydroxy-3-methylglutaryl-CoA reductase	HMGCR	LDLCQ3	9606	HGNC:5006
A0A7P0TBP1	3156	3-hydroxy-3-methylglutaryl-CoA reductase	HMGCR	LDLCQ3	9606	HGNC:5006
A0A7P0Z481	3156	3-hydroxy-3-methylglutaryl-CoA reductase	HMGCR	LDLCQ3	9606	HGNC:5006
P04035	3156	3-hydroxy-3-methylglutaryl-CoA reductase	HMGCR	LDLCQ3	9606	HGNC:5006
A8KA27	3156	3-hydroxy-3-methylglutaryl-CoA reductase	HMGCR	LDLCQ3	9606	HGNC:5006
B2R649	3156	3-hydroxy-3-methylglutaryl-CoA reductase	HMGCR	LDLCQ3	9606	HGNC:5006
K7E023	4864	NPC intracellular cholesterol transporter 1	NPC1	NPC, POGZ, SLC65A1	9606	HGNC:7897
Q15118	4864	NPC intracellular cholesterol transporter 1	NPC1	NPC, POGZ, SLC65A1	9606	HGNC:7897
A0A0S2A5C8	4864	NPC intracellular cholesterol transporter 1	NPC1	NPC, POGZ, SLC65A1	9606	HGNC:7897
A0A193DRS0	4864	NPC intracellular cholesterol transporter 1	NPC1	NPC, POGZ, SLC65A1	9606	HGNC:7897
A0A0A8JCD0	4864	NPC intracellular cholesterol transporter 1	NPC1	NPC, POGZ, SLC65A1	9606	HGNC:7897
Q59GR1	4864	Niemann-Pick disease, type C1 variant	NPC1	NPC, POGZ, SLC65A1	9606	HGNC:7897
A0A0C4DFX6	29881	NPC1 like intracellular cholesterol transporter 1	NPC1L1	LDLCQ7, NPC11L1, SLC65A2	9606	HGNC:7898
A0A0C4DGG6	29881	NPC1 like intracellular cholesterol transporter 1	NPC1L1	LDLCQ7, NPC11L1, SLC65A2	9606	HGNC:7898
Q9UHC9	29881	NPC1 like intracellular cholesterol transporter 1	NPC1L1	LDLCQ7, NPC11L1, SLC65A2	9606	HGNC:7898
H0Y3B8	5727	patched 1	PTCH1	BCNS, NBCCS, PTC, PTC1, PTCH	9606	HGNC:9585
H3BLX7	5727	patched 1	PTCH1	BCNS, NBCCS, PTC, PTC1, PTCH	9606	HGNC:9585
Q13635	5727	patched 1	PTCH1	BCNS, NBCCS, PTC, PTC1, PTCH	9606	HGNC:9585
Q3LFT4	5727	patched 1	PTCH1	BCNS, NBCCS, PTC, PTC1, PTCH	9606	HGNC:9585
Q3LG18	5727	patched 1	PTCH1	BCNS, NBCCS, PTC, PTC1, PTCH	9606	HGNC:9585
A0A1W5YL14	5727	patched 1	PTCH1	BCNS, NBCCS, PTC, PTC1, PTCH	9606	HGNC:9585
A0A1W5YL17	5727	patched 1	PTCH1	BCNS, NBCCS, PTC, PTC1, PTCH	9606	HGNC:9585
Q9Y6C5	8643	patched 2	PTCH2	PTC2	9606	HGNC:9586
Q96NR3	139411	patched domain containing 1	PTCHD1	AUTSX4	9606	HGNC:26392
X5DNX9	139411	patched domain containing 1	PTCHD1	AUTSX4	9606	HGNC:26392
A0A0N9HU02	139411	patched domain containing 1	PTCHD1	AUTSX4	9606	HGNC:26392
A0A087WVH3	374308	patched domain containing 3 (gene/pseudogene)	PTCHD3	PTR	9606	HGNC:24776
Q3KNS1	374308	patched domain containing 3 (gene/pseudogene)	PTCHD3	PTR	9606	HGNC:24776
F6LPT1	374308	patched domain containing 3 (gene/pseudogene)	PTCHD3	PTR	9606	HGNC:24776
I0CMK0	374308	patched domain containing 3 (gene/pseudogene)	PTCHD3	PTR	9606	HGNC:24776
A0A7P0TAD5	442213	patched domain containing 4	PTCHD4	C6orf138, PTCH53, dJ402H5.2	9606	HGNC:21345
H0Y3Q6	442213	patched domain containing 4	PTCHD4	C6orf138, PTCH53, dJ402H5.2	9606	HGNC:21345
Q6ZW05	442213	patched domain containing 4	PTCHD4	C6orf138, PTCH53, dJ402H5.2	9606	HGNC:21345
A0A0A0MTG6	22937	SREBF chaperone	SCAP		9606	HGNC:30634
B7Z6H0	22937	SREBF chaperone	SCAP		9606	HGNC:30634
F8WEH8	22937	SREBF chaperone	SCAP		9606	HGNC:30634
Q12770	22937	SREBF chaperone	SCAP		9606	HGNC:30634
A8K619	22937	SREBF chaperone	SCAP		9606	HGNC:30634
Q6PIX8	22937	SREBF chaperone	SCAP		9606	HGNC:30634
Q8N966	283576	zinc finger DHHC-type palmitoyltransferase 22	ZDHHC22	C14orf59	9606	HGNC:20106









## 2.3 Exploring Ptchd1 localization and potential interactors

Ptchd1 is a multi-spanning transmembrane protein of cellular membranes. Regardless of whether Ptchd1 acts as a cholesterol sensor or transporter, knowledge of its sub-cellular localization is important to understand its function. Previous studies (Tora et al., 2017), suggest that Ptchd1 interacts with components of retromer (Vps35, Vps26B and Snx27), a protein complex implicated in capturing transmembrane cargo proteins and directing their transport between cellular organelles and the plasmamembrane. Currently no antibodies are available to detect endogenous Ptchd1 in immunohistochemical applications. To nevertheless obtain insights into the subcellular localization of Ptchd1, we inserted a triple HA tag into the carboxy-terminal cytoplasmic tail of Ptchd1 and generated expression vectors for expression in mammalian cells. We used biochemical experiments with recombinant protein to confirm that the tag insertion did not impair binding to retromer and other Ptchd1 interacting proteins (data not shown).

As Ptchd1 is expressed throughout the body and as its subcellular localization is likely to be shared between cell types, we expressed Ptchd1-3xHA in cultured HEK293T cells. The expression vector was titrated to low levels to minimize over-expression artefacts. We then immunostained the cells with anti-HA antibodies and antibodies to antigens that serve as markers for cellular compartments (endosomes, lysosomes, Golgi apparatus) to examine co-localization profiles (**Fig. 6A-B**). Confocal images suggest that Ptchd1 is expressed at the plasma membrane and but also in intracellular compartments. Notably, some signal might be attributed to over-expression and may not reflect endogenous Ptchd1 localization. Images also show that Ptchd1 partially co-localize with EEA1 endosomal marker and Vps35, the retromer complex component. Some co-localization can be found between *Ptchd1* and the Golgi marker GM130, which may be due to the fact that as a transmembrane protein, Ptchd1 matures passing through the Golgi apparatus. However, Ptchd1 does not co-localize with the lysosomal marker Lamp1.

These in vitro results suggests that upon maturation through the Golgi apparatus, Ptchd1 protein can be localized at the plasma membrane. Ptchd1 can then be endocytosed and recycled by the retromer machinery from early endosomes back to the plasma membrane through its interactions with Vps35, Vps26B and Snx27 at the carboxyterminal domain. Indeed, the retromer machinery is responsible for endosome-to-plasma recycling of proteins (Wang et al., 2018) and Snx27 has been implicated specifically for recycling of transmembrane proteins with PDZ-binding motifs (Steinberg et al., 2013) such as Ptchd1. These findings need to be

confirm in other cell population in vitro and in vivo as well as bio-chemically by immunoprecipitation, pull-down or proteomics experiments.

**Figure 6**

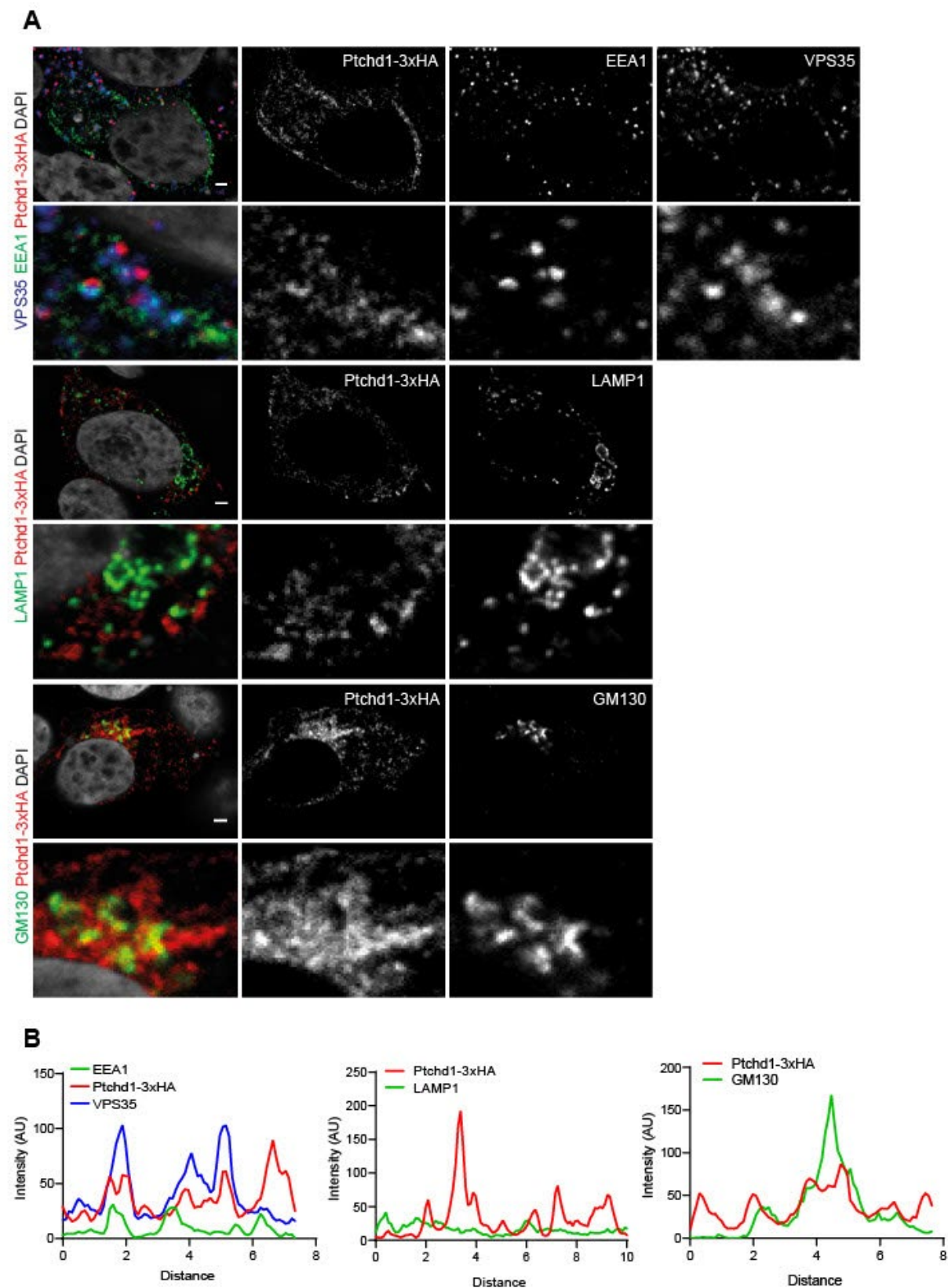




### Figure 6 : Ptchd1 sub-cellular localization *in vitro*

(A) Confocal images of HEK293T cells transfected with 80ng of Syn-*Ptchd1*-3xHA plasmid. 24h post-transfected, cells were fixed and subsequently stained with antibodies for cellular compartments (*Eea1*: early endosome, *Vps35*: retromer machinery, *Lamp1*: lysosome, *GM130*: Golgi apparatus) and for *Ptchd1*-3xHA using specific HA antibody. Scale bar: 2 $\mu$ m. (B) Visualization of co-localization between *Ptchd1*-3xHA and compartment markers signals using the ImageJ histogram function. Lines were drawn on a portion of the images displayed above. Peak overlap indicates signal co-localization.

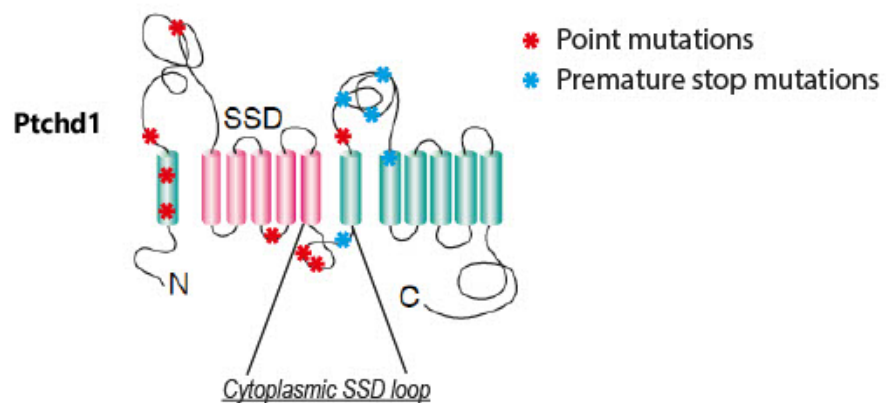
*Ptchd1* is mutated in individuals with neurodevelopmental disorders but the functional impact of most mutations is unknown. In order to uncover other protein interactions that are essential for *Ptchd1* biological function, we mapped pathogenic mutations found in the *Ptchd1* gene from human patients diagnosed with a neurodevelopmental disorder as reported in the SFARI database. As depicted below in **Fig. 7A**, we found 8 point mutations and 5 premature stop mutations in the *Ptchd1* gene. Interestingly, 2 point mutations were found in the cytoplasmic loop (Gly422-Lys501) directly after the sterol-sensing domain (SSD). Ala470Asp and Glu479Gly are maternally-inherited mutations reported in patients diagnosed with ID and ASD respectively. When expressing *Ptchd1*-3XHA in HEK293T, the mutant variants ( $\Delta$ A470D-*Ptchd1*-3xHA and  $\Delta$ E479G-*Ptchd1*-3xHA) did not show mis-expression or mis-localization when compared to wild-type *Ptchd1*-3xHA, which was also reported by Halewa et al. Thus, it suggests that the mutations pathogenicity does not stem from a mis-folded or mis-localized protein but most likely through impairment of essential protein interactions.

To identify interacting partners, we designed a yeast two-hybrid (Y2H) with the aforementioned cytoplasmic sequence as bait against a mouse adult brain library (performed by the Hybrigenics company using the ULTImate Y2H™ protein interactions screening protocol). The screen revealed only one potential interaction with a high confidence score between *Ptchd1* and Uba3 (**Fig. 7B**). Uba3 (NEDD8-activating enzyme E1 catalytic subunit) is an enzyme involved in the neddylation process. Neddylation is a post-translational protein modification similar to ubiquitination, however neddylated proteins are not targeted for degradation but rely on the neddylation/deneddylation process for proper functioning. Neddylation has gathered interest as it has been implicated in several neurological disorders (Dil Kuazi et al., 2003) and cancers (Zhou et al., 2019). The potential *Ptchd1*-Uba3 interaction at the cytoplasmic loop after SSD is therefore very interesting as it could indicate that *Ptchd1* itself is a target of neddylation

or that Ptchd1 could regulate the neddylation of other protein targets. This result will be confirmed by pull-down experiments using GST-conjugated Ptchd1 peptides with the cytoplasmic loop sequence (wild-type, A470D or E479G variants) and brain lysate. The hypothesis is that Uba3 will bound the wild-type GST-Ptchd1 peptide but that the mutants will modify the Uba3 interaction. This confirmation experiment is currently ongoing. The other potential interactors detected in the Y2H assay did not possess a confidence score warranting further investigation, D being the lowest confidence score before non-specific interactions or technical artefacts.

Figure 7

A



GSSLVFTGYIENNYQHSIFCRKVPKPDVLQEQPAWYRFLLTARFSEETAEGEEANTYESHLLVCFKRYCDWITNTYVK

B

Protein name	Interaction confidence	# Interactions	GO class
NEDD8-activating enzyme E1 catalytic subunit (Uba3)	A: Very High	11	- NEDD8 activating enzyme activity - BLOC-1 complex - Nucleus - Protein neddylation
Receptor-type tyrosine-protein phosphatase N2 (Ptpn2)	D: Moderate	3	- Protein tyrosine phosphatase activity - Secretory granule - Cell junction
Mitochondrial import receptor subunit TOM34 (Tomm34)	D: Moderate	1	- Mitochondrion - Cytosol - Heat shock protein binding
Septin-7 (Sept7)	D: Moderate	1	- Protein binding - Septin complex - GTP binding
DnaJ homolog subfamily C member 7 (Dnajc7)	E: may be non specific	8	- Chaperone cofactor-dependent protein refolding - Cytoplasm - Cytoskeleton
Zinc finger and BTB domain-containing 16 (Zbtb16)	E: may be non specific	1	- Nucleus - Skeletal system development - RNA polymerase II cis-regulatory region sequence-specific DNA binding
SNARE-associated protein Snapin (Snapin)	F: experimentally proven technical artefact	7	- Protein binding - BLOC-1 complex - Regulation of synaptic vesicle exocytosis
Transcription initiation factor TFIID subunit 1 (Taf1)	F: experimentally proven technical artefact	1	- Protein binding - Transcription factor TFIID complex - RNA polymerase II general transcription initiation factor activity
Ran-binding protein 9	F: experimentally proven technical artefact	1	- Protein binding - Cytoplasm - Nucleus
E3 ubiquitin-protein ligase RING2 (Rnf2)	F: experimentally proven technical artefact	1	- Protein binding - PcG protein complex - Chromatin binding
Zinc finger protein Pegasus (Ikzf5)	N/A	1	- DNA binding - DNA binding transcription factor activity - DNA binding transcription repressor activity, RNA polymerase II-specific

**Figure 7 : Ptchd1 pathogenic mutations and potential protein interactors**

**(A)** Schematic structure of Ptchd1 modified from Kuwabara and Labouesse, 2002, with stars indicating the position of pathogenic mutations found in human patients (red: point mutation, blue: premature stop mutation). *Ptchd1* mutations were found in the SFARI database. Below, the cytoplasmic loop structure (Gly422-Lys501) used for the yeast two-hybrid assay is indicated with the few last amino acid from the previous TM domain highlighted in pink. **(B)** Summary result table from the yeast two-hybrid assay, with cytoplasmic loop sequence from Ptchd1 as bait (Gly422-Lys501) against a mouse adult brain library as prey.

### ***3. Discussion and future directions***

### 3.1 Conclusions

The main goal of my PhD was to investigate the biological function of the *Ptchd1* protein, a neurodevelopmental risk gene. Due to its sequence similarity with *Ptch1* and the presence of a sterol-sensing domain, we hypothesized that *Ptchd1* may be a cholesterol transporter or sensor and potentially have a role in cholesterol homeostasis. Thus, we wanted to probe potential cholesterol-related phenotypes that the absence of *Ptchd1* may trigger. We also sought to localize *Ptchd1* sub-cellularly and uncover potential interacting partners to further unravel the cellular pathways in which *Ptchd1* may be involved.

To achieve the aforementioned goals, we used various techniques to assess cholesterol levels and distribution in neuronal cell populations of interest, namely *Ptchd1*-expressing cells. As conventional tools for cholesterol detection do not allow for cell-type-specific investigations, we adapted the existing D4H cholesterol sensors for in vivo cell-type-specific use by viral delivery. As the dentate granule cells express high levels of *Ptchd1* protein and have shown an electrophysiological phenotype in absence of *Ptchd1*, we delivered the D4H ratiometric probe in those cells by stereotaxic injection in adolescent *Ptchd1*<sup>KO</sup> mice. We did not observe any significant difference in probe distribution between *Ptchd1* KO and WT counterparts, indicating that absence of *Ptchd1* does not significantly affect cholesterol homeostasis in this cell population. We are confident in this finding as the D4H probe was able to recapitulate a well-described cholesterol accumulation phenotypes in the *NPC1*<sup>KO</sup> mice, another NDD disease model, in the same cell population. We also used lipidomic analysis to assess global lipid levels in the cerebellum of *Ptchd1*<sup>KO</sup> mice. The cerebellum was chosen for this analysis as it represents the site of highest *Ptchd1* expression in the mouse brain. We examined two developmental stages (pre- and post-myelination), and did not find significant changes in cholesterol and other lipid species when compared to WT littermates. As our *Ptchd1*<sup>KO</sup> mice are a global KO and *Ptchd1* is also expressed outside of the CNS, we used standard blood sampling for detection of peripheral cholesterol and cholesterol-related metabolites in the plasma of *Ptchd1*<sup>KO</sup> mice at the same developmental stages. This blood analysis is routinely performed on patients and a subset of ASD patients exhibit abnormal blood cholesterol profiles, speaking to the high translational value of this method. However, no significant differences were observed between *Ptchd1* WT and KO mice at both ages.

Taken together, these results suggest that *Ptchd1* is unlikely to be a cholesterol transporter such as *NPC1* or *Ptch1*. Indeed, the lack of any differences in cholesterol distribution or overall levels does not align with the expected consequences of ablation of a cholesterol transporter.

Furthermore, the essential amino acids in the SSD sequence for cholesterol transport identified in the Ptch1 protein and mainly conserved in NPC1 protein are not present in the Ptchd1 SSD, thus, further suggesting that Ptchd1 is unlikely to act as a cholesterol transporter. The lack of observable cholesterol-related phenotypes also seems to preclude any major involvement of Ptchd1 in the cholesterol metabolism and homeostasis, as those pathways are tightly regulated and any disruptions are likely to result in discernable phenotypes.

Although Ptchd1 does not seem to be involved in cholesterol homeostasis, uncovering its biological function is essential to further understand the pathophysiology in the *Ptchd1*<sup>KO</sup> NDD model. From previous work, Ptchd1 was posited to interact with components of the retromer machinery (Vps35, Vps26B and Snx27) (Tora et al., 2017). Co-localization studies in HEK293T revealed that over-expressed Ptchd1-3xHA does seem to co-localize with the retromer protein Vps35 in early endosomes (EEA1). Those findings indicate that Ptchd1 is located at the plasma membrane, can be endocytosed and recycled by the retromer machinery back to the plasma membrane. We also investigated other potential interactors by yeast two-hybrid assay, which yielded one interesting result: the neddylation enzyme Uba3. Notably, neddylation plays important roles in sub-cellular trafficking. Thus, further investigations into the potential Ptchd1-Uba3 interaction may help to understand the cellular function of Ptchd1.

## 3.2 Ptchd1 – cholesterol transporter or sensor?

*Ptchd1* has been identified as a NDD risk gene and severe phenotypes resulting from *Ptchd1* mutations were reported in human patients as well as in animal models. However, no biological function was uncovered for this transmembrane protein. The presence of a sterol-sensing domain in *Ptchd1* is indicative of a cholesterol-related role, as other SSD-containing proteins such as NPC1 or Hmgcr are involved in cholesterol transport and/or homeostasis. SSD-containing proteins can be loosely categorized as cholesterol transporters or cholesterol sensors. In the case of *Ptchd1*, the present evidence does not allow for a definitive categorization of this SSD-containing protein (**Fig. 1A**).

Some evidence pointing to a cholesterol transport activity was found in a recent study by Maza et al., which posited that *Ptchd1* controls the internalization of the  $\mu$ -opoid receptor in GABAergic thalamic neurons through local cholesterol transport. They demonstrated that *Ptchd1* overexpression can reduce the pool of D4H-accessible cholesterol using a BRET assay. However, this experiment was performed *in vitro* using over-expressed *Ptchd1* and, and the reported cholesterol reduction appears minimal, thus requiring further validation before the statement that *Ptchd1* is a local PM cholesterol transporter similar to *Ptch1* can be made. Similarly, an *in vitro* cholesterol export assay performed in HEK293 cells by a collaborator in the Spang lab seemed to indicate a low (if any) cholesterol transport activity of *Ptchd1*, inferior to the known cholesterol transport of *Ptch1* used as a control. Assessment of protein expression and other controls are needed to validate a potential cholesterol transport activity for the *Ptchd1* protein.

Other evidence seems to exclude a cholesterol transport activity therefore leaving a sensor role for *Ptchd1*. As mentioned above, *Ptchd1* amino acid sequence does not contain the amino acid motifs identified in *Ptch1* as essential for cholesterol transport, similarly to other cholesterol sensing SSD protein such as Scap and Hmgcr. Furthermore, no cholesterol differences were observed in *Ptchd1*<sup>KO</sup> mice using the D4H probe, enzymatic or lipidomics analysis in various cell populations, unlike in the case of *NPC1*<sup>KO</sup> mice where a clear phenotype can be observed. Absence of differences in cholesterol distribution in *Ptchd1*<sup>KO</sup> mice tends to indicate that *Ptchd1* is not a major cellular cholesterol transporter like NPC1. It would be interesting to observe if there are cholesterol differences in *Ptch1*<sup>KO</sup> mice as *Ptch1* is a local cholesterol transporter at the PM, although it may be difficult given the impaired cellular proliferation caused by the absence of *Ptch1* *in vivo*. Lack of differences in cholesterol levels in *Ptchd1*<sup>KO</sup> mice also seems to indicate that *Ptchd1* is not essential for cholesterol homeostasis contrary to other cholesterol sensing proteins. Indeed, absence of either Scap, Hmgcr or 7dhcr, cholesterol synthesis



enzymes, would likely trigger detectable changes in cellular cholesterol levels. Conversely, changes in cholesterol levels trigger up- or down-regulation of the aforementioned enzymes. The most studied regulation is the up-regulation of the Hmgcr protein upon cholesterol depletion. Cholesterol depletion by methyl  $\beta$ -cyclodextrin (MbCDX) induces up-regulation of Hmgcr transcription and subsequent translation to replenish the cellular cholesterol pool and maintain cholesterol homeostasis. We performed this experiment on cultured cerebellar granule cells treated with MbCDX and quantified Ptchd1 and Hmgcr mRNA levels by RT-qPCR (**Fig. 1B**). As expected, Hmgcr was significantly up-regulated 3h and 12h after MbCDX treatment whereas Ptchd1 mRNA levels remained unchanged indicating that Ptchd1 is not involved in cholesterol synthesis and homeostasis. Taken together, it remains unclear whether Ptchd1 acts as a local cholesterol transporter similarly to Ptch1 or acts as a cholesterol-sensing protein, which triggers a cellular response depending on membrane cholesterol levels (**Fig. 1A**). However, it seems likely that the cellular pathway down-stream of Ptchd1 is not part of the cholesterol homeostasis/synthesis pathway.

The potential interaction between Ptchd1 and Uba3 could help unravel which signaling pathway is connected to Ptchd1. The Uba3 protein is part of the heterodimeric Nedd8-activating enzyme E1, which part of the neddylation machinery. Neddylation is a post-translational modification similar to ubiquitination, and consists of the reversible covalent binding of the neuronal precursor cell-expressed developmentally down-regulated protein 8 (Nedd8) to substrate proteins. In a similar fashion to ubiquitin, Nedd8 is binding to specific protein substrates by an isopeptide chain between its carboxy-terminal glycine residue (Gly76) and a lysine residue of the target protein (Kamitani et al., 1997). The most studied substrate of neddylation is the cullin protein family and neddylated cullin proteins constitute the largest ubiquitin E3 family (Zhao et al., 2014). Down-regulation of the cullin neddylation results in decreased levels of active ubiquitin E3s leading to altered ubiquitination levels. Dysfunction of ubiquitination will then results in the accumulation of several proteins contributing to neurodegenerative diseases pathology such as Alzheimer's and Parkinson's disease (Chen et al., 2012, Xiong et al., 2009). Other protein targets of neddylation are involved in cell cycle progression such as p53, which is why neddylation was also studied in the context of cancer (Xirodimas et al., 2004). More interestingly, neddylation was found to be involved in neuronal developmental and dendritic maturation. Indeed, inhibition of neddylation pharmacologically or genetically has major effects on neurons both *in vitro* and *in vivo*, including synaptic loss, altered synaptic plasticity, and impaired neurotransmission (Vogl et al., 2015, Scudder and Patrick, 2015, Brockmann et al., 2019). The effect of neddylation on spine maturation and synaptic transmission is mediated by the neddylation of Psd95 on the lysine residue 202 which is essential for the pro-active role of this synaptic scaffolding protein (Vogl et al., 2015). In a

biochemical assay, Tora et al. showed that Ptchd1 can bind Psd95 through its carboxy-terminal PDZ-binding motif. It would be interesting to study whether neddylation of Psd95 is regulated by Ptchd1 as disruption of spine stability and/or synaptic transmission could potentially explain the electrophysiological changes detected in *Ptchd1<sup>KO</sup>* mice. In a more global fashion, defining the specific proteome of neddylated proteins in Ptchd1-expressing cells could reveal important differences in *Ptchd1<sup>KO</sup>* mice, which could help pinpoint Ptchd1 biological function and underlying cellular pathways. Independently of neddylation, another interesting experiment would be to use spatial proteomic methods such as LOPIT-DC (Geladaki et al., 2019) to identify up- or down-regulated proteins in specific cellular compartments of *Ptchd1<sup>KO</sup>* cells. Pilot experiments were conducted on wild-type cerebellar samples using the LOPIT-DC differential ultracentrifugation protocol, which results in 10 fractions representing different cellular compartments. Although segregation of cellular compartments markers in their respective fractions was not as clear-cut due to the heterogeneity of cerebellar cell populations, this method could provide valuable insights into underlying cellular pathways and/or compensatory mechanisms induced by the absence of Ptchd1. Identification of the biological role of Ptchd1 remains a primary goal to understand the pathophysiology of this NDD risk gene.

**Figure 1**

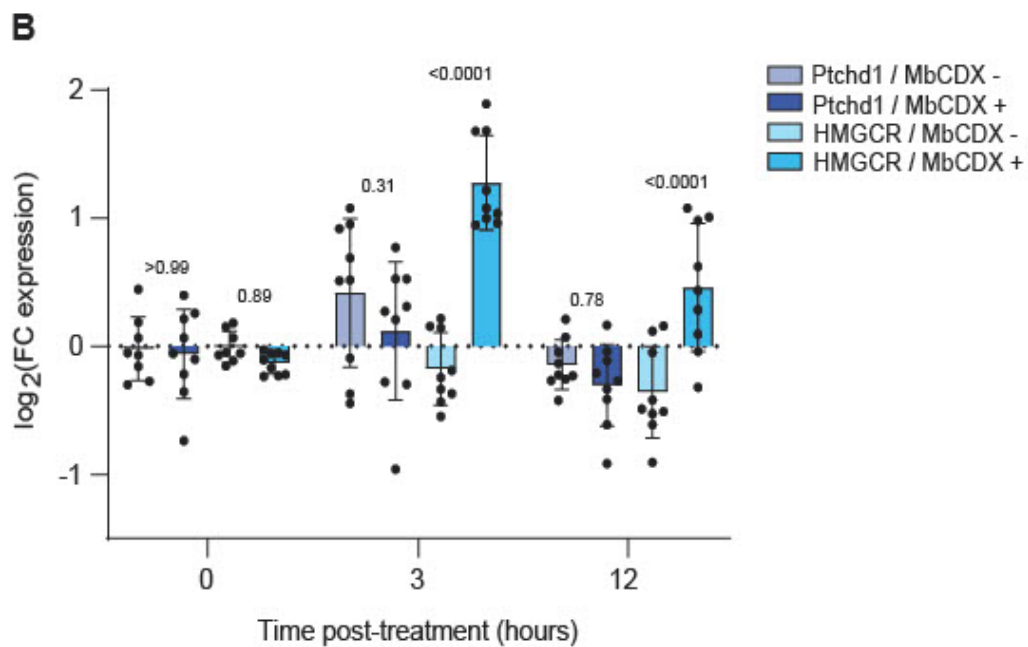
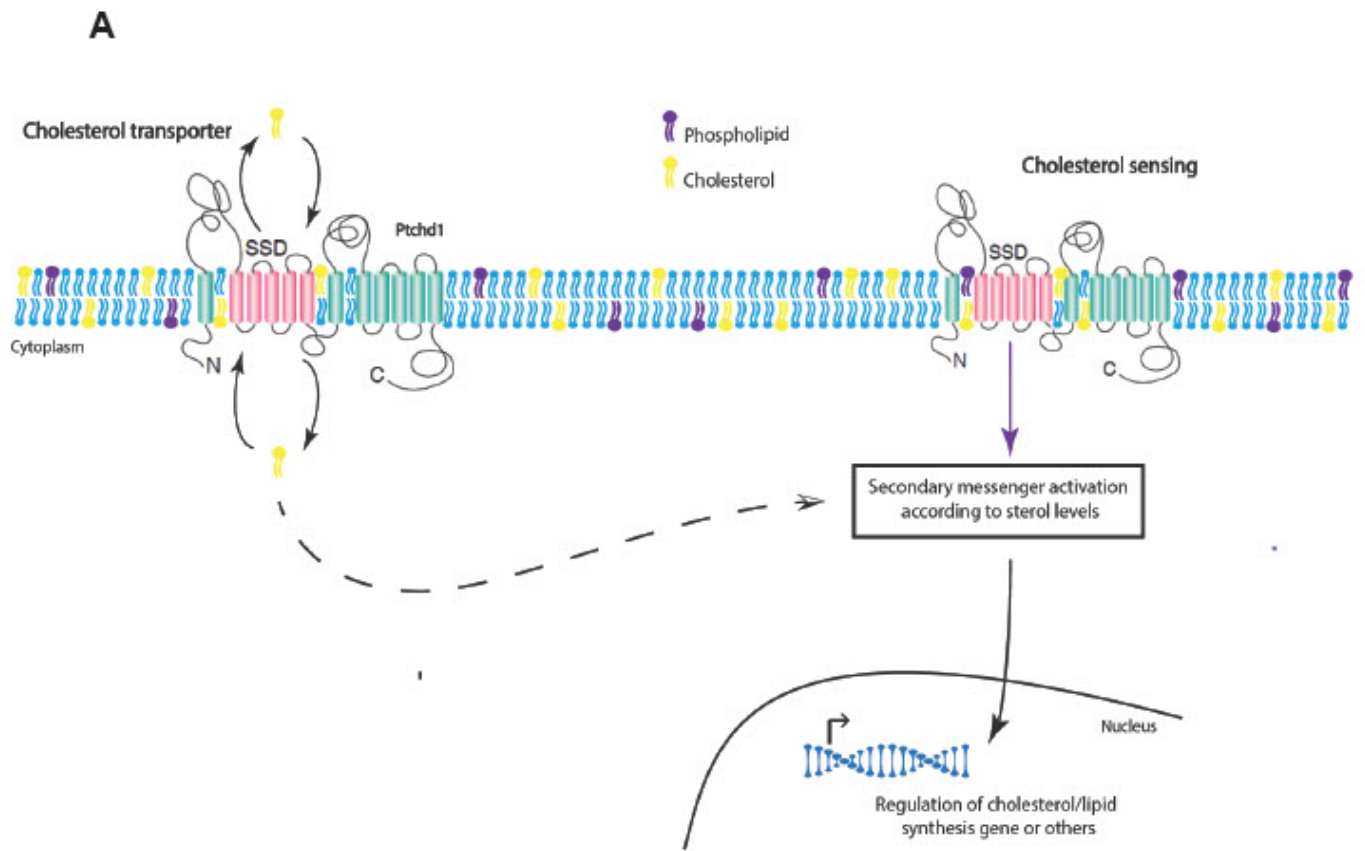


## Figure 1 : Assessment of Ptchd1 biological function

**(A)** Illustration of the potential function of Ptchd1 protein as a cholesterol transporter or sensor. Schematic structure Ptchd1 was modified from Kuwabara and Labouesse, 2002. **(B)** RT-qPCR results from MbCDX-treated cultured cerebellar granule cells. Expression fold-change (FC) is compared between treated and non-treated conditions for the *Ptchd1* and *Hmgcr* genes at different time points (normalized to *Hprt* house-keeping gene), Ordinary two-way ANOVA with Tukey's multiple comparisons tests, with individual variances computed for each comparison. Mean  $\pm$  SD, n=3 technical replicates, N=3 independent culture experiments.

### 3.3 Cell-type specific cholesterol differences

In this work, we relied on the D4H probe to visualize differences in cholesterol levels and distribution *in vivo*. One striking observation was that the D4H probe pattern vastly differs between neuronal cell populations, and with non-neuronal cells (**Fig. 2A**). Some of those differences can be explained by varying amount of membrane structures between cells such as between dentate granule cells and hilar interneurons, as was made evident by the Myr\_mCherry control probe. But others are due to actual cholesterol differences detected by the D4H sensor. Notably, D4H signals do not directly report cholesterol concentration in the cytoplasmic leaflets of membrane but pools of cholesterol accessible for probe binding. Cholesterol accessibility is in part dependent on the lipid composition of the membrane, e.g. the sphingomyelin content. Regardless, our experiments revealed that dentate granule cells display high plasma membrane signals, in particular along the dendrites. Granule cells exhibited only few presumptive intracellular puncta. By contrast, parvalbumin interneurons in the same brain region primarily show cytoplasmic puncta and little plasma membrane signal. Similarly, astrocytes in the dentate gyrus display intense and large D4H puncta that are rarely seen in neuronal populations. The observed differences in cholesterol distribution between neurons and astrocytes could be explained by the fundamentally different cholesterol handling of these cells. Indeed, astrocytes are the main cholesterol supplier of mature neurons through cholesterol-loaded ApoE vesicles which may be what is detected by the D4H probe. However, the different D4H patterns between two neuronal populations such as the glutamatergic dentate granule cells and GABAergic parvalbumin interneurons is very interesting and harder to grasp. It has been shown that some synaptic receptors and channels need to be localized in cholesterol-rich microdomains for correct functioning. As synaptic proteins differ between excitatory and inhibitory cells, could the plasma membrane cholesterol differences detected by the D4H be explained by a lesser need for cholesterol-rich membrane domains in inhibitory cells? Alternatively, differing lipid composition may significantly limit D4H probe access to plasma membrane cholesterol in these cell types. This question would be an interesting avenue to pursue, looking at the cholesterol distribution of other excitatory and inhibitory cell types in several brain regions and across development. It has been demonstrated that brain regions can differ in the expression of cholesterol-synthesis enzymes such as Hmgcr independently of astrocytes number where cholesterol synthesis mainly occurs in the brain (Pfrieger and Ungerer, 2011). Indeed, Hmgcr levels are found to be low in the brain stem region while higher levels were detected in the hippocampus, cortex and cerebellum of adult male rats (Segatto et al., 2012), reflecting distinct cholesterol metabolism handling across cells and brain regions. Furthermore, cholesterol homeostasis changes are age- and sex-dependent

(Armstrong et al., 2019, Martin et al., 2010). Therefore, dissecting cholesterol distribution in specific cell populations and regions is essential to further understanding into cholesterol handling and its dysfunction in various diseases.

Our work was mainly focused on the hippocampal dentate region due to the expression pattern of the Ptchd1 protein. It would however be valuable to map cholesterol differences between cell types throughout the whole brain. Preliminary experiments were performed to deliver the D4H probe globally using stereotaxic techniques optimized for whole-brain expression. Injections of adeno-associated viruses in the retro-orbital or transverse sinus regions have been shown to allow for whole-brain expression (Chan et al., 2017, Hamodi et al., 2020). The same methods were used with the D4H probe virus (**Fig. 2B**) but some brain regions seem more prone to infection than others such as the hippocampus. The PhP.eB capsid was shown to improve expression across the brain but requires high titer virus preparation for successful injections (Chan et al., 2017). Further optimization is required to achieve homogenous infection across the brain, which would allow for comparison of cholesterol level and distribution between cell types and brain regions. The individual cholesterol profile of various cell populations would provide valuable insights into the etiology of several brain diseases where cholesterol alterations have been implicated in disease pathology.

## Figure 2

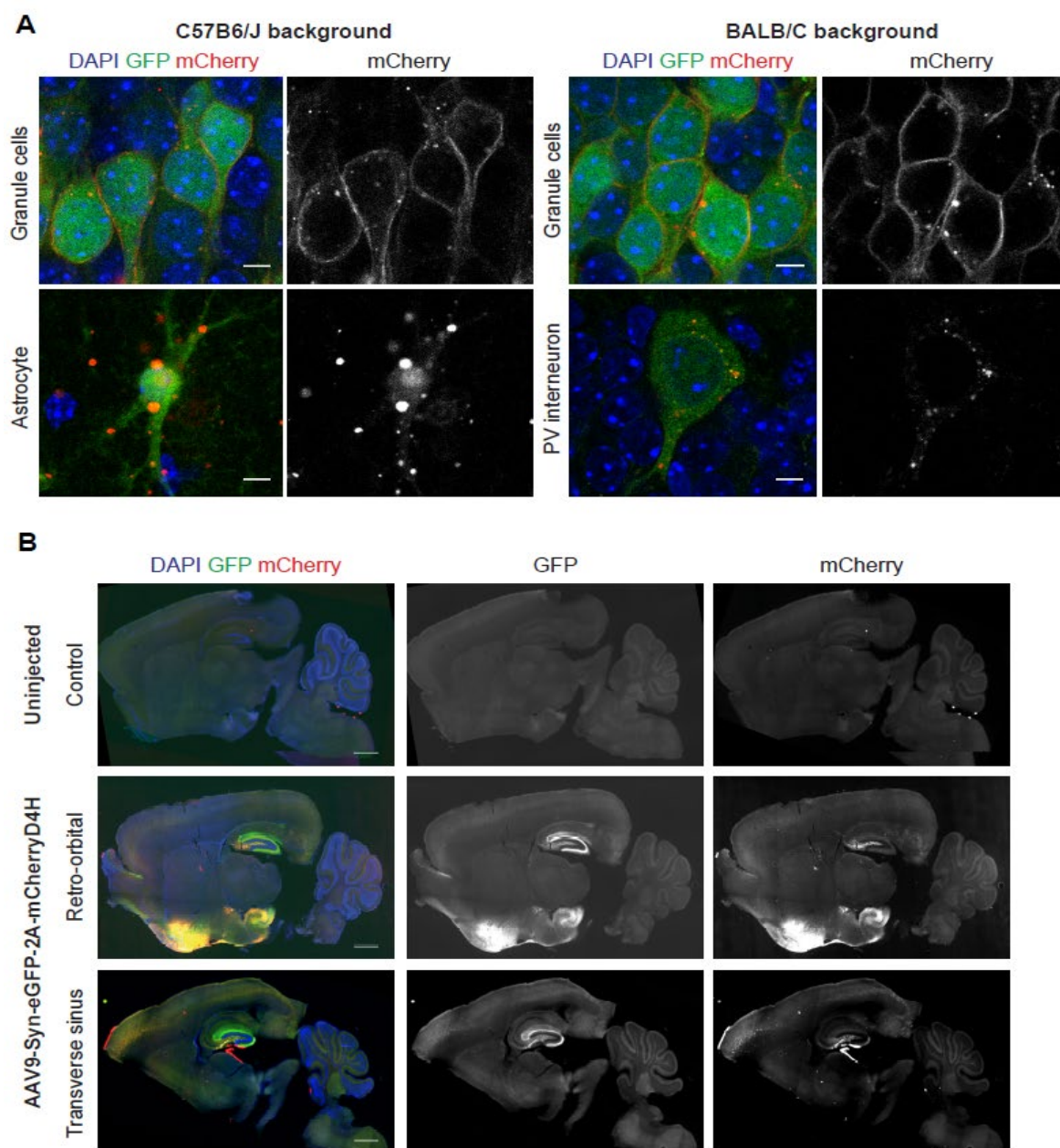


**Figure 2 : Cell-type specific cholesterol distribution in the mouse brain**

**(A)** Confocal images of 50µm coronal brain sections of P27-32 wild-type C57B6/J or Balb/C mice (pAAV9-eGFP-2A-mCherryD4H  $1,6 \cdot 10^{11}$  GC/mL). 63X magnification of granule cells (GC), astrocyte or Parvalbumin (PV) interneuron, scale bar: 5µm. **(B)** Wide-field images of 50µm sagittal brain sections of P14 wild-type C57B6/J mice, control or injected retro-orbitally or in the transverse sinus at P2 (pAAV-Syn-eGFP-2A-mCherryD4H  $2,4 \cdot 10^{12}$  GC/mL). 5X magnification, scale bar: 1000µm.

### 3.4 Cholesterol alterations in neurodevelopmental disorders

In the central nervous system, cholesterol has essential roles as a major component of myelin sheaths and neuronal membranes. As such, cholesterol levels can greatly affect synaptic transmission. At the pre-synapse, synaptic vesicle formation and release properties are dependent on cholesterol levels (Linetti et al., 2010) whereas post-synaptically cholesterol controls the organization and optimal positioning of neurotransmitter receptors, ion channels and downstream effectors (Segatto et al., 2014. Korade and Kenworthy, 2008). Reduction in post-synaptic cholesterol levels has been shown to impair neurotransmission and induce synaptic loss (Sebastiao et al., 2012). The link between cholesterol abnormalities and neurodevelopmental disorders was clearly identified in the context of SLOS and NPC1 diseases (Elias and Irons, 1995, Pfrieger, 2003). Indeed, both NDDs are caused by non-functional proteins involved in cholesterol homeostasis, respectively the cholesterol synthesis enzyme *7dhcr* and the lysosomal cholesterol transporter NPC1. Abnormalities in cholesterol metabolism were also detected in non-syndromic ASD patients (Tierney et al., 2006) including Asperger syndrome subset (Dziobek et al., 2007), although the cellular mechanisms connecting cholesterol alterations and ASD dysfunctions remain largely unknown. One converging link between ASD and cholesterol are lipid rafts, which are cholesterol-rich membrane micro-domains enriched at synaptic sites (Pristera and Okuse, 2011). Numerous synaptic proteins are thought to cluster in lipid rafts for correct functioning, and interestingly amongst those proteins many are found to be implicated in ASD pathology such as NMDA receptors and metabotropic glutamate receptors (mGluRs) (Delorme et al., 2013). Therefore, lipid rafts could be the convergence point where cholesterol alterations trigger the synaptic deficits observed in ASD pathology (Lee and Tierney, 2011).

Manipulation of cholesterol metabolism by genetic or pharmacological means was reported to alleviate ASD behaviors in mouse models. Indeed, statin treatment or mutation of a cholesterol synthesis rate-limiting enzyme were found to rescue some phenotypes in the *Mecp2* mouse model of Rhatt syndrome (Buchovecky et al., 2013). Statin treatments were also used in other ASD models such as Fragile X syndrome and neurofibromatosis type 1 (Li et al., 2005, Osterweil et al., 2013). These results support the notion that cholesterol metabolism may participate to ASD phenotypes and may be a therapeutic avenue for a subset of ASD individuals. As ASD shares overlapping symptoms and etiology with other NDDs, it is reasonable to assume that cholesterol metabolism could also play a role in the pathology of ID, ADHD or other NDDs. Alterations in cholesterol metabolism have also been associated with



several neurodegenerative diseases such as Alzheimer's, Parkinson's and Huntington diseases), mood disorders and depression (Jeong et al., 2019, Hu et al., 2008, Leoni et al., 2011, Troisi, 2011, Ruljancic et al., 2011), highlighting a critical role of cholesterol metabolism in neuronal function in a wide-array of brain disorders. Therefore, studying cellular cholesterol metabolism becomes essential to further define the pathological effects of cholesterol alterations in specific cell types in many neurological diseases, which would help in finding potential therapeutic avenues with high translational value. Indeed, lipophilic statin treatments have been used in Fragile X individuals and Alzheimer's patients to alleviate symptoms with no or moderate success (Hoglund and Blennow, 2007). Dietary cholesterol supplementation is a therapy used for SLOS patients which has controversial effects reported with some improvements in ASD-like behaviors (Aneja and Tierney, 2008) while developmental progress was not ameliorated in children and adolescents (Sikora et al., 2004). However, it remains unclear how peripheral cholesterol addition can significantly modulate brain cholesterol homeostasis. A more targeted and individualized approach to regulate cholesterol homeostasis in affected neuronal populations may prove beneficial compared to global cholesterol reduction or dietary supplementation. Therefore, the D4H cholesterol probes used in this work will be a helpful tool for achieving this goal.

## ***4. Materials and methods***

## 4.1 Materials and methods from the manuscript

### Mice and animal experimentation

All animal experiments were approved by the Cantonal Veterinary Office of Basel-Stadt (Switzerland), and performed in accordance with Swiss laws. The following transgenic mouse lines were used in this study: *Npc1*<sup>KO</sup> (BALB/cNctr-Npc1<m1N>/J, The Jackson Laboratory, strain #003092), *Ptchd1*<sup>KO</sup> (Tora et al., 2017) (B6.Cg-Ptchd1tm1d(KOMP)lcsOrl/Mmucd, MMRRC, stock n° 043797-UCD), PV-cre (B6;129P2-Pvalbtm1(cre)Arbr/J, The Jackson Laboratory, strain #008069). For all experiments, mice were strain-matched, age-matched, and wild-type littermates were used as controls. For the *Ptchd1*<sup>KO</sup> line, only males were used in experiments.

### Viral and plasmid vectors

cDNAs for genetically-encoded mCherry-D4H/YDA cholesterol probes were kindly provided by Dr. Sophie Martin (UNIL, Lausanne, Switzerland) (pSM2056\_Pact\_mCherry\_D4H-Tdh2). The mCherry-D4H/YDA coding sequence was fused to a eGFP and T2A sequence and inserted in an adenoviral backbone under control of the human Synapsin promoter (hSyn). As cholesterol-independent membrane probe, a myristoylated/palmitoylated-mCherry was used. For astrocyte-specific expression, the hSyn promoter was replaced by the minimal GFAP-promoter (GfaABC1D) (Lee et al., 2008). Viruses were generated in HEK293T cells using standard protocols with AAV9 capsid. Viral preparations were concentrated in 100K Millipore Amicon columns at 4°C. Samples were then suspended in PBS, aliquoted and stored at -80°C. Viral titers were determined by qPCR and were >10<sup>13</sup> particles/mL.

### GeneTrek analysis

A curated list of sterol-sensing domain (SSD) proteins and sterol metabolism genes was created using KEGG pathways and HGNC nomenclature (Supplementary table 1), and entered in the GeneTrek search tool. GeneTrek is used to explore association of human genes with several neurodevelopmental disorders (NDD) including autism-spectrum disorders (ASD), intellectual disability (ID) and others (Leblond et al., 2021).

### Cell culture experiments

HEK293T cells were grown on 10mm glass coverslips in 24-well plates in DMEM medium (Thermo Fisher, cat n°10566016) supplemented with fetal bovine serum 10% and penicillin/streptomycin 1%. 24h after plating, cells were transfected with 800ng of plasmid vectors (50ng/750ng or 200ng/600ng of pAAV-Syn-eGFP-2A-mCherry\_D4H/YDA or pAAV-

Syn-Myr\_mCherry-2A-eGFP and pAAV-iCre control respectively) using the FuGene6 transfection protocol (Roche, cat n°11 844 443 001) with 3:1 DNA:FuGene ratio. 24h post-transfection, cells were fixed with PFA 4% in PBS 1X (Electron Microscopy Sciences, cat n°15700) for 10min, washed twice with PBS 1X, stained with DAPI 1/10 000 and finally washed with PBS 1X. Coverslips were subsequently mounted on glass microscopy slides using Fluoromount G (Thermo Fisher, cat n°00-4958-02).

### **Surgeries and stereotaxic injections**

Mice (postnatal day 27 - P32) were placed in a stereotaxic frame (Kopf Instrument) under isoflurane anesthesia (Baxter AG). Stereotaxic injections in the Dentate Gyrus (DG) region (ML 1.25mm, AP -1.9mm, DV -1.9mm in C57Bl6/J background and ML 1.5mm, AP -2.0mm, DV -2.0mm in BALB/C background) were performed using a Picospritzer III pressure injection system (Parker) with borosilicate glass capillaries (Hilgenberg, length 100mm, OD 1mm, ID 0.25mm, wall thickness 0.375mm). Each mouse was injected bilaterally and for each injection, 200nL total volume was delivered through multiple spaced bursts over several minutes ( $1,6 \cdot 10^{11}$  GC/mL viral titer). After 7-9 days of incubation, mice were deeply anesthetized with ketamine/xylazine and transcardially perfused with PBS followed by 4% PFA in PBS (Electron Microscopy Sciences, cat n°15700). Extracted brains were incubated in PFA 4% overnight for post-fixation at 4°C and stored in PBS at 4°C. Coronal brain slices were cut at 50µm thickness with a vibratome (Leica Microsystems VT1000) and kept in PBS before staining with DAPI 1/10 000 for 5min and washed with PBS. Slices were subsequently mounted on glass microscopy slides with Fluoromount G (Thermo Fisher, cat n°00-4958-02).

### **Immunohistochemistry**

For brain slices coming from the PV-cre injected animals, further staining was performed to confirm virus cell-specificity. After vibratome cutting, the 50µm coronal sections were permeated in PBS 1X + Triton X 0,05% for 5 min at RT with gentle shaking and washed with PBS 1X. Blocking was performed 1h at RT in 10% Neutral Donkey Serum (Jackson ImmunoResearch, 017-000-121) and Triton-X 0,05% with gentle horizontal shaking. Primary anti-parvalbumin (PV, Columbia University) antibody was added onto the slices and incubated overnight at 4°C with gentle shaking. Slices were washed with PBS 1X and incubated in Cy5-conjugated donkey anti-chicken secondary antibody (Jackson ImmunoResearch, 703-175-155) for 1h at RT. Slices were again washed with PBS 1X, stained with DAPI 1/10 000 for 5 min and washed with PBS 1X. Slices were subsequently mounted on glass microscopy slides with Fluoromount G (Thermo Fisher, 00-4958-02) and imaged within one week.

### **Image analysis and quantification**

Confocal snapshot images and stacks were also taken from fixed HEK293T cells and brain slices with a Zeiss point scanning LSM700 confocal microscope (10X NA 0.45, 20X NA 0.80, 63X NA 1.3). For the analysis of mCherry<sub>D4H/YDA</sub> or M/P<sub>mCherry</sub> signal enrichment at the plasma membrane, lines (10 pixels width) were drawn across cells from single planes of 63X image stacks in Fiji. Histograms of GFP and mCherry signals were derived from the lines and transferred to an Excel file. Further analysis and quantification was performed in GraphPad Prism software. To determine puncta aggregation of mCherry signal in cells, single planes of 63X image stacks were inputted in Fiji where cells were manually drawn and added to the ROI manager using the eGFP cytoplasmic filler as template. Images were then thresholded to generate binary mask images and particles for each cell were defined using the analyze particles function. The calculated particles were added to the ROI manager. Area and intensity of cell and particles region were calculated for the eGFP and mCherry channels respectively and the data transferred to an Excel file. A post-hoc size cut-off of 0,04 $\mu\text{m}^2$  (=2 pixels) was applied to filter particles. Further analysis and quantification was performed in GraphPad Prism software. For global qualitative assessment of in vivo injection success, full coronal slices images were obtained from the Zeiss AxioScan Z1 microscope (5X NA 0.25).

### **Image analysis and quantification**

For plasma metabolites analysis, P6 or P30 Ptchd1 KO or wild-type male mice were deeply anesthetized using isoflurane (Baxter AG) and decapitated with scissors. Decapitation blood from the body was collected in 300 $\mu\text{L}$  Li-Heparin microvette (Sarstedt) on ice and centrifugated at 200g for 5min at 4°C. The supernatant (plasma) was transferred to an Eppendorf tube and stored at -20°C. Samples were diluted 1:3 in ddH<sub>2</sub>O on ice in a 45 $\mu\text{L}$  total volume before analysis in the Cobas c111 Analyzer (Roche). The Cobas c111 Analyzer is a platform for clinical chemistry testing of human samples but can also be used to analyze mouse samples. In this study, the following metabolites were measured: cholesterol (CHOL2), cholesterol HDL (HDL3), cholesterol LDL (LDL-C) and triglycerides (TRIGL).

### **Lipidomics analysis**

For lipid extraction, P6 or P26-28 Ptchd1 KO and wild-type male mice were deeply anesthetized using isoflurane (Baxter AG), the cerebellum was dissected out, flash frozen in liquid nitrogen and stored at -80°C. Cerebellums were subsequently crushed into a fine powder using a custom-made metal mortar on dry ice to keep the tissue frozen. Samples were then analyzed by the Riezman lab (UNIGE, Geneva, Switzerland) using the following methyl-ter-butyl ether (MTBE) modified protocol for extraction. In summary, 5-10mg of dry tissue was resuspended on ice in 100 $\mu\text{L}$  H<sub>2</sub>O where 50 $\mu\text{L}$  1.4mm Zirconium oxide glass beads (Bertin

Technologies), 360µL methanol and internal standard mix were added. The tissue was broken with 3 bursts of 45s at 6200rpm with 45s interruptions in a pre-cooled Cryolysis System (Bertin Technologies) at 4°C. 1.2mL MTBE was added before a 1h incubation in room temperature (RT) with shaking at 750rpm. 200µL ddH<sub>2</sub>O was added to the mixture to induce phase separation. After 10min of incubation at RT, the samples were centrifuged at 1000g for 10min. The upper organic phase was transferred to a 13mm glass tube. The lower phase was extracted using 400µL of artificial upper phase (MBTE/methanol/water, 10:3:1.5, v/v) with the same incubation/centrifugation parameters. Both upper phases were combined and total lipid extract was divided in 3 equal aliquots: one for phospholipid analysis (TL), one for sphingolipid analysis (SL) and one for sterol analysis (S). Aliquots were dried in a Centrivap at 50°C or under a nitrogen flow. The TL aliquots were ready for mass-spectrometry analysis and stored at -80°C. SL aliquot underwent further deacylation to eliminate phospholipids by methylamine treatment (Clarke method). 0.5mL monomethylamine reagent (MeOH/H<sub>2</sub>O/n-butanol/Methylamine, 4:3:1:5, v/v) was added to the dried lipid. Samples were then sonicated and incubated for 1h at 53°C and dried as described above. The monomethylamine treated lipids were desalted by n-butanol extraction where 300µL H<sub>2</sub>O saturated n-butanol was added to the dried lipids. The samples were vortexed, sonicated and 150µL MS grade water was added. The mixture was vortexed and centrifuged at 3200g for 10min. The upper phase was collected and the lower phase was extracted twice more with 300µL H<sub>2</sub>O saturated n-butanol. The upper phases were combined and dried as described above.

For phospholipid and sphingolipid detection, samples were pipetted into a 96-well plate with a final volume of 100µL and LC-MS or HPLC grade solvent were used (positive mode solvent: Chloroform/Methanol/H<sub>2</sub>O 2:7:1 v/v + 5mM Ammonium Acetate, negative mode solvent: Chloroform/Methanol 1:2 v/v + 5mM Ammonium Acetate. The TL and SL aliquots were resuspended in 500µL Chloroform/Methanol (1:1 v/v) solution and sonicated. The TL and SL fractions were diluted 1:10 and 1:5 respectively in a negative and positive mode solvents. For the identification and quantification of phospho- and sphingolipid molecular species, all diluted fractions were infused onto the mass spectrometer where tandem mass spectrometry was performed using multiple reaction monitoring (MRM) with a TSQ Vantage Triple Stage Quadrupole Mass Spectrometer (Thermo Fisher) equipped with a robotic nanoflow ion source (Nanomate HD, Advion Biosciences). Ceramide species were also quantified with a loss of water. Lipid concentrations were calculated according to the standard curves with the internal standards and normalized to the total lipid extract content. Data were also normalized between experiments. The data were not corrected for isotope distribution.

For sterol detection, the S aliquots were resuspended in 500 $\mu$ L Chloroform/Methanol (HPLC/CHROMASOLV LC-MS grade 1:1) and sonicated. 5 $\mu$ L of samples were loaded onto a VARIAN CP-3800 Gas Chromatograph equipped with a Factor Four Capillary Column VF-5ms and analyzed by a VARIAN 320 mass spectrometer triple quadrupole with electron energy set to -70eV at 250°C and the transfer line at 280°C. Temperature was held for 4min at 45°C and ramped successively to 195°C (20°C/min), 230°C (4°C/min), 325°C (20°C/min) and 350°C (6°C/min) before colling back to 45°C. Free sterols were eluted during the linear gradient from 195°C to 230°C. For each sterol, specific ions (m/z) were extracted: Ergosterol (396.4, 363.3 and 337.3), Cholesterol (386.4, 368 and 275.2) and Cholesterol esters (368.4, 353.4 and 147.1). The area under the peak was integrated and the values were transferred into Excel. The sterol concentrations were determined using the standard curves of ergosterol, cholesterol and cholesterol esters.

### **Statistical methods and data availability**

Sample sizes were determined based on the 3R principles, past experience with the experiments and literature surveys. Pre-established exclusion criteria were defined to ensure success and reliability of the experiments: for stereotaxic injection, all mice with mistargeted injections were excluded from analysis (e.g. if no eGFP signal was detected in the granule cell layer of the DG). Furthermore, all mice exhibiting visible behavioral abnormalities or disease symptoms, in the case of the NPC1  $-/-$  mice, were excluded. Investigators performing image analysis and quantification were blinded to genotype. The applied statistical tests were chosen based on sample size, normality of data distribution and number of groups compared. Appropriate correction for variance differences was applied when necessary. Details on n numbers, pvalues and specific tests are found in figure legends. All raw data files, excel analysis tables and additional data supporting the findings of this study could not be included in the manuscript due to space constraints but are available from the corresponding author upon reasonable request.

## **4.2 Additional materials and methods**

### **Mice and reagents**

All animal experiments were approved by the Cantonal Veterinary Office of Basel-Stadt (Switzerland), and performed in accordance with Swiss laws. The following mouse lines were used in stereotaxic injections: C57B6/JRj, *Npc1*<sup>KO</sup> (BALB/cNctr-Npc1<m1N>/J, The Jackson Laboratory, strain #003092), *Ptchd1*<sup>KO</sup> (B6.Cg-Ptchd1tm1d(KOMP)lcsOrl/Mmucd, MMRRC, stock n° 043797-UCD). For stereotaxic injections, mice were strain-matched, age-matched and

the pAAV9-Syn-eGFP-2A-mCherryD4H was used for cholesterol distribution assessment.

For HEK293T cells experiments, the pAAV9-Syn-PTCHD1-3xHA plasmid was used. The triple HA tag was inserted in the Cter domain of PTCHD1 without disruption to previously identified interacting partners. The following commercial primary antibodies were used: anti-HA (Cell signaling, 3724), anti-HA (Roche, 11867431001), anti-EEA1 (BD, E41120), anti-VPS35 (Abcam, ab10099), anti-LAMP1 (Abcam, ab24170), anti-GM130 (BD, 610822). The following commercial secondary antibodies were used: A488-conjugated donkey anti-mouse (Thermo Fisher, A-21202) and anti-rabbit (Thermo Fisher, A-21206), Cy3-conjugated donkey anti-rabbit (Jackson ImmunoResearch, 711-165-152) and anti-rat (Jackson ImmunoResearch, 711-165-153), Cy5-conjugated donkey anti-goat (Jackson ImmunoResearch, 705-715-147).

### **Cell culture experiments and immunocytochemistry**

HEK293T cells were grown on 10mm glass coverslips in 24-well plates in DMEM media (Thermo Fisher, 10566016) supplemented with fetal bovine serum 10% and penicillin/streptomycin 1%. 24h after plating, cells were transfected with 80ng of plasmid pAAV9-Syn-Ptchd1-3xHA using the FuGene6 transfection protocol (Roche, 11 844 443 001) with 3:1 DNA:FuGene ratio. 24h post-transfection, cells were fixed with PFA 4% in PBS 1X (Electron Microscopy Sciences, 15700) for 10min, washed with PBS 1X, permeated in PBS 1X + Triton X 0,01% for 5 min and washed again with PBS 1X. Blocking was performed by incubation 1h at RT in 10% Neutral Donkey Serum (Jackson ImmunoResearch, 017-000-121) with gentle horizontal shaking. Coverslips were transferred to a humidified chamber and primaries antibodies were added for overnight incubation at 4°C. Coverslips were washed 3x with PBS 1X and incubated 1h at RT in secondary antibodies. Coverslips were washed with PBS 1X, stained with DAPI 1/10 000 for 5min and finally washed with PBS 1X. Coverslips were subsequently mounted on glass microscopy slides using Fluoromount G (Thermo Fisher, 00-4958-02), left overnight at RT to dry and stored at -20°C until imaging.

### **Yeast-two hybrid assay**

Yeast two-hybrid screening was performed by Hybrigenics Services, S.A.S., Evry, France. The coding sequence for *Mus musculus* - Ptchd1 (NM\_001093750.1) cytoplasmic loop sequence (Gly422-Lys501) was PCR-amplified and cloned into pB27 and pB66 as a C-terminal fusion to LexA (LexA-Ptchd1) and the Gal4 DNA-binding domain (Gal4-Ptchd1), respectively. The constructs were checked by sequencing and used as a bait to screen a random-primed Mouse Adult Brain cDNA library constructed into pP6. pB27 derives from the original pBTM116 vector (Vojtek and Hollenberg, 1995; Béranger et al., 1997), pB66 derives from the original pAS2ΔΔ vector (Fromont-Racine et al., 1997) and pP6 is based on the pGADGH plasmid (Bartel et al.,



1993).

For the N-LexA-Ptchd1-C bait construct, 109 million (10-fold the complexity of the library) clones were screened using a mating approach with YHGX13 (Y187 *ade2-101::loxP-kanMX-loxP, mata $\alpha$* ) and L40 $\Delta$ Gal4 (*mata*) yeast strains as previously described (Fromont-Racine et al., 1997). Only one His<sup>+</sup> colony, was selected on a medium lacking tryptophan, leucine and histidine. For the N-Gal4-Ptchd1-C bait construct, 90 million (9 -fold the complexity of the library) clones were screened using the same mating approach with YHGX13 (Y187 *ade2-101::loxP-kanMX-loxP, mata $\alpha$* ) and CG1945 (*mata*) yeast strains 36 His<sup>+</sup> colonies were selected on a medium lacking tryptophan, leucine and histidine and supplemented with 0.5 mM 3-aminotriazole to handle bait autoactivation. The prey fragments of the positive clones were amplified by PCR and sequenced at their 5' and 3' junctions. The resulting sequences were used to identify the corresponding interacting proteins in the GenBank database (NCBI) using a fully automated procedure. A confidence score (PBS, for Predicted Biological Score) was attributed to each interaction as previously described (Formstecher et al., 2005).

The PBS relies on two different levels of analysis. Firstly, a local score takes into account the redundancy and independency of prey fragments, as well as the distribution of reading frames and stop codons in overlapping fragments. Secondly, a global score takes into account the interactions found in all the screens performed at Hybrigenics using the same library. This global score represents the probability of an interaction being nonspecific. For practical use, the scores were divided into four categories, from A (highest confidence) to D (lowest confidence). A fifth category (E) specifically flags interactions involving highly connected prey domains previously found several times in screens performed on libraries derived from the same organism. Finally, several of these highly connected domains have been confirmed as false-positives of the technique and are now tagged as F. The PBS scores have been shown to positively correlate with the biological significance of interactions (Rain et al., 2001; Wojcik et al., 2002).

### **Primary cell culture experiments and pharmacological treatment**

Dissociated cultures of cerebellar granule cells were prepared from P5-P6 C57B6/J wild-type mice. The mouse pups were decapitated with scissors and the cerebellum was isolated. Cells were dissociated by addition of 0,05% trypsin-EDTA and 1mg/mL DNase and incubation for 10-15min at 37°C with intermittent swirling. The trypsin-EDTA was then neutralized by adding 5mg/mL soy bean trypsin inhibitor and incubation for 1min at 37°C. Mechanical dissociation was then performed before centrifugation at 290 rpm for 10min at 4°C on a 4% BSA cushion to isolate granule cells from other cell population. Granule cells (60-80,000 cells/cm<sup>2</sup>) were

maintained in neurobasal medium (Gibco, 21103-049) containing 2% B27 supplement (Gibco, 17504-044), 1% Glutamax (Gibco, 35050-61), and 1% penicillin/streptomycin (Bioconcept, 4-01F00-H) for 5 days. Cells were depleted in cholesterol by addition of 0,5mM methyl- $\beta$ -cyclodextrin (MbCDX, Sigma, C4555) for 30 minutes. Following the treatment, the culture medium was replaced and cells were processed for mRNA extraction and qPCR analysis.

### **RNA isolation and qPCR**

Cells were lysed using Trizol reagent (Sigma, T9424) followed by addition of chloroform. After vigorous shaking, samples were centrifuged at 16,000g for 10min at 4°C. Total RNAs were isolated from the supernatant and DNase treated on columns (RNeasy micro kit, Qiagen, 74004) following the manufacturer's instructions. cDNAs were generated using 500ng total RNA reverse transcribed with ImProm-II reverse transcriptase (Promega, A3800) in corresponding reaction buffer, dNTP mix (Promega, C1141), MgCl<sub>2</sub> (Promega, A3511), RNasin ribonuclease inhibitor (Promega, N2511), random primers (Promega, C1181) and oligo(dT)<sub>15</sub> primer (Promega, C1101).

Real-time quantitative PCRs were performed with FastStart Universal SYBR GreenMaster (Roche, 04-913-850-001). PCRs were carried out in a StepOnePlus qPCR system (Applied Biosystems) with the following thermal profile: 10 min at 95°C, 40 cycles of 15s at 95°C and 1 min at 60°C. Real-time quantitative PCR assays were analyzed with the StepOne software with the comparative C<sub>T</sub> method and normalization to the HPRT house-keeping gene. Primer sequences used were as follows: *PTCHD1*: 5'-CAAGATCGAGCGCAACCTAG-3' and 5'-ATGTTGGCTTTCTGGTAGGAG-3'; *HMGCR*: 5'-CTCATGAACGTGGTGTGTCTAT-3' and 5'-GCTCCCATCACCAAGGAATAA-3'; *HPRT*: 5'-GATGAACCAGGTATGACCTAGATTTG-3' and 5'-ATGGCCTCCCATCTCCTTCAT-3';

### **Surgeries and stereotaxic injections**

Wild-type mice (postnatal day 27 - P32) were placed in a stereotaxic frame (Kopf Instrument) under isoflurane anesthesia (Baxter AG). Injections in the Dentate Gyrus (DG) region (ML 1.25mm, AP -1.9mm, DV -1.9mm in C57Bl6/J background and ML 1.5mm, AP -2.0mm, DV -2.0mm in BALB/C background) were performed using a Picospritzer III pressure injection system (Parker) with borosilicate glass capillaries (Hilgenberg, length 100mm, OD 1mm, ID 0.25mm, wall thickness 0.375mm). Each mouse was injected bilaterally and for each injection, 200nL total volume was delivered through multiple spaced bursts over several minutes (1,6.10<sup>11</sup> GC/mL viral titer). After 7-9 days of incubation, mice were deeply anesthetized with ketamine/xylazine and transcardially perfused with PBS 1X followed by 4% PFA in PBS 1X

(Electron Microscopy Sciences, 15700). Extracted brains were then incubated in PFA 4% overnight for post-fixation at 4°C followed by storage in PBS 1X at 4°C. Coronal brain slices were cut at 50µm with a vibratome (Leica Microsystems VT1000) and kept in PBS 1X before staining with DAPI 1/10 000 for 5min and washed with PBS 1X. Slices were subsequently mounted on glass microscopy slides with Fluoromount G (Thermo Fisher, 00-4958-02) and imaged within one week.

For retro-orbital injections, wild-type P2 mice were placed on a heating pad under isoflurane anesthesia (Baxter AG) and 5µL of virus diluted in PBS 1X was injected behind the eye using a BD micro-fine + 0,3mL (BD). For transverse sinus injections, wild-type P2 mice were placed in a stereotaxic frame (Kopf Instrument) under isoflurane anesthesia (Baxter AG). Injections in the transverse sinuses was performed using a Picospritzer III pressurized injection system (Parker) with borosilicate glass capillaries (Hilgenberg, length 100mm, OD 1mm, ID 0.25mm, wall thickness 0.375mm). Transverse sinus localization was done visually and at DV -0.4mm as described in Hamodi et al., 2019. Each mice was injected bilaterally and for each injection, 200nL total volume was delivered through multiple spaced bursts over several minutes ( $2,4 \cdot 10^{12}$  GC/mL viral titer). At P14, mice were deeply anesthetized with ketamine/xylazine and transcardially perfused with PBS 1X followed by 4% PFA in PBS 1X (Electron Microscopy Sciences, 15700). Extracted brains were then incubated in PFA 4% overnight for post-fixation at 4°C followed by storage in PBS 1X at 4°C. Sagittal brain slices were cut at 50µm with a vibratome (Leica Microsystems VT1000) and kept in PBS 1X before staining with DAPI 1/10 000 for 5min and washed with PBS 1X. Slices were subsequently mounted on glass microscopy slides with Fluoromount G (Thermo Fisher, 00-4958-02) and imaged within one week.

## ***5. Appendix***

# Index of figures

## Introduction

<b>Figure 1:</b> Representation of the core ASD symptoms and associated co-morbidities....	12
<b>Figure 2:</b> Schematic representation of pre- and post-synaptic proteins involved in ASD pathophysiology .....	15
<b>Figure 3:</b> Neurodevelopmental continuum hypothesis and ASD-associated co-morbidity rates.....	17
<b>Figure 4:</b> <i>Ptchd1</i> protein structure and potential interactors .....	23
<b>Figure 5:</b> SSD-containing proteins and their cellular functions.....	29
<b>Figure 6:</b> Cholesterol metabolism and transport in the brain.....	33
<b>Figure 7:</b> PFO cholesterol-binding D4 domain structure and mutations .....	44

## Results

<b>Figure 1:</b> Adaptation of perfringolysin O-derived cholesterol probes for analysis of cholesterol distribution in rodent models.....	56
<b>Figure 2:</b> Application of ratiometric D4H cholesterol probes in mice .....	58
<b>Figure 3:</b> Neuronal cholesterol distribution in <i>Npc1<sup>KO</sup></i> mice.....	60
<b>Figure 4:</b> Neuronal cholesterol distribution in <i>Ptchd1<sup>KO</sup></i> mice .....	62
<b>Figure 5:</b> Adaptation of D4H probes for probing astrocyte-specific cholesterol distribution .....	64
<b>Figure supplement 1 – related to figure 4</b> Summary of lipidomic comparison of wild-type and <i>Ptchd1<sup>KO</sup></i> tissue .....	65
<b>Figure supplement 2 – related to figure 5</b> AAV vectors for cell-type specific visualization of cholesterol distribution.....	66
<b>Figure supplement 3</b> Comparison of key amino acid residues in sterol-sensing domains in mouse proteins.....	68
<b>Figure 6:</b> <i>Ptchd1</i> sub-cellular localization in vitro .....	76
<b>Figure 7:</b> <i>Ptchd1</i> pathogenic mutations and potential protein interactors .....	79

## **Discussion and future directions**

**Figure 1:** Assessment of Ptchd1 biological function..... 87

**Figure 2:** Cell-type specific cholesterol distribution in the mouse brain ..... 91

# Index of abbreviations

A = Alanine  
AAV = Adeno-associated virus  
Abca1 = ATP-binding cassette transporter  
AchR = Acetylcholine receptor  
ADHD = Attention deficit/hyperactivity disorder  
AIMS2-TRIALS = Autism Innovative Medicine Studies-2-Trials  
Akt = RAC-alpha serine/threonine-protein kinase  
AMPA =  $\alpha$ -amino-3-hydroxy-5-methyl-4-isoxazolepropionic acid  
ApoE = Apolipoprotein E  
AS = Asperger's Syndrome  
ASD = Autism spectrum disorders  
AU = Arbitrary unit  
audTRN = auditory TRN  
BBB = Blood-brain barrier  
BRET = Bioluminescence resonance energy transfer  
Bsn = Bassoon presynaptic cytomatrix protein  
C = Cytosine  
CANDY = Comorbid Analysis of Neurodevelopmental Disorders and Epilepsy  
CamK2a = Calcium/calmodulin-dependent protein kinase type II subunit alpha  
CAT = Cliff avoidance test  
CA<sub>v</sub> = voltage-gated P-type calcium channel  
CER = Ceramide  
CL = Cardiolipin  
CNS = Central nervous system  
CNV = Copy number variation  
CTEP = 2-chloro-4-((2,5-dimethyl-1-(4-(trifluoromethoxy)phenyl)-1H-imidazol-4-yl)ethynyl)pyridine, mGluR5 inhibitor  
Cyp46a1 = Cytochrome P450 46A1, cholesterol 24-hydroxylase  
D = Aspartic acid  
D4 = PFO-derived domain 4  
D4H = D4 with higher affinity  
DG = Dentate gyrus  
7Dhcr = 7-dehydrocholesterol reductase  
Dhcr24 = Delta(24)-sterol reductase  
DiO = Double-floxed inverted orientation  
Disp1 = Dispatched-1 protein  
DNA = Deoxyribonucleic acid  
DSM-5 = Diagnostic and statistical manual of mental disorders  
DTI = Diffusion tensor imaging  
E = Glutamic acid  
1-EBIO = 1-ethyl-2-benzimidazolinone, activator of calcium-activated potassium channels  
EEA1 = Early endosome antigen 1

EEG = Electroencephalogram  
eGFP = enhanced GFP  
Egr1 = Early growth response protein 1  
E/I = Excitation/Inhibition  
EPSC = Excitatory post-synaptic current  
ER = Endoplasmic reticulum  
FC = Fold-change  
FCA = Fluorescent cholesterol analog  
Fmrp = Fragile X mental retardation protein  
FXS = Fragile X Syndrome  
G = Guanine (for nucleotides) or Glycine (for amino acids)  
GABA =  $\gamma$ -aminobutyric acid  
GC = Granule cell  
GCL = Granule cell layer  
GfaABC1D = truncated GFAP promoter  
GFAP = Glial fibrillary acidic protein  
GFP = Green fluorescent protein  
GI = Gastro-intestinal  
GlcCER = Glucosylceramide  
GLI = *Glioma-associated oncogene*  
GM130 = 130 kDa cis-Golgi matrix protein  
HA = Hemagglutinin  
HEK293T = Human embryonic kidney 293T cells  
HDL = *High-density lipoprotein*  
Hh = Hedgehog  
Hmgcr = 3-hydroxy-3-methylglutaryl-coenzyme A reductase  
Hprt = Hypoxanthine Phosphoribosyltransferase  
hSyn = human Synapsin promoter  
I = Isoleucine  
ID = Intellectual disability  
Insig = Insuline-induced gene protein  
iPSC = induced Pluripotent stem cell  
IPSC = Inhibitory post-synaptic current  
KEGG = Kyoto Encyclopedia of Genes and Genomes  
KO = Knock-Out  
Lamp1 = Lysosome-associated membrane glycoprotein 1  
LE/LY= Late endosome/Lysosome  
LDL = Low-density lipoprotein  
LOPIT-DC = Localisation of organelle proteins by isotope tagging after differential ultracentrifugation  
Lrp1 = Low-density lipoprotein receptor-related protein 1  
LTD = Long-term depression  
LTP = Long-term potentiation  
March6 = E3 ubiquitin-protein ligase MARCH6  
MbCDX = methyl  $\beta$ -cyclodextrin



Mecp2 = methyl CpG binding protein 2  
mGluR = metabotropic Glutamatergic receptor  
miRNA = micro RNA  
MPEP = 2-Methyl-6-(phenylethynyl)pyridine, mGluR5 inhibitor  
MRI = Magnetic resonance imaging  
mRNA = messenger RNA  
mTOR = mammalian Target of rapamycin (Serine/threonine-protein kinase)  
Myr/P = Myristoylated/Palmitoylated  
Na<sup>+</sup> = sodium  
NAD = Nicotinamide adenine dinucleotide  
ncRNA = non-coding RNA  
NDD = Neurodevelopmental disorders  
NEDD8 = Neuronal precursor cell-expressed developmentally down-regulated protein 8  
NMDA = N-methyl-D-aspartate  
Npas4 = Neuronal PAS domain protein 4  
NPC = Niemann-Pick disease type C  
NPC1 = NPC intracellular cholesterol transporter 1  
NPC1L1 = NPC1-like 1 protein  
NPC2 = NPC intracellular cholesterol transporter 2  
24-OHC = 24-hydroxycholesterol  
OFT = Open-field test  
P = Proline  
p53 = Cellular tumor antigen p53  
pA = Polyadenylation sequence  
PC = Phosphatidylcholine  
PDD-NOS = Pervasive developmental disorder – not otherwise specified  
PDZbm = PDZ-binding motif  
PE = Phosphatidylethanolamine  
PFC = Prefrontal cortex  
PFO = Perfringolysin O  
PI = Phosphatidylinositol  
PI3K = Phosphoinositide 3-Kinase  
PM = Plasma membrane  
PS = Phosphatidylserine  
Psd95 = Post-synaptic density 95 protein  
Ptch1 = Protein patched homolog 1  
Ptchd1 = Patched-domain containing 1  
Ptchd1-AS = Ptchd1 anti-sense ncRNA  
Pten = Phosphatidylinositol 3,4,5-trisphosphate 3-phosphatase and dual-specificity protein phosphatase  
PV = Parvalbumin  
Q = Glutamine  
Rab9 = Ras-related protein Rab-9A  
RNA = Ribonucleic acid  
RND = Resistance/nodulation/division

Rnf145 = RING finger protein 145  
RS = Rett Syndrome  
RT-qPCR = Reverse transcription quantitative real-time polymerase chain reaction  
S = Serine  
Scap = Sterol regulatory element-binding protein cleavage-activating protein  
SCD = Social communication disorder  
SD = Standard deviation  
SEM = Standard deviation of error of measurement  
SFARI = Simons Foundation Autism Research Initiative  
SHANK = SH3 and multiple ankyrin repeat domain  
SK = Small conduction calcium-activated potassium channel  
SLOS = Smith-Lemli-Opitz Syndrome  
SM = Sphingomyelin  
Smo = Smoothed  
SNARE = *Soluble N-ethylmaleimide-sensitive-factor attachment protein receptor*  
SNP = Single nucleotide polymorphism  
SNV = Single nucleotide variant  
Snx27 = Sortin nexin-27 protein  
Sqle = Squalene epoxidase  
SRE = Sterol regulatory elements  
SREBP = Sterol regulatory elements-binding protein  
SSD = Sterol-sensing domain  
SSDL = Sterol-sensing domain-like  
SV = Synaptic vesicle  
Syn = Synapsin promoter  
Syngap1 = Ras/Rap GTPase-activating protein SynGAP  
Syt1 = Synaptotagmin-1 protein  
T = Threonine  
T2A = self-cleaving 2A peptide  
TF = Transcription factor  
TM = Transmembrane  
Trem2 = Triggering receptor expressed on myeloid cells 2  
TRN = Thalamic reticular nucleus  
Uba3 = NEDD8-activating enzyme E1 catalytic subunit  
UI = Unsaturation index  
3'UTR = 3' untranslated region  
Vamp3 = Vesicle-associated membrane protein 3  
Vps26 = Vacuolar protein sorting-associated 26 protein  
Vps35 = Vacuolar protein sorting-associated 35 protein  
W = Tryptophan  
WPRE = Woodchuck hepatitis virus post-transcriptional regulatory element  
Y = Tyrosine  
YDA = D4 with Y415A/D434W/A463W mutations  
YQDA = D4 with Y415A/Q433W/D434W/A463W mutations

## **6. *References***

## References

- Allen J.A., Halverson-Tamboli R.A., Rasenick M.M. (2007). Lipid raft microdomains and neurotransmitter signalling. *Nat Rev Neurosci* 8, 128-140.
- Amir R.E., Van den Veyver I.B., Wan M., Tran C.Q., Francke U., Zoghbi H.Y. (1999). Rett syndrome is caused by mutations in X-linked MECP2, encoding methyl-CpG-binding protein 2. *Nat Genet.* 23, 185-188.
- American Psychiatric Association (2013). Diagnostic and statistical manual of mental disorders (DSM-5). Washington DC: American Psychiatric Publishing
- Anderson J.S., Druzgal T.J., Froehlich A., DuBray M.B., Lange N., Alexander A.L., Abildskov T., Lainhart J.E., *et al.* (2011). Decreased interhemispheric functional connectivity in autism. *Cereb Cortex.* 21, 1134-46.
- Aneja A., Tierney E. Autism: the role of cholesterol in treatment. (2008). *Int Rev Psychiatry.* 2, 165-70.
- Armstrong N.M., An Y., Beason-Held L., Doshi J., Erus G., Ferrucci L., Davatzikos C., Resnick S.M. (2019). Sex differences in brain aging and predictors of neurodegeneration in cognitively healthy older adults. *Neurobiol Aging.* 81, 146-156.
- Aksoy-Aksel, A., Zampa, F., and Schrott, G. (2014). MicroRNAs and synaptic plasticity— a mutual relationship. *Philos. Trans. R. Soc. B Biol. Sci.* 369, 20130515.
- Asiminas, A., Jackson, A.D., Louros, S.R., Till, S.M., Spano, T., Dando, O., Bear, M.F., Chattarji, S., *et al.* (2019). Sustained correction of associative learning deficits after brief, early treatment in a rat model of Fragile X Syndrome. *Science translational medicine* 11.
- Atasoy, D., Aponte, Y., Su, H.H., and Sternson, S.M. (2008). A FLEX switch targets Channelrhodopsin-2 to multiple cell types for imaging and long-range circuit mapping. *J Neurosci* 28, 7025-7030.
- Bai D., Marrus N., Yip B.H.K., Reichenberg A., Constantino J.N., Sandin S. (2020) Inherited Risk for Autism Through Maternal and Paternal Lineage. *Biol Psychiatry.* 88, 480-487.
- Baier C.J., Fantini J., Barrantes F.J. (2011). Disclosure of cholesterol recognition motifs in transmembrane domains of the human nicotinic acetylcholine receptor. *Sci Rep.* 1, 69.
- Barrantes F.J. (2007). Cholesterol effects on nicotinic acetylcholine receptor. *J Neurochem.* 103, 72-80.
- Basilico, B., Morandell, J., and Novarino, G. (2020). Molecular mechanisms for targeted ASD treatments. *Curr Opin Genet Dev* 65, 126-137.
- Baxter A.J., Brugha T.S., Erskine H.E., Scheurer R.W., Vos T., Scott J.G. (2015). The epidemiology and global burden of autism spectrum disorders. *Psychol Med.* 45, 601-13.
- Beggiato A., Peyre H., Maruani A., Scheid I., Rastam M., Amsellem F., Gillberg C.I., Leboyer M., Bourgeron T., Gillberg C., Delorme R. (2017). Gender differences in autism spectrum disorders: Divergence among specific core symptoms. *Autism Res.* 10, 680-689.

- Berghoff S.A., Spieth L., Sun T., Hosang L., Depp C., Sasmita A.O., Vasileva M.H., Scholz P., Zhao Y., Saher G., *et al.* (2021). Neuronal cholesterol synthesis is essential for repair of chronically demyelinated lesions in mice. *Cell Rep.* **37**, 109889.
- Berry-Kravis E. (2021). Niemann-Pick Disease, Type C: Diagnosis, Management and Disease-Targeted Therapies in Development. *Semin Pediatr Neurol.* **37**, 100879.
- Berry-Kravis, E., Levin, R., Shah, H., Mathur, S., Darnell, J.C., and Ouyang, B. (2015). Cholesterol levels in fragile X syndrome. *Am J Med Genet A* **167A**, 379-384.
- Bhakar, A.L., Dolen, G., and Bear, M.F. (2012). The pathophysiology of fragile X (and what it teaches us about synapses). *Annu Rev Neurosci* **35**, 417-443.
- Björkhem I., Meaney S. (2004). Brain cholesterol: long secret life behind a barrier. *Arterioscler Thromb Vasc Biol.* **24**, 806-15.
- Bohlen C.J., Bennett F.C., Tucker A.F., Collins H.Y., Mulinyawe S.B., Barres B.A. (2017). Diverse Requirements for Microglial Survival, Specification, and Function Revealed by Defined-Medium Cultures. *Neuron.* **94**, 759-773.
- Bolard J. (1986). How do the polyene macrolide antibiotics affect the cellular membrane properties? *Biochim Biophys Acta.* **864**, 257-304.
- Bourgeron T. (2015). From the genetic architecture to synaptic plasticity in autism spectrum disorder. *Nat Rev Neurosci.* **16**, 551-563.
- Brachet, A., Norwood, S., Brouwers, J.F., Palomer, E., Helms, J.B., Dotti, C.G., and Esteban, J.A. (2015). LTP-triggered cholesterol redistribution activates Cdc42 and drives AMPA receptor synaptic delivery. *The Journal of cell biology* **208**, 791-806.
- Brockmann, M. M., Döngi, M., Einsfelder, U., Körber, N., Refojo, D., and Stein, V. (2019). neddylation regulates excitatory synaptic transmission and plasticity. *Scientific Reports* **9**, 1-10.
- Brown M.S., Goldstein J.L. (1999). A proteolytic pathway that controls the cholesterol content of membranes, cells, and blood. *Proc Natl Acad Sci USA* **96**, 11041-11048.
- Brown M.S., Radhakrishnan A., Goldstein J.L. (2018). Retrospective on Cholesterol Homeostasis: The Central Role of Scap. *Annu Rev Biochem.* **87**, 783-807.
- Buchovecky, C.M., Turley, S.D., Brown, H.M., Kyle, S.M., McDonald, J.G., Liu, B., Pieper, A.A., Huang, W., *et al.* (2013). A suppressor screen in *Mecp2* mutant mice implicates cholesterol metabolism in Rett syndrome. *Nat Genet* **45**, 1013-1020.
- Butler J.D., Comly M.E., Kruth H.S., Vanier M., Filling-Katz M., Fink J., Barton N., Weintraub H., Tokoro T., *et al.* (1987). Niemann-pick variant disorders: comparison of errors of cellular cholesterol homeostasis in group D and group C fibroblasts. *Proc Natl Acad Sci USA.* **84**, 556-560.
- Cadena Del Castillo, C.E., Hannich, J.T., Kaech, A., Chiyoda, H., Brewer, J., Fukuyama, M., Faergeman, N.J., Riezman, H., *et al.* (2021). Patched regulates lipid homeostasis by controlling cellular cholesterol levels. *Nat Commun* **12**, 4898.

- Cantuti-Castelvetri L., Fitzner D., Bosch-Queralt M., Weil M.T., Su M., Sen P., Ruhwedel T., Mitkovski M., Trendelenburg G., Lütjohann D., Möbius W., Simons M. (2018). Defective cholesterol clearance limits remyelination in the aged central nervous system. *Science*. 359, 684-688.
- Castro J., Mellios N., Sur M. (2013). Mechanisms and therapeutic challenges in autism spectrum disorders: insights from Rett syndrome. *Curr Opin Neurol*. 26, 154-159.
- Chahrour M., Jung S.Y., Shaw C., Zhou X., Wong S.T., Qin J., Zoghbi H.Y. (2008). MeCP2, a key contributor to neurological disease, activates and represses transcription. *Science*. 320, 1224-9.
- Chamberlain L.H., Burgoyne R.D., Gould G.W. (2001). SNARE proteins are highly enriched in lipid rafts in PC12 cells: implications for the spatial control of exocytosis. *Proc Natl Acad Sci USA* 98, 5619-562.
- Champigny C., Morin-Parent F., Bellehumeur-Lefebvre L., Çaku A., Lepage J.F., Corbin F. (2021). Combining Lovastatin and Minocycline for the Treatment of Fragile X Syndrome: Results From the LovaMiX Clinical Trial. *Front Psychiatry*. 12, 762967.
- Chan K.Y., Jang M.J., Yoo B.B., Greenbaum A., Ravi N., Wu W.L., Sánchez-Guardado L., Lois C., Mazmanian S.K., Deverman B.E., Gradinaru V. (2017). Engineered AAVs for efficient noninvasive gene delivery to the central and peripheral nervous systems. *Nat Neurosci*. 2, 1172-1179.
- Chaudhry, A., Noor, A., Degagne, B., Baker, K., Bok, L.A., Brady, M.F., Chitayat, D., Chung, B.H., Dymont, D. *et al.* (2015). Phenotypic spectrum associated with PTCHD1 deletions and truncating mutations includes intellectual disability and autism spectrum disorder. *Clin. Genet*. 88, 224-233.
- Chen, Y., Neve, R. L., and Liu, H. (2012). Neddylation dysfunction in Alzheimer's disease. *Journal of Cellular and Molecular Medicine*, 16 ,2583-2591.
- Cheroni C., Caporale N., Testa G. (2020). Autism spectrum disorder at the crossroad between genes and environment: contributions, convergences, and interactions in ASD developmental pathophysiology. *Mol Autism*. 11, 69.
- Christensen J., Overgaard M., Parner E.T., Vestergaard M., Schendel D. (2016). Risk of epilepsy and autism in full and half siblings-A population-based cohort study. *Epilepsia*. 57, 2011-2018.
- Colombo, A., Dinkel, L., Muller, S.A., Sebastian Monasor, L., Schifferer, M., Cantuti-Castelvetri, L., Konig, J., Vidatic, L., *et al.* (2021). Loss of NPC1 enhances phagocytic uptake and impairs lipid trafficking in microglia. *Nat Commun* 12, 1158.
- Coman D., Vissers L., Waterham H., Christodoulou J., Wevers R.A., Pitt J. (2020). Squalene Synthase Deficiency. *GeneReviews*® Seattle.
- Cooper M.K., Porter J.A., Young K.E., Beachy P.A. (1998). Teratogen-mediated inhibition of target tissue response to Shh signaling. *Science*. 280, 1603-7.
- Crawford D.C., Acuña J.M., Sherman S.L. (2001). FMR1 and the fragile X syndrome: human genome epidemiology review. *Genet Med*. 3, 359-371.
- Croen L.A., Zerbo O., Qian Y., Massolo M.L., Rich S., Sidney S., Kripke C. (2015). The health status of adults on the autism spectrum. *Autism*. 19, 814-823.

- Cunniff C., Kratz L.E., Moser A., Natowicz M.R., Kelley R.I. (1997). Clinical and biochemical spectrum of patients with RSH/Smith-Lemli-Opitz syndrome and abnormal cholesterol metabolism. *Am J Med Genet.* *68*, 263-269.
- Darnell J.C., Van Driesche S.J., Zhang C., Hung K.Y., Mele A., Fraser C.E., Stone E.F., Chen C., Darnell R.B., *et al.* (2011). FMRP stalls ribosomal translocation on mRNAs linked to synaptic function and autism. *Cell.* *146*, 247-261.
- Das, A., Goldstein, J.L., Anderson, D.D., Brown, M.S., Radhakrishnan, A. (2013). Use of mutant 125I-perfringolysin O to probe transport and organization of cholesterol in membranes of animal cells. *Proc. Natl. Acad. Sci. USA* *110*, 10580-10585.
- David, M.M., Enard, D., Ozturk, A., Daniels, J., Jung, J.Y., Diaz-Beltran, L., and Wall, D.P. (2016). Comorbid Analysis of Genes Associated with Autism Spectrum Disorders Reveals Differential Evolutionary Constraints. *PLoS One* *11*, e0157937.
- Davidson C.D., Ali N.F., Micsenyi M.C., Stephney G., Renault S., Dobrenis K., Ory D.S., Vanier M.T., Walkley S.U. (2009). Chronic cyclodextrin treatment of murine Niemann-Pick C disease ameliorates neuronal cholesterol and glycosphingolipid storage and disease progression. *PLoS One.* *4*, 6951.
- DeBarber A.E., Eroglu Y., Merkens L.S., Pappu A.S., Steiner R.D. (2011). Smith-Lemli-Opitz syndrome. *Expert Rev Mol Med.* *13*, 24.
- DeBose-Boyd R.A. (2008). Feedback regulation of cholesterol synthesis: sterol-accelerated ubiquitination and degradation of HMG CoA reductase. *Cell Res.* *18*, 609-621.
- de la Torre-Ubieta L., Won H., Stein J.L., Geschwind D.H. (2016). Advancing the understanding of autism disease mechanisms through genetics. *Nat Med.* *22*, 345-61.
- Delorme, R., Ey, E., Toro, R., Leboyer, M., Gillberg, C., and Bourgeron, T. (2013). Progress toward treatments for synaptic defects in autism. *Nat. Med.* *19*, 685-694.
- Dehorter N., Del Pino I. (2020). Shifting Developmental Trajectories During Critical Periods of Brain Formation. *Front Cell Neurosci.* *14*, 283.
- Diaz-Stransky A., Tierney E. (2012). Cognitive and behavioral aspects of Smith-Lemli-Opitz syndrome. *Am J Med Genet C Semin Med Genet.* *160C*, 295-300.
- Dietschy J.M., Turley S.D. (2004). Thematic review series: brain Lipids. Cholesterol metabolism in the central nervous system during early development and in the mature animal. *Lipid Res.* *45*, 1375-1397.
- Dil Kuazi A., Kito K., Abe Y., Shin R.W., Kamitani T., Ueda N. (2003). NEDD8 protein is involved in ubiquitinated inclusion bodies. *J Pathol.* *199*, 259-266.
- Duncan, A.L., Song, W., and Sansom, M.S.P. (2020). Lipid-Dependent Regulation of Ion Channels and G Protein-Coupled Receptors: Insights from Structures and Simulations. *Annu Rev Pharmacol Toxicol* *60*, 31-50.
- Dworzynski K., Ronald A., Bolton P., Happé F. (2012). How different are girls and boys above and below the diagnostic threshold for autism spectrum disorders? *J Am Acad Child Adolesc Psychiatry.* *51*, 788-97.

- Dziobek I., Gold S.M., Wolf O.T., Convit A. (2007). Hypercholesterolemia in Asperger syndrome: Independence from lifestyle, obsessive-compulsive behavior, and social anxiety. *Psychiatry Res* 149, 321– 324.
- Ebrahimi-Fakhari D., Sahin M. (2015). Autism and the synapse: emerging mechanisms and mechanism-based therapies. *Curr Opin Neurol.* 1, 1-12.
- Elsabbagh M., Divan G., Koh Y.J., Kim Y.S., Kauchali S., Marcín C., Montiel-Nava C., Patel V., Paula C.S., Wang C., Yasamy M.T., Fombonne E. (2012). Global prevalence of autism and other pervasive developmental disorders. *Autism Res.* 5, 160-79.
- Esposito C.M., Buoli M., Ciappolino V., Agostoni C., Brambilla P. (2021). The Role of Cholesterol and Fatty Acids in the Etiology and Diagnosis of Autism Spectrum Disorders. *Int J Mol Sci.* 22, 3550.
- Firth, H.V., Richards, S.M., Bevan, A.P., Clayton, S., Corpas, M., Rajan, D., van Vooren, S., Moreau, Y., Pettett, R.M., Carter, N.P. (2009). DECIPHER: Database of Chromosomal Imbalance and Phenotype in Humans Using Ensembl Resources. *Am. J. Hum. Genet.* 84, 524–533.
- Fogerson, P.M., Huguenard, J.R. (2016). Tapping the Brakes: Cellular and Synaptic Mechanisms that Regulate Thalamic Oscillations. *Neuron* 92, 687-704.
- Frank C., Giammarioli A.M., Pepponi R., Fiorentini C., Rufini S. (2004). Cholesterol perturbing agents inhibit NMDA-dependent calcium influx in rat hippocampal primary culture. *FEBS Lett.* 566, 25-29.
- Franklin T.B., Russig H., Weiss I.C., Gräff J., Linder N., Michalon A., Vizi S., Mansuy I.M. (2010). Epigenetic transmission of the impact of early stress across generations. *Biol Psychiatry.* 68, 408-415.
- Fromer M., Pocklington A.J., Kavanagh D.H., Williams H.J., Dwyer S., Gormley P., Rees E., O'Donovan M.C., *et al.* (2014). De novo mutations in schizophrenia implicate synaptic networks. *Nature.* 506, 179-184.
- Fünfschilling U., Jockusch W.J., Sivakumar N., Möbius W., Corthals K., Li S., Quintes S., Kim Y., Schaap I.A., Rhee J.S., Nave K.A., Saher G. (2012). Critical time window of neuronal cholesterol synthesis during neurite outgrowth. *J Neurosci.* 32, 7632-45.
- Ganley I.G., Pfeffer S.R. (2006). Cholesterol accumulation sequesters Rab9 and disrupts late endosome function in NPC1-deficient cells. *J Biol Chem.* 281, 17890-9.
- Gaugler T., Klei L., Sanders S.J., Bodea C.A., Goldberg A.P., Lee A.B., Mahajan M., Manaa D., Pawitan Y., Reichert J., Buxbaum J.D., *et al.* (2014). Most genetic risk for autism resides with common variation. *Nat Genet.* 46, 881-5.
- Gaylor J.L. (2002). Membrane-bound enzymes of cholesterol synthesis from lanosterol. *Biochem Biophys Res Commun.* 292, 1139-46.
- Geberhiwot T., Moro A., Dardis A., Ramaswami U., Sirrs S., Marfa M.P., Vanier M.T., Walterfang M., Patterson M., *et al.* (2018). Consensus clinical management guidelines for Niemann-Pick disease type C. *Orphanet J Rare Dis.* 13, 50.



- Geladaki, A., Kočevár Britovšek, N., Breckels, L.M., Smith T.S., Vennard O.L., Mulvey C.M., Crook O.M., Gatto L. and Lilley K.S. (2019). Combining LOPIT with differential ultracentrifugation for high-resolution spatial proteomics. *Nat Commun* 10, 331.
- Gelsthorpe M.E., Baumann N., Millard E., Gale S.E., Langmade S.J., Schaffer J.E., Ory D.S. (2008). Niemann-Pick type C1 I1061T mutant encodes a functional protein that is selected for endoplasmic reticulum-associated degradation due to protein misfolding. *J Biol Chem*. 283, 8229-36.
- Giles C., Takechi R., Lam V., Dhaliwal S.S., Mamo J.C.L. (2018). Contemporary lipidomic analytics: opportunities and pitfalls. *Prog Lipid Res*. 71, 86-100.
- Gillberg, C., Fernell, E., Kocovska, E., Minnis, H., Bourgeron, T., Thompson, L., and Allely, C.S. (2017). The role of cholesterol metabolism and various steroid abnormalities in autism spectrum disorders: A hypothesis paper. *Autism Res* 10, 1022-1044.
- Gimpl G., Gehrig-Burger K. (2007). Cholesterol reporter molecules. *Biosci Rep*. 27, 335-358.
- Gimpl, G., and Fahrenholz, F. (2001). The oxytocin receptor system: structure, function, and regulation. *Physiological reviews* 81, 629-683.
- Girirajan S., Brkanac Z., Coe B.P., Baker C., Vives L., Vu T.H., Shafer N., Bernier R., Ferrero G.B., Silengo M., Eichler E.E., *et al.* (2011). Relative burden of large CNVs on a range of neurodevelopmental phenotypes. *PLoS Genet*. 7, 1002334.
- Goldstein J.L., Brown M.S. (1990). Regulation of the mevalonate pathway. *Nature*. 343, 425-430.
- Gong, X., Qian, H., Cao, P., Zhao, X., Zhou, Q., Lei, J., and Yan, N. (2018). Structural basis for the recognition of Sonic Hedgehog by human Patched1. *Science*. 361.
- Gong X., Qian H., Zhou X., Wu J., Wan T., Cao P., Huang W., Zhao X., Wang X., Wang P., Shi Y., Gao G.F., Zhou Q., Yan N. (2016). Structural Insights into the Niemann-Pick C1 (NPC1)-Mediated Cholesterol Transfer and Ebola Infection. *Cell*. 165, 1467-1478.
- Göritz C., Mauch D.H., Pfrieder F.W. (2005). Multiple mechanisms mediate cholesterol-induced synaptogenesis in a CNS neuron. *Mol Cell Neurosci* 29, 190-201.
- Guttenplan K.A., Weigel M.K., Prakash P., Wijewardhane P.R., Hasel P., Rufen-Blanchette U., Münch A.E., Blum J.A., Fine J., Neal M.C., Bruce K.D., Gitler A.D., Chopra G., Liddel S.A., Barres B.A. (2021). Neurotoxic reactive astrocytes induce cell death via saturated lipids. *Nature*. 599,102-107.
- Hagerman R.J., Berry-Kravis E., Hazlett H.C., Bailey D.B. Jr., Moine H., Kooy R.F., Tassone F., Hagerman P.J., *et al.* (2017). Fragile X syndrome. *Nat Rev Dis Primers*. 3, 17065.
- Halassa, M.M., Chen, Z., Wimmer, R.D., Brunetti, P.M., Zhao, S., Zikopoulos, B., Wang, F., Brown, E.N., Wilson, M.A. (2014). State-dependent architecture of thalamic reticular subnetworks. *Cell* 158, 808-821.
- Halewa, J., Marouillat, S., Dixneuf, M., Thépault, R.A., Ung, D.C., Chatron, N., Gérard, B., Ghomid, J., *et al.* (2021). Novel missense mutations in PTCHD1 alter its plasma membrane subcellular localization and cause intellectual disability and autism spectrum disorder. *Hum. Mutat*. 42, 848-861.

- Hallmayer J., Cleveland S., Torres A., Phillips J., Cohen B., Torigoe T., Miller J., Fedele A., Collins J., Smith K., Lotspeich L., Croen L.A., Ozonoff S., Lajonchere C., Grether J.K., Risch N. (2011). Genetic heritability and shared environmental factors among twin pairs with autism. *Arch Gen Psychiatry*. *68*, 1095-102.
- Hamodi A.S., Martinez Sabino A., Fitzgerald N.D., Moschou D., Crair M.C. (2020). Transverse sinus injections drive robust whole-brain expression of transgenes. *Elife*. *18*, 53639.
- Herz, J., and Bock, H.H. (2002). Lipoprotein receptors in the nervous system. *Annu Rev Biochem* *71*, 405-434.
- Heuck, A.P., Savva, C.G., Holzenburg, A., Johnson, A.E. (2007). Conformational changes that effect oligomerization and initiate pore formation are triggered throughout perfringolysin O upon binding to cholesterol. *J. Biol. Chem.* *282*, 22629–37.
- Hewitson L. (2013). Scientific challenges in developing biological markers for autism. *OA Autism* *1*, 7.
- Higgins M.E., Davies J.P., Chen F.W., Ioannou Y.A. (1999). Niemann-Pick C1 is a late endosome-resident protein that transiently associates with lysosomes and the trans-Golgi network. *Mol Genet Metab.* *68*, 1-13.
- Hoglund, K., Blennow, K. (2007). Effect of HMG-CoA reductase inhibitors on beta-amyloid peptide levels: implications for Alzheimer's disease. *CNS Drugs* *21*, 449-462.
- Hornberg, H., Perez-Garci, E., Schreiner, D., Hatstatt-Burkle, L., Magara, F., Baudouin, S., Matter, A., Nacro, K., *et al.* (2020). Rescue of oxytocin response and social behaviour in a mouse model of autism. *Nature* *584*, 252-256.
- Hu, A., Song, B.L. (2019). The interplay of Patched, Smoothed and cholesterol in Hedgehog signaling. *Curr. Opin. Cell Biol.* *61*, 31-38.
- Hu G, Antikainen R, Jousilahti P, Kivipelto M, Tuomilehto J. (2008). Total cholesterol and the risk of Parkinson disease. *Neurology* *70*, 1972-1979.
- Hua X., Sakai J., Brown M.S., Goldstein J.L. (1996). Regulated cleavage of sterol regulatory element binding proteins requires sequences on both sides of the endoplasmic reticulum membrane. *J Biol Chem.* *271*, 10379-84.
- Ikonen, E., and Zhou, X. (2021). Cholesterol transport between cellular membranes: A balancing act between interconnected lipid fluxes. *Dev Cell* *56*, 1430-1436.
- Iossifov I., O'Roak B.J., Sanders S.J., Ronemus M., Krumm N., Levy D., Stessman H.A., Wigler M., *et al.* (2014). The contribution of de novo coding mutations to autism spectrum disorder. *Nature*. *515*, 216-221.
- Ismail F.Y., Shapiro B.K. (2019). What are neurodevelopmental disorders? *Curr Opin Neurol.* *32*, 611-616.
- Itoh N., Itoh Y., Tassoni A., Ren E., Kaito M., Ohno A., Ao Y., Farkhondeh V., Johnsonbaugh H., Burda J., Sofroniew M.V., Voskuhl R.R. (2018). Cell-specific and region-specific transcriptomics in the multiple sclerosis model: Focus on astrocytes. *Proc Natl Acad Sci USA.* *115*, 302-309.

- Iwamoto M., Morita I., Fukuda M., Murota S., Ando S., Ohno-Iwashita Y. (1997). A biotinylated perfringolysin O derivative: a new probe for detection of cell surface cholesterol. *Biochim Biophys Acta.* 1327, 222-230.
- Jeong W., Lee H., Cho S., Seo J. (2019). ApoE4-Induced Cholesterol Dysregulation and Its Brain Cell Type-Specific Implications in the Pathogenesis of Alzheimer's Disease. *Mol Cells.* 42,739-746.
- Jiang L.Y., Jiang W., Tian N., Xiong Y.N., Liu J., Wei J., Wu K.Y., Luo J., Shi X.J., Song B.L. (2018). Ring finger protein 145 (RNF145) is a ubiquitin ligase for sterol-induced degradation of HMG-CoA reductase. *J Biol Chem.* 293, 4047-4055.
- Johnson, M. (2001). Functional brain development in humans. *Nat Rev Neurosci.* 2, 475–483.
- Johnson, B.B., Moe, P.C., Wang, D., Rossi, K., Trigatti, B.L., Heuck, A.P. (2012). Modifications in perfringolysin O domain 4 alter the cholesterol concentration threshold required for binding. *Biochemistry* 51, 3373-3382.
- Joubert B.R., Felix J.F., Yousefi P., Bakulski K.M., Just A.C., Breton C., Reese S.E., Markunas C.A., Richmond R.C., *et al.* (2016). DNA Methylation in Newborns and Maternal Smoking in Pregnancy: Genome-wide Consortium Meta-analysis. *Am J Hum Genet.* 98, 680-696.
- Kadish I., Thibault O., Blalock E.M., Chen K.C., Gant J.C., Porter N.M., Landfield P.W. (2009). Hippocampal and cognitive aging across the lifespan: a bioenergetic shift precedes and increased cholesterol trafficking parallels memory impairment. *J Neurosci.* 29, 1805-16.
- Kalinowska M., Castillo C., Francesconi A. (2015). Quantitative profiling of brain lipid raft proteome in a mouse model of fragile X syndrome. *PLoS One.* 10, 0121464.
- Kamitani, T., Kito, K., Nguyen, H. P., and Yeh, E. T. H. (1997). Characterization of NEDD8, a developmentally down-regulated ubiquitin-like protein. *Journal of Biological Chemistry* 272, 28557-28562.
- Kanungo S., Soares N., He M., Steiner R.D. (2013). Sterol metabolism disorders and neurodevelopment—an update. *Dev Disabil Res Rev.* 17, 197-210.
- Karaca, E., Harel, T., Pehlivan, D., Jhangiani, S.N., Gambin, T., Akdemir, Z.C., Gonzaga-Jauregui, C., *et al.* (2015). Genes that Affect Brain Structure and Function Identified by Rare Variant Analyses of Mendelian Neurologic Disease. *Neuron* 88, 499-513.
- Kelleher R.J. 3rd, Bear M.F. (2008). The autistic neuron: troubled translation? *Cell.* 135, 401-6.
- Keown C.L., Shih P., Nair A., Peterson N., Mulvey M.E., Müller R.A. (2013). Local functional overconnectivity in posterior brain regions is associated with symptom severity in autism spectrum disorders. *Cell Rep.* 5, 567-572.
- Kim, T.K., Hemberg, M., Gray, J.M., Costa, A.M., Bear, D.M., Wu, J., Harmin, D.A., Laptewicz, M., Kuersten, S., *et al.* (2010). Widespread transcription at neuronal activity-regulated enhancers. *Nature* 465, 182-187.
- Kim S.M., Mun B.R., Lee S.J., Joh Y., Lee H.Y., Ji K.Y., Choi H.R., Lee E.H., Kim E.M., Jang J.H., Song H.W., Mook-Jung I., Choi W.S., Kang H.S. (2017). TREM2 promotes A $\beta$  phagocytosis by upregulating C/EBP $\alpha$ -dependent CD36 expression in microglia. *Sci Rep.* 7, 11118.

- Kirov G., Rees E., Walters J.T., Escott-Price V., Georgieva L., Richards A.L., Chambert K.D., Davies G., Owen M.J., *et al.* (2014). The penetrance of copy number variations for schizophrenia and developmental delay. *Biol Psychiatry*. *75*, 378-385.
- Ko, S.Y., Epp, J., Mittal, K., Sheikh, T., Ha, V., Degagne, B., Mikhailov, A., French, L., Vincent, J.B., *et al.* (2019). Ptchd1 exon3 truncating mutations recapitulate more clinically relevant autistic-like traits in mice. *IBRO Rep*. *6*, 346-562.
- Koide T., Hayata T., Cho K.W. (2006). Negative regulation of Hedgehog signaling by the cholesterologenic enzyme 7-dehydrocholesterol reductase. *Development*. *133*, 2395-405.
- Knobloch M., Pilz G.A., Ghesquière B., Kovacs W.J., Wegleiter T., Moore D.L., Hruzova M., Zamboni N., Carmeliet P., Jessberger S. (2017). A Fatty Acid Oxidation-Dependent Metabolic Shift Regulates Adult Neural Stem Cell Activity. *Cell Rep*. *20*, 2144-2155.
- Koponen A., Arora A., Takahashi K., Kentala H., Kivelä A.M., Jääskeläinen E., Peränen J., Olkkonen V.M., *et al.* (2019). ORP2 interacts with phosphoinositides and controls the subcellular distribution of cholesterol. *Biochimie*. *158*, 90-101.
- Koponen A., Pan G., Kivelä A.M., Ralko A., Taskinen J.H., Arora A., Kosonen R., Kari O.K., Ndika J., Olkkonen V.M., *et al.* (2020). ORP2, a cholesterol transporter, regulates angiogenic signaling in endothelial cells. *FASEB J*. *34*, 14671-14694.
- Korade, Z., and Kenworthy, A. K. (2008). Lipid rafts, cholesterol, and the brain. *Neuropharmacology*. *55*, 1265–1273.
- Krakowski M., Czobor P. (2011). Cholesterol and cognition in schizophrenia: a double-blind study of patients randomized to clozapine, olanzapine and haloperidol. *Schizophr Res*. *130*, 27-33.
- Kudinov AR, Kudinova NV, Berezov TT (2006) Cholesterol is an important molecule in the processes of the synaptic plasticity and degeneration of neurons. *Vestn Ross Akad Med Nauk*. 61-66.
- Kuwabara, P.E., and Labouesse, M. (2002). The sterol-sensing domain: multiple families, a unique role? *Trends Genet* *18*, 193-201.
- Kyle S.M., Vashi N., Justice M.J. (2018). Rett syndrome: a neurological disorder with metabolic components. *Open Biol*. *8*, 170216.
- Ladd-Acosta C., Fallin M.D. (2016). The role of epigenetics in genetic and environmental epidemiology. *Epigenomics*. *8*, 271-283.
- Lai, M.C., Lombardo, M.V., Baron-Cohen, S. (2014). Autism. *Lancet*. *383*, 896-910.
- Lasič E., Lisjak M., Horvat A., Božić M., Šakanović A., Anderluh G., Verkhatsky A., Vardjan N., Jorgačevski J., Stenovec M., Zorec R. (2019). Astrocyte Specific Remodeling of Plasmalemmal Cholesterol Composition by Ketamine Indicates a New Mechanism of Antidepressant Action. *Sci Rep*. *9*, 10957.
- LeBlanc J.J., Fagiolini M. (2011). Autism: a "critical period" disorder? *Neural Plast*. *921680*.
- Leblond, C.S., Le, T.L., Malesys, S., Cliquet, F., Tabet, A.C., Delorme, R., Rolland, T., and Bourgeron, T. (2021). Operative list of genes associated with autism and neurodevelopmental disorders based on database review. *Mol Cell Neurosci* *113*, 103623.

- Lee B.K., Magnusson C., Gardner R.M., Blomström Å., Newschaffer C.J., Burstyn I., Karlsson H., Dalman C. (2015). Maternal hospitalization with infection during pregnancy and risk of autism spectrum disorders. *Brain Behav Immun.* *44*, 100-105.
- Lee, Y., Messing, A., Su, M., and Brenner, M. (2008). GFAP promoter elements required for region-specific and astrocyte-specific expression. *Glia* *56*, 481-493.
- Lee, R. W., and Tierney, E. (2011). Hypothesis: the role of sterols in autism spectrum disorder. *Autism Res. Treat.* *653570*.
- Leoni V., Mariotti C., Nanetti L., Salvatore E., Squitieri F., Bentivoglio A.R., Bandettini di Poggio M., Piacentini S., Monza D., Valenza M., Cattaneo E., Di Donato S. (2011). Whole body cholesterol metabolism is impaired in Huntington's disease. *Neurosci Lett* *494*, 245– 249.
- Li L.H., Dutkiewicz E.P., Huang Y.C., Zhou H.B., Hsu C.C. (2019). Analytical methods for cholesterol quantification. *J Food Drug Anal.* *27*, 375-386.
- Li, W., Cui, Y., Kushner, S. A., Brown, R. A., Jentsch, J. D., Frankland, P. W., et al. (2005). The HMG-CoA reductase inhibitor lovastatin reverses the learning and attention deficits in a mouse model of neurofibromatosis type 1. *Curr. Biol.* *15*, 1961-1967.
- Li, D., Zhang, J., and Liu, Q. (2022). Brain cell type-specific cholesterol metabolism and implications for learning and memory. *Trends in neurosciences* *45*, 401-414.
- Li Q., Barres B.A. (2018). Microglia and macrophages in brain homeostasis and disease. *Nat Rev Immunol.* *18*, 225-242.
- Lim C.Y., Davis O.B., Shin H.R., Zhang J., Berdan C.A., Jiang X., Counihan J.L., Ory D.S., Nomura D.K., Zoncu R. (2019). ER-lysosome contacts enable cholesterol sensing by mTORC1 and drive aberrant growth signalling in Niemann-Pick type C. *Nat Cell Biol.* *21*, 1206-1218.
- Lingwood D., Simons K. (2010). Lipid rafts as a membrane-organizing principle. *Science* *327*, 46-50.
- Lisik M.Z., Gutmajster E., Sieroń A.L. (2016). Low Levels of HDL in Fragile X Syndrome Patients. *Lipids.* *51*, 189-192.
- Liu Q., Trotter J., Zhang J., Peters M.M., Cheng H., Bao J., Han X., Weeber E.J., Bu G. (2010). Neuronal LRP1 knockout in adult mice leads to impaired brain lipid metabolism and progressive, age-dependent synapse loss and neurodegeneration. *J Neurosci.* *30*, 17068-78.
- Liu, S.L., Sheng, R., Jung, J.H., Wang, L., Stec, E., O'Connor, M.J., Song, S., Bikkavilli, R.K., Winn, R.A., Lee, D., *et al.* (2017). Orthogonal lipid sensors identify transbilayer asymmetry of plasma membrane cholesterol. *Nat. Chem. Biol.* *13*, 268-274.
- Lloyd-Evans E., Morgan A.J., He X., Smith D.A., Elliot-Smith E., Sillence D.J., Churchill G.C., Schuchman E.H., Galione A., Platt F.M. (2008). Niemann-Pick disease type C1 is a sphingosine storage disease that causes deregulation of lysosomal calcium. *Nat Med.* *14*, 1247-55.
- Lloyd-Evans E., Platt F.M. (2010). Lipids on trial: the search for the offending metabolite in Niemann-Pick type C disease. *Traffic.* *11*, 419-28.

- Linetti, A., Fratangeli, A., Taverna, E., Valnegri, P., Francolini, M., Cappello, V., et al. (2010). Cholesterol reduction impairs exocytosis of synaptic vesicles. *J. Cell Sci.* 123, 595-605.
- Lopez A.M., Chuang J.C., Posey K.S., Turley S.D. (2017). Suppression of brain cholesterol synthesis in male *Mecp2*-deficient mice is age dependent and not accompanied by a concurrent change in the rate of fatty acid synthesis. *Brain Res.* 1654, 77-84.
- Lopez, M.E., Klein, A.D., Dimbil, U.J., and Scott, M.P. (2011). Anatomically defined neuron-based rescue of neurodegenerative Niemann-Pick type C disorder. *J Neurosci* 31, 4367-4378.
- Lord C., Bishop S.L. (2015). Recent advances in autism research as reflected in DSM-5 criteria for autism spectrum disorder. *Annu Rev Clin Psychol.* 11, 53-70.
- Luo, Y., Eran, A., Palmer, N., Avillach, P., Levy-Moonshine, A., Szolovits, P., and Kohane, I.S. (2020). A multidimensional precision medicine approach identifies an autism subtype characterized by dyslipidemia. *Nature medicine* 26, 1375-1379.
- Lütjohann D., Lopez A.M., Chuang J.C., Kerksiek A., Turley S.D. (2018). Identification of Correlative Shifts in Indices of Brain Cholesterol Metabolism in the C57BL6/*Mecp2*<sup>tm1.1Bird</sup> Mouse, a Model for Rett Syndrome. *Lipids.* 53, 363-373.
- Lyall K., Croen L., Daniels J., Fallin M.D., Ladd-Acosta C., Lee B.K., Park B.Y., Snyder N.W., Schendel D., Volk H., Windham G.C., Newschaffer C. (2017). The Changing Epidemiology of Autism Spectrum Disorders. *Annu Rev Public Health.* 38, 81-102.
- Maas D.A., Martens M.B., Priovoulos N., Zuure W.A., Homberg J.R., Nait-Oumesmar B., Martens G.J.M. (2020). Key role for lipids in cognitive symptoms of schizophrenia. *Transl Psychiatry.* 10, 399.
- Maekawa, M. (2017). Domain 4 (D4) of Perfringolysin O to Visualize Cholesterol in Cellular Membranes-The Update. *Sensors (Basel)* 17.
- Maekawa, M., and Fairn, G.D. (2014). Molecular probes to visualize the location, organization and dynamics of lipids. *J Cell Sci* 127, 4801-4812.
- Maekawa, M., Fairn, G.D. (2015). Complementary probes reveal that phosphatidylserine is required for the proper transbilayer distribution of cholesterol. *J. Cell Sci.* 128, 1422-1433.
- Marek M., Vincenzetti V., Martin S.G. (2020). Sterol biosensor reveals LAM-family *Ltc1*-dependent sterol flow to endosomes upon *Arp2/3* inhibition. *J Cell Biol.* 219, 202001147.
- Maresca G., Formica C., Nocito V., Latella D., Leonardi S., De Cola M.C., Triglia G., Bramanti P., Corallo F. (2021). Neuropsychological assessment in Niemann-Pick disease type C: a systematic review. *Neurol Sci.* 42, 3167-3175.
- Marshall, C.R., Noor, A., Vincent, J.B., Lionel, A.C., Feuk, L., Skaug, J., Shago, M., Moessner, R., Pinto, D., Ren, Y., et al. (2008). Structural variation of chromosomes in autism spectrum disorder. *Am. J. Hum. Genet.* 82, 477-488.
- Martin M., Dotti C.G., Ledesma M.D. (2010). Brain cholesterol in normal and pathological aging. *Biochim Biophys Acta.* 1801, 934-44.
- Martin, M.G., Pfrieger, F., and Dotti, C.G. (2014). Cholesterol in brain disease: sometimes determinant and frequently implicated. *EMBO Rep* 15, 1036-1052.

- Mathews E.S., Appel B. (2016). Cholesterol Biosynthesis Supports Myelin Gene Expression and Axon Ensheathment through Modulation of P13K/Akt/mTor Signaling. *J Neurosci.* 36, 7628-39.
- Mathews E.S., Mawdsley D.J., Walker M., Hines J.H., Pozzoli M., Appel B. (2014). Mutation of 3-hydroxy-3-methylglutaryl CoA synthase I reveals requirements for isoprenoid and cholesterol synthesis in oligodendrocyte migration arrest, axon wrapping, and myelin gene expression. *J Neurosci.* 34, 3402-12.
- Matson J.L., Cervantes P.E. (2014). Commonly studied comorbid psychopathologies among persons with autism spectrum disorder. *Res Dev Disabil.* 35, 952-62.
- Mauch D.H., Nägler K., Schumacher S., Göritz C., Müller E.C., Otto A., Pfrieder F.W. (2001). CNS synaptogenesis promoted by glia-derived cholesterol. *Science* 294, 1354-1357.
- Maza, N., Wang, D., Kowalski, C., Stoveken, H.M., Dao, M., Sial, O.K., Giles, A.C., Grill, B., *et al.* (2022). Ptchd1 mediates opioid tolerance via cholesterol-dependent effects on mu-opioid receptor trafficking. *Nature neuroscience*, 25, 1179-1190.
- Menzies S.A., Volkmar N., van den Boomen D.J., Timms R.T., Dickson A.S., Nathan J.A., Lehner P.J. (2018). The sterol-responsive RNF145 E3 ubiquitin ligase mediates the degradation of HMG-CoA reductase together with gp78 and Hrd1. *Elife.* 7, 40009.
- Millat G., Chikh K., Naureckiene S., Sleat D.E., Fensom A.H., Higaki K., Elleder M., Lobel P., Vanier M.T. (2001). Niemann-Pick disease type C: spectrum of HE1 mutations and genotype/phenotype correlations in the NPC2 group. *Am J Hum Genet.* 69, 1013-1021.
- Millat G., Marcais C., Rafi M.A., Yamamoto T., Morris J.A., Pentchev P.G., Ohno K., Wenger D.A., Vanier M.T. (1999). Niemann-Pick C1 disease: the I1061T substitution is a frequent mutant allele in patients of Western European descent and correlates with a classic juvenile phenotype. *Am J Hum Genet.* 65, 1321-1329.
- Mitroi, D.N., Pereyra-Gomez, G., Soto-Huelin, B., Senovilla, F., Kobayashi, T., Esteban, J.A., and Ledesma, M.D. (2019). NPC1 enables cholesterol mobilization during long-term potentiation that can be restored in Niemann-Pick disease type C by CYP46A1 activation. *EMBO Rep* 20, e48143.
- Mondal M., Mesmin B., Mukherjee S., Maxfield F.R. (2009). Sterols are mainly in the cytoplasmic leaflet of the plasma membrane and the endocytic recycling compartment in CHO cells. *Mol Biol Cell* 20, 581-588.
- Morris-Rosendahl D.J., Crocq M.A. (2020). Neurodevelopmental disorders-the history and future of a diagnostic concept. *Dialogues Clin Neurosci.* 22, 65-72.
- Mullin A.P., Gokhale A., Sanyal S., Moreno-De-Luca A., Waddington J.L., Faundez V. (2013). Neurodevelopmental disorders: mechanisms and boundary definitions from genomes, interactomes and proteomes. *Transl Psychiatry.* 3, 329-336.
- Murakami, Y., Imamura, Y., Saito, K., Sakai, D., Motoyama, J. (2019). Altered kynurenine pathway metabolites in a mouse model of human attention-deficit hyperactivity/autism spectrum disorders: A potential new biological diagnostic marker. *Sci. Rep.* 9, 13182.

- Murakami S., Nakashima R., Yamashita E., Yamaguchi A. (2002). Crystal structure of bacterial multidrug efflux transporter AcrB. *Nature*. *419*, 587-593.
- Muscas M., Louros S.R., Osterweil E.K. (2019). Lovastatin, not Simvastatin, Corrects Core Phenotypes in the Fragile X Mouse Model. *eNeuro*. *6*.
- Myers B.R., Neahring L., Zhang Y., Roberts K.J., Beachy P.A. (2017). Rapid, direct activity assays for Smoothed reveal Hedgehog pathway regulation by membrane cholesterol and extracellular sodium. *Proc Natl Acad Sci U S A*. *114*, 11141-11150.
- Nakajima, M., Schmitt, L.I., Feng, G., Halassa, M.M. (2019). Combinatorial Targeting of Distributed Forebrain Networks Reverses Noise Hypersensitivity in a Model of Autism Spectrum Disorder. *Neuron* *104*, 488-500.
- Nakanishi, M., Anderson, M.P., and Takumi, T. (2019). Recent genetic and functional insights in autism spectrum disorder. *Curr Opin Neurol* *32*, 627-634.
- Nelson S.B., Valakh V. (2015). Excitatory/Inhibitory Balance and Circuit Homeostasis in Autism Spectrum Disorders. *Neuron*. *87* , 684-698.
- Neufeld E.B., Wastney M., Patel S., Suresh S., Cooney A.M., Dwyer N.K., Roff C.F., Ohno K., Morris J.A., Blanchette-Mackie E.J. (1999). The Niemann-Pick C1 protein resides in a vesicular compartment linked to retrograde transport of multiple lysosomal cargo. *J Biol Chem*. *274*, 9627-9635.
- Newschaffer C.J., Croen L.A., Daniels J., Giarelli E., Grether J.K., Levy S.E., Mandell D.S., Miller L.A., Windham GC., *et al.* (2007). The epidemiology of autism spectrum disorders. *Annu Rev Public Health*. *28*, 235-58.
- Nohturfft A., Brown M.S., Goldstein J.L. (1998). Topology of SREBP cleavage-activating protein, a polytopic membrane protein with a sterol-sensing domain. *J Biol Chem*. *273*, 17243-50.
- Noor, A., Whibley, A., Marshall, C.R., Gianakopoulos, P.J., Piton, A., Carson, A.R., Orlic-Milacic, M., Lionel, A.C., *et al.* (2010). Disruption at the PTCHD1 Locus on Xp22.11 in Autism spectrum disorder and intellectual disability. *Science translational medicine* *2*, 49ra68.
- Nowaczyk M.J., Irons M.B. (2012). Smith-Lemli-Opitz syndrome: phenotype, natural history, and epidemiology. *Am J Med Genet C Semin Med Genet*. *160C*, 250-262.
- Oates, J., and Watts, A. (2011). Uncovering the intimate relationship between lipids, cholesterol and GPCR activation. *Curr Opin Struct Biol* *21*, 802-807.
- Osterweil, E. K., Chuang, S. C., Chubykin, A. A., Sidorov, M., Bianchi, R., Wong, R. K., et al. (2013). Lovastatin corrects excess protein synthesis and prevents epileptogenesis in a mouse model of fragile X syndrome. *Neuron* *77*, 243-250.
- Owen M.J., O'Donovan M.C. (2017). Schizophrenia and the neurodevelopmental continuum:evidence from genomics. *World Psychiatry*. *16*, 227-235.
- Owen M.J., O'Donovan M.C., Thapar A., Craddock N. (2011). Neurodevelopmental hypothesis of schizophrenia. *Br J Psychiatry*. *198*, 173-175.



- Ozonoff S., Young G.S., Carter A., Messinger D., Yirmiya N., Zwaigenbaum L., Bryson S., Carver L.J., Constantino J.N., Stone W.L., *et al.* (2011). Recurrence risk for autism spectrum disorders: a Baby Siblings Research Consortium study. *Pediatrics*. *128*, 488-95.
- Pacheco N.L., Heaven M.R., Holt L.M., Crossman D.K., Boggio K.J., Shaffer S.A., Flint D.L., Olsen M.L. (2018). RNA sequencing and proteomics approaches reveal novel deficits in the cortex of *Mecp2*-deficient mice, a model for Rett syndrome. *Mol Autism*. *8*, 56.
- Papandreou A., Gissen P. (2016). Diagnostic workup and management of patients with suspected Niemann-Pick type C disease. *Ther Adv Neurol Disord*. *9*, 216-29.
- Parkhurst C.N., Yang G., Ninan I., Savas J.N., Yates J.R. 3rd, Lafaille J.J., Hempstead B.L., Littman D.R., Gan W.B. (2013). Microglia promote learning-dependent synapse formation through brain-derived neurotrophic factor. *Cell*. *155*, 1596-609.
- Pastore S.F., Ko S.Y., Frankland P.W., Hamel P.A., Vincent J.B. (2022). *PTCHD1*: Identification and Neurodevelopmental Contributions of an Autism Spectrum Disorder and Intellectual Disability Susceptibility Gene. *Genes (Basel)*. *13*, 527.
- Paul S.M., Doherty J.J., Robichaud A.J., Belfort G.M., Chow B.Y., Hammond R.S., Crawford D.C., Izumi Y., *et al.* (2013). The major brain cholesterol metabolite 24(S)-hydroxycholesterol is a potent allosteric modulator of N-methyl-D-aspartate receptors. *J Neurosci* *33*, 17290-17300.
- Pelletier R.M., Vitale M.L. (1994). Filipin vs enzymatic localization of cholesterol in guinea pig, mink, and mallard duck testicular cells. *J Histochem Cytochem*. *42*, 1539-54.
- Penagarikano O., Mulle J.G., Warren S.T. (2007). The pathophysiology of fragile x syndrome. *Annu Rev Genomics Hum Genet*. *8*, 109-129.
- Pfeiffer P., Egorov A.V., Lorenz F., Schleimer J.H., Draguhn A., Schreiber S. (2020). Clusters of cooperative ion channels enable a membrane-potential-based mechanism for short-term memory. *Elife*. *9*, 49974.
- Pfriege, F.W. (2003). Cholesterol homeostasis and function in neurons of the central nervous system. *Cell Mol Life Sci* *60*, 1158-1171.
- Pfriege, F.W., and Ungerer, N. (2011). Cholesterol metabolism in neurons and astrocytes. *Prog Lipid Res* *50*, 357-371.
- Pinto, D., Pagnamenta, A.T., Klei, L., Anney, R., Merico, D., Regan, R., Conroy, J., Magalhaes, T.R., Correia, C., Abrahams, B.S. *et al.* (2010). Functional impact of global rare copy number variation in autism spectrum disorders. *Nature* *466*, 368-372.
- Poliani P.L., Wang Y., Fontana E., Robinette M.L., Yamanishi Y., Gilfillan S., Colonna M. (2015). TREM2 sustains microglial expansion during aging and response to demyelination. *J Clin Invest*. *125*, 2161-70.
- Porter F.D., Herman G.E. (2011). Malformation syndromes caused by disorders of cholesterol synthesis. *J Lipid Res* *52*, 6-34.
- Priester, A., and Okuse, K. (2011). Building excitable membranes: lipid rafts and multiple controls on trafficking of electrogenic molecules. *Neuroscientist* *18*, 70-81.

- Qi X., Schmiede P., Coutavas E., Wang J., Li X. (2018). Structures of human Patched and its complex with native palmitoylated sonic hedgehog. *Nature*. 560, 128-132.
- Qian H., Wu X., Du X., Yao X., Zhao X., Lee J., Yang H., Yan N. (2020). Structural Basis of Low-pH-Dependent Lysosomal Cholesterol Egress by NPC1 and NPC2. *Cell*. 182, 98-111.
- Qin Q., Teng Z., Liu C., Li Q., Yin Y., Tang Y. (2021). TREM2, microglia, and Alzheimer's disease. *Mech Ageing Dev*. 195, 111438.
- Ramachandran, R., Heuck, A.P., Tweten, R.K., Johnson, A.E. (2002). Structural insights into the membrane-anchoring mechanism of a cholesterol-dependent cytolysin. *Nat. Struct. Biol*. 9, 823-827.
- Ribeiro I., Marcao A., Amaral O., Sa Miranda M.C., Vanier M.T., Millat G. (2001). Niemann-Pick type C disease: NPC1 mutations associated with severe and mild cellular cholesterol trafficking alterations. *Hum Genet*. 109, 24-32.
- Rochtus, A., Olson, H.E., Smith, L., Keith, L.G., El Achkar, C., Taylor, A., Mahida, S., Park, M., Kelly, M., Shain, C., *et al.* (2020). Genetic diagnoses in epilepsy: The impact of dynamic exome analysis in a pediatric cohort. *Epilepsia* 61, 249-258.
- Ronald A., Hoekstra R.A. (2011). Autism spectrum disorders and autistic traits: a decade of new twin studies. *Am J Med Genet B Neuropsychiatr Genet*. 156B, 255-74.
- Rosen T.E., Mazefsky C.A., Vasa R.A., Lerner M.D. (2018). Co-occurring psychiatric conditions in autism spectrum disorder. *Int Rev Psychiatry*. 30, 40-61.
- Ross, P.J., Zhang, W.B., Mok, R.S., Zaslavsky, K., Deneault, E., D'Abate, L., Rodrigues, D.C., Yuen, R.K., *et al.* (2020) Synaptic Dysfunction in Human Neurons With Autism-Associated Deletions in PTCHD1-AS. *Biol. Psychiatry* 87, 139-149.
- Rossjohn J., Feil S.C., McKinstry W.J., Tweten R.K., Parker M.W. (1997). Structure of a cholesterol-binding, thiol-activated cytolysin and a model of its membrane form. *Cell*. 89, 685-692.
- Roy, D.S., Zhang, Y., Aida, T., Choi, S., Chen, Q., Hou, Y., Lea, N.E., Skaggs, K.M., Quay, J.C., Liew, M., *et al.* (2021). Anterior thalamic dysfunction underlies cognitive deficits in a subset of neuropsychiatric disease models. *Neuron* 109, 2590-2603.
- Ruljancic N., Mihanovic M., Cepelak I. (2011). Thrombocyte serotonin and serum cholesterol concentration in suicidal and non-suicidal depressed patients. *Prog Neuropsychopharmacol Biol Psychiatry* 35, 1261-1267.
- Ryan A.K., Bartlett K., Clayton P., Eaton S., Mills L., Donnai D., Winter R.M., Burn J. (1998). Smith-Lemli-Opitz syndrome: a variable clinical and biochemical phenotype. *J Med Genet*. 35, 558-565.
- Saher G., Brügger B., Lappe-Siefke C., Möbius W., Tozawa R., Wehr M.C., Wieland F., Ishibashi S., Nave K.A. (2005). High cholesterol level is essential for myelin membrane growth. *Nat Neurosci*. 8, 468-475.
- Sahin, M., and Sur, M. (2015). Genes, circuits, and precision therapies for autism and related neurodevelopmental disorders. *Science*. 350.

- Salvioli R., Scarpa S., Ciaffoni F., Tatti M., Ramoni C., Vanier M.T., Vaccaro A.M. (2004). Glucosylceramidase mass and subcellular localization are modulated by cholesterol in Niemann-Pick disease type C. *J Biol Chem.* 279, 17674-17680.
- Scudder, S. L., and Patrick, G. N. (2015). Synaptic structure and function are altered by the neddylation inhibitor MLN4924. *Molecular and Cellular Neuroscience* 65, 52-57.
- Sebastiao, A. M., Colino-Oliveira, M., Assaife-Lopes, N., Dias, R. B., and Ribeiro, J. A. (2012). Lipid rafts, synaptic transmission and plasticity: impact in age-related neurodegenerative diseases. *Neuropharmacology* 64, 97-107.
- Segatto M., Trapani L., Lecis C., Pallottini V. (2012). Regulation of cholesterol biosynthetic pathway in different regions of the rat central nervous system. *Acta Physiol.* 206, 62-71.
- Segatto M., Leboffe L., Trapani L., Pallottini V. (2014). Cholesterol homeostasis failure in the brain: Implications for synaptic dysfunction and cognitive decline. *Curr Med Chem* 21, 2788-2802.
- Sestan N., State M.W. (2018). Lost in Translation: Traversing the Complex Path from Genomics to Therapeutics in Autism Spectrum Disorder. *Neuron.* 100, 406-423.
- Sever N., Song B.L., Yabe D., Goldstein J.L., Brown M.S., DeBose-Boyd R.A. (2003). Insig-dependent ubiquitination and degradation of mammalian 3-hydroxy-3-methylglutaryl-CoA reductase stimulated by sterols and geranylgeraniol. *J Biol Chem.* 278, 52479-90.
- Severs N.J., Simons H.L. (1983). Failure of filipin to detect cholesterol-rich domains in smooth muscle plasma membrane. *Nature.* 303, 637-638.
- Sezgin E., Can F.B., Schneider F., Clausen M.P., Galiani S., Stanly T.A., Waithe D., Colaco A., Honigsmann A., Wüstner D., Platt F., Eggeling C. (2016). A comparative study on fluorescent cholesterol analogs as versatile cellular reporters. *J Lipid Res.* 57, 299-309.
- Shan L., Zhang T., Fan K., Cai W., Liu H. (2021). Astrocyte-Neuron Signaling in Synaptogenesis. *Front Cell Dev Biol.* 9, 680301.
- Sharp L., Salari R., Brannigan G. (2019). Boundary lipids of the nicotinic acetylcholine receptor: Spontaneous partitioning via coarse-grained molecular dynamics simulation. *Biochim Biophys Acta Biomembr.* 1861, 887-896.
- Shimada, Y., Maruya, M., Iwashita, S., Ohno-Iwashita, Y. (2002). The C-terminal domain of perfringolysin O is an essential cholesterol-binding unit targeting to cholesterol-rich microdomains. *Eur. J. Biochem.* 269, 6195-6203.
- Sikora D.M., Ruggiero M., Petit-Kekel K., Merkens L.S., Connor W.E., Steiner R.D. (2004). Cholesterol supplementation does not improve developmental progress in Smith-Lemli-Opitz syndrome. *J Pediatr.* 144, 783-91.
- Sikora, D.M., Pettit-Kekel, K., Penfield, J., Merkens, L.S., and Steiner, R.D. (2006). The near universal presence of autism spectrum disorders in children with Smith-Lemli-Opitz syndrome. *Am J Med Genet A* 140, 1511-1518.
- Singh T., Walters J.T.R., Johnstone M., Curtis D., Suvisaari J., Torniaainen M., Rees E., Blackwood D., Barrett J.C., *et al.* (2017). The contribution of rare variants to risk of schizophrenia in individuals with and without intellectual disability. *Nat Genet.* 49, 1167-1173.

- Snipes G., Suter U. (1998). Cholesterol and myelin. Cholesterol New York Plenum Press.
- Smith D.W., Lemli L., Opitz J.M. (1964). A newly recognized syndrome of multiple congenital anomalies. *J Pediatr.* *64*, 210-217.
- Steer C.J., Bisher M., Blumenthal R., Steven A.C. (1984). Detection of membrane cholesterol by filipin in isolated rat liver coated vesicles is dependent upon removal of the clathrin coat. *J Cell Biol.* *99*, 315-319.
- Steinberg F., Gallon M., Winfield M., Thomas E.C., Bell A.J., Heesom K.J., Tavaré J.M., Cullen P.J. (2013). A global analysis of SNX27-retromer assembly and cargo specificity reveals a function in glucose and metal ion transport. *Nat Cell Biol.* *5*, 461-71.
- Sticozzi C., Belmonte G., Pecorelli A., Cervellati F., Leoncini S., Signorini C., Ciccoli L., De Felice C., Hayek J., Valacchi G. (2013). Scavenger receptor B1 post-translational modifications in Rett syndrome. *FEBS Lett.* *587*, 2199-204.
- Stiles, J., Jernigan, T.L. (2010). The Basics of Brain Development. *Neuropsychol Rev.* *20*, 327-348.
- Suzuki, K. (2007). Neuropathology of developmental abnormalities. *Brain and Development.* *29*, 129-141.
- Svennerholm L., Bostrom K., Helander C.G., Jungbjer B. (1991). Membrane lipids in the aging human brain. *J Neurochem* *56*, 2051-2059.
- Takamori S., Holt M., Stenius K., Lemke E.A., Grønborg M., Riedel D., Urlaub H., Schenck S., Brügger B, Jahn R., *et al.* (2006). Molecular anatomy of a trafficking organelle. *Cell.* *127*, 831-846.
- Tau, G., Peterson, B. (2010). Normal Development of Brain Circuits. *Neuropsychopharmacol.* *35*, 147-168.
- Thapar A., Cooper M., Rutter M. (2017). Neurodevelopmental disorders. *Lancet Psychiatry.* *4*, 339-346.
- Thiele C., Hannah M.J., Fahrenholz F., Huttner W.B. (2000). Cholesterol binds to synaptophysin and is required for biogenesis of synaptic vesicles. *Nat Cell Biol* *2*, 42-49.
- Thomson, S.R., Seo, S.S., Barnes, S.A., Louros, S.R., Muscas, M., Dando, O., Kirby, C., Wyllie, D.J.A., *et al.* (2017). Cell-Type-Specific Translation Profiling Reveals a Novel Strategy for Treating Fragile X Syndrome. *Neuron* *95*, 550-563.
- Thurman A.J., Potter L.A., Kim K., Tassone F., Banasik A., Potter S.N., Bullard L., Nguyen V., McDuffie A., Hagerman R., Abbeduto L. (2020). Controlled trial of lovastatin combined with an open-label treatment of a parent-implemented language intervention in youth with fragile X syndrome. *J Neurodev Disord.* *12*, 12.
- Tierney, E., Bukelis, I., Thompson, R.E., Ahmed, K., Aneja, A., Kratz, L., and Kelley, R.I. (2006). Abnormalities of cholesterol metabolism in autism spectrum disorders. *Am J Med Genet B Neuropsychiatr Genet* *141B*, 666-668.
- Tierney, E., Nwokoro, N.A., Porter, F.D., Freund, L.S., Ghuman, J.K., and Kelley, R.I. (2001). Behavior phenotype in the RSH/Smith-Lemli-Opitz syndrome. *Am J Med Genet* *98*, 191-200.

- Tomson-Johanson K., Harro J. (2018). Low cholesterol, impulsivity and violence revisited. *Curr Opin Endocrinol Diabetes Obes.* 25, 103-107.
- Tora, D., Gomez, A.M., Michaud, J.F., Yam, P.T., Charron, F., and Scheiffele, P. (2017). Cellular Functions of the Autism Risk Factor PTCHD1 in Mice. *J Neurosci* 37, 11993-12005.
- Toro R., Konyukh M., Delorme R., Leblond C., Chaste P., Fauchereau F., Coleman M., Leboyer M., Gillberg C., Bourgeron T. (2010). Key role for gene dosage and synaptic homeostasis in autism spectrum disorders. *Trends Genet.* 26, 363-372.
- Torrico, B., Fernández-Castillo, N., Hervás, A., Milà, M., Salgado, M., Rueda, I., Buitelaar, J.K., Rommelse, N., *et al.* (2015). Contribution of common and rare variants of the PTCHD1 gene to autism spectrum disorders and intellectual disability. *Eur. J. Hum. Genet.* 23, 1694-1701.
- Toupin A., Benachenhou S., Abolghasemi A., Laroui A., Galarneau L., Fülöp T., Corbin F., Çaku A. (2022). Association of lipid rafts cholesterol with clinical profile in fragile X syndrome. *Sci Rep.* 12, 2936.
- Troisi A. (2011). Low cholesterol is a risk factor for attentional impulsivity in patients with mood symptoms. *Psychiatry Res* 188, 83-87.
- Tunyasuvunakool K., Adler J., Wu Z., Green T., Zielinski M., Žídek A., Bridgland A., Cowie A., Hassabis D., *et al.* (2021). Highly accurate protein structure prediction for the human proteome. *Nature.* 596, 590-596.
- Tweten R.K., Parker M.W., Johnson A.E. (2001). The cholesterol-dependent cytolysins. *Curr Top Microbiol Immunol.* 257, 15-33.
- Ung, D.C., Iacono, G., Meziane, H., Blanchard, E., Papon, M.A., Selten, M., van Rhijn, J.R., Montjean, R., *et al.* (2018). Ptchd1 deficiency induces excitatory synaptic and cognitive dysfunctions in mouse. *Molecular psychiatry.* 23, 1356-1367.
- van den Bogaart, G., Lang, T., and Jahn, R. (2013). Microdomains of SNARE proteins in the plasma membrane. *Curr Top Membr* 72, 193-230.
- Vanier M.T. (2010). Niemann-Pick disease type C. *Orphanet J Rare Dis.* 5, 16.
- Vanier M.T., Millat G. (2003). Niemann-Pick disease type C. *Clin Genet.* 64, 269-281.
- van Karnebeek C.D., Bowden K., Berry-Kravis E. (2016). Treatment of Neurogenetic Developmental Conditions: From 2016 into the Future. *Pediatr Neurol.* 65, 1-13.
- Varma V.R., Büşra Lüleci H., Oommen A.M., Varma S., Blackshear C.T., Griswold M.E., An Y., Thambisetty M., *et al.* (2021). Abnormal brain cholesterol homeostasis in Alzheimer's disease—a targeted metabolomic and transcriptomic study. *NPJ Aging Mech Dis.* 7, 11.
- Verkerk A.J., Pieretti M., Sutcliffe J.S., Fu Y.H., Kuhl D.P., Pizzuti A., Reiner O., Richards S., Victoria M.F., Zhang F.P., *et al.* (1991). Identification of a gene (FMR-1) containing a CGG repeat coincident with a breakpoint cluster region exhibiting length variation in fragile X syndrome. *Cell.* 65, 905-14.
- Villani C., Sacchetti G., Bagnati R., Passoni A., Fusco F., Carli M., Invernizzi R.W. (2016). Lovastatin fails to improve motor performance and survival in *methyl-CpG-binding protein2*-null mice. *Elife.* 5, 22409.

- Vogl, A. M., Brockmann, M. M., Giusti, S. A., MacCarrone, G., Vercelli, C. A., Bauder, C. A., Richter, J. S., Roselli, F., Refojo, D., *et al.* (2015). Neddylation inhibition impairs spine development, destabilizes synapses and deteriorates cognition. *Nature Neuroscience* 2, 239-251.
- Voskuhl R.R., Itoh N., Tassoni A., Matsukawa M.A., Ren E., Tse V., Jang E., Suen T.T., Itoh Y. (2019). Gene expression in oligodendrocytes during remyelination reveals cholesterol homeostasis as a therapeutic target in multiple sclerosis. *Proc Natl Acad Sci U S A.* 116, 10130-10139.
- Walkley S.U., Vanier M.T. (2009). Secondary lipid accumulation in lysosomal disease. *Biochim Biophys Acta.* 1793, 726-736.
- Walsh P., Elsabbagh M., Bolton P., Singh I. (2011). In search of biomarkers for autism: scientific, social and ethical challenges. *Nat Rev Neurosci.* 12, 603-12.
- Wang J., Fedoseienko A., Chen B., Burstein E., Jia D., Billadeau D.D. (2018). Endosomal receptor trafficking: Retromer and beyond. *Traffic.* 8, 578-590.
- Wang C., Yue H., Hu Z., Shen Y., Ma J., Li J., Wang X.D., Wang L., Sun B., Shi P., Wang L., Gu Y. (2020). Microglia mediate forgetting via complement-dependent synaptic elimination. *Science.* 367, 688-694.
- Waye M.M.Y., Cheng H.Y. (2018). Genetics and epigenetics of autism: A Review. *Psychiatry Clin Neurosci.* 72, 228-244.
- Weiss L.E., Milenkovic L., Yoon J., Stearns T., Moerner W.E. (2019). Motional dynamics of single Patched1 molecules in cilia are controlled by Hedgehog and cholesterol. *Proc Natl Acad Sci USA.* 116, 5550-5557.
- Wells, M.F., Wimmer, R.D., Schmitt, L.I., Feng, G., and Halassa, M.M. (2016). Thalamic reticular impairment underlies attention deficit in *Ptchd1*(Y/-) mice. *Nature* 532, 58-63.
- Wheeler S., Sillence D.J. (2020). Niemann-Pick type C disease: cellular pathology and pharmacotherapy. *J Neurochem.* 153, 674-692.
- Whibley, A.C., Plagnol, V., Tarpey, P.S., Abidi, F., Fullston, T., Choma, M.K., Boucher, C.A., Shepherd, L., Willatt, L., Parkin, G., *et al.* (2010). Fine-scale survey of X chromosome copy number variants and indels underlying intellectual disability. *Am. J. Hum. Genet.* 87, 173-188.
- Wilhelm L.P., Voilquin L., Kobayashi T., Tomasetto C., Alpy F. (2019). Intracellular and Plasma Membrane Cholesterol Labeling and Quantification Using Filipin and GFP-D4. *Methods Mol Biol.* 1949, 137-152.
- Won, H., Mah, W., and Kim, E. (2013). Autism spectrum disorder causes, mechanisms, and treatments: focus on neuronal synapses. *Frontiers in molecular neuroscience* 6, 19.
- Wraith J.E., Baumgartner M.R., Bembi B., Covanis A., Levade T., Mengel E., Pineda M., Sedel F., Vanier M.T., *et al.* (2009). Recommendations on the diagnosis and management of Niemann-Pick disease type C. *Mol Genet Metab.* 98, 152-165.
- Wu, X., Yan, R., Cao, P., Qian, H., and Yan, N. (2022). Structural advances in sterol-sensing domain-containing proteins. *Trends in biochemical sciences* 47, 289-300.

- Wüstner D., Lund F.W., Röhrl C., Stangl H. (2016). Potential of BODIPY-cholesterol for analysis of cholesterol transport and diffusion in living cells. *Chem Phys Lipids*. 194, 12-28.
- Xiong, H., Wang, D., Chen, L., Choo, Y. S., Ma, H., Tang, C., Xia, K., Jiang, W., Ronai, Z., Zhuang, X., and Zhang, Z. (2009). Parkin, PINK1, and DJ-1 form a ubiquitin E3 ligase complex promoting unfolded protein degradation, *119*.
- Xirodimas, D. P., Saville, M. K., Bourdon, J. C., Hay, R. T., and Lane, D. P. (2004). Mdm2-mediated NEDD8 conjugation of p53 inhibits its transcriptional activity. *Cell*, 118, 83-97.
- Yeh F.L., Wang Y., Tom I., Gonzalez L.C., Sheng M. (2016). TREM2 Binds to Apolipoproteins, Including APOE and CLU/APOJ, and Thereby Facilitates Uptake of Amyloid-Beta by Microglia. *Neuron*. 91, 328-340.
- You H., Lu W., Zhao S., Hu Z., Zhang J. (2013). The relationship between statins and depression: a review of the literature. *Expert Opin Pharmacother*. 14, 1467-76.
- Young A., Wimmer R.D. (2017). Implications for the thalamic reticular nucleus in impaired attention and sleep in schizophrenia. *Schizophr Res*. 180, 44-47.
- Zelcer N., Sharpe L.J., Loregger A., Kristiana I., Cook E.C., Phan L., Stevenson J., Brown A.J. (2014). The E3 ubiquitin ligase MARCH6 degrades squalene monooxygenase and affects 3-hydroxy-3-methyl-glutaryl coenzyme A reductase and the cholesterol synthesis pathway. *Mol Cell Biol*. 34, 1262-70.
- Zerbo O., Traglia M., Yoshida C., Heuer L.S., Ashwood P., Delorenze G.N., Hansen R.L., Kharrazi M., Croen L.A., *et al.* (2016). Maternal mid-pregnancy C-reactive protein and risk of autism spectrum disorders: the early markers for autism study. *Transl Psychiatry*. 6, 783.
- Zhao, Y., Morgan, M. A., and Sun, Y. (2014). Targeting Neddylatation Pathway to Inactivate Cullin-RING Ligases for Anticancer Therapy. *Antioxidants and Redox Signaling*, 17, 2383-2400.
- Zhang, Y., Bulkley, D.P., Xin, Y., Roberts, K.J., Asarnow, D.E., Sharma, A., Myers, B.R., Cho, W., *et al.* (2018). Structural Basis for Cholesterol Transport-like Activity of the Hedgehog Receptor Patched. *Cell* 175, 1352-1364.
- Zhou L., Jiang Y., Luo Q., Li L., Jia L. (2019). Neddylatation: a novel modulator of the tumor microenvironment. *Mol Cancer*. 1, 77.

# Acknowledgements

I would first and foremost like to thank Peter for his unwavering support and guidance throughout my PhD. You gave me the great opportunity to work on a subject which holds personal importance for me while helping me grow scientifically. I have learned so much from you and it shapes the scientist I am today and that I will be in the future. I will always be grateful for your understanding when things were complicated due to my health problems.

Secondly, many thanks to the people you supported my laboratory work while I could not do it. Without Shirley Dixit, Sabrina Innocenti and Caroline Bornmann, I would not have been able to finish both publication and thesis manuscripts. I am so grateful for your help and support.

To the Scheiffele lab, past and present members, thank you for the great collaborating and enjoyable work atmosphere. I really was a pleasure to work with all of you. Helping each other, discussing science or laughing about something... you all made my PhD a good time, even when experiments would not necessarily cooperate! I hope to keep contact with many of you in the future.

Thank you to Anne Spang and Markus Rüegg, my committee members, for their advice and guidance. Your input during the committee meetings was always helpful and constructive for my project. I would also like to thank you for collaborating on some parts of the project.

The biggest thanks goes to my family members and friends. Having you in my life made it possible for me to complete my PhD. Your love, friendship and support helped me in more ways that you can know. Especially to my parents and grand-parents, I know you were so proud of me for doing this PhD but I am so much prouder to be your daughter and grand-daughter. I would not be where I am without your love and your help in all things.

To my love, Mark, thank you for loving me, accepting me as I am and bearing with me while I was working on this thesis with my messy back. I would not have made it this far without you. I know our future is filled with even more love and joy, I cannot wait to spend it all with you. You are the best and I love you, pinky swear.



# Curriculum Vitae

## Personal data

Name: Charlotte  
Surname: Czernecki  
Date of birth: 28/08/1993  
Nationality: French  
Email: charlotte.czernecki@live.fr  
Phone: +33 6 27 53 12 45  
Current address: 22 rue de Huningue, 68300 Saint-Louis, France

## Education

2017 - Now                    **PhD degree in Molecular neuroscience**  
Basel - Switzerland      University of Basel

2013 - 2016                **Engineering degree in Biology,  
sp. bioinformatics and modelling**  
Nice - France              Polytech' Nice-Sophia Antipolis

2011 - 2013                **Preparatory program to biological engineering**  
Montpellier - France      Polytech' Montpellier

2011                         **Baccalauréat, with honors (French high school diploma)**  
Cannes - France            Jules Ferry High School

## **Scientific experience**

**Jun. - Sep. 2017**                    **Sr. Associate in Pharmacological Research & Development,  
Neurodegeneration & Regeneration, Roche**

### **Basel, Switzerland**

Responsible for the maintenance of several transgenic mouse line, testing and developing new tools and experimental protocols, and performing general lab management tasks. Techniques used included animal handling and breeding, genotyping, in vivo dosing and organ collection.

**Feb. 2016 - May. 2017**           **Intern in Behavioral Pharmacology, Dr. Biemans' lab  
Neuroscience and Rare Disease, Roche**

### **Basel, Switzerland**

Establishment a protocol to perform pharmacological testing and detect cognitive, impulsive, spontaneous and anxious behaviors in disease mouse models using an automated mouse cage system.

**Jun. - Aug. 2015**                    **Intern in Drug Design and Pharmacology,  
Dr. Boonen's lab, University of Copenhagen**

### **Copenhagen, Denmark**

Correlation matrix analysis of an animal study investigating vascular reactivity of mesenteric resistance-sized arteries in the Angiotensin II-infusion model including possible protective effects of  $\alpha$ CGRP.

## **Working experience**

**Aug. 2014/'15**                    Bank teller, Caisse d'Epargne Côte d'Azur, France

**Aug. 2011/'13**                    Secretary at lawyer firm, Cannes, France

## **Publications**

Cell type-specific assessment of cholesterol distribution in models of neurodevelopmental disorders

Charlotte Czernecki<sup>1</sup>, Shirley Dixit<sup>1</sup>, Sabrina Innocenti<sup>1</sup>, Caroline Bornmann<sup>1</sup>, Isabelle Riezman<sup>2</sup>, Howard Riezman<sup>2</sup>, Peter Scheiffele<sup>1</sup> *in preparation*

## **Contribution to international conferences**

AIMS2-TRIALS GA meeting 2019	Poster presentation, Fuerteventura, Spain Poster title: Investigations of ASD risk gene PTCHD1
CANDY Kick-off meeting 2020	Workshop participation, online
CANDY GA meeting 2021	Workshop participation, online

## **Teaching activities**

April/May 2018/'19/'20/'21	Teaching assistance in “Blockkurs” for Bachelor students, University of Basel, Switzerland.
----------------------------	---

## **Additional education**

“**Applied Statistics using R**”; University of Basel, Switzerland.

“**Cellular signaling**”; University of Basel, Switzerland.

“**Genes & Behavior**”; University of Basel, Switzerland.

“**Molecular Neurobiology I**”; University of Basel, Switzerland.

“**Molecular Neurobiology II**”; University of Basel, Switzerland.

LTK Module 1: “**Introductory course in Laboratory Animal Science**”, Basel, Switzerland.

## **Personal skills**

Languages: English (fluent), French (native language) and Spanish (basic)

Programming: moderate skills with R/Rstudio and basic knowledge of programming languages (Python, Java, SQL)

Software: Illustrator, ImageJ, GraphPad, SnapGene, EthoVision, Microsoft Office

Techniques: Nucleic acid work (isolation, purification, amplification), RT-PCR/qPCR, primary neuronal culture, stable cell lines usage, transfection, western blot, pharmacological treatments, stereotaxic injections, behavior testing, perfusion and organ collection, immunocytochemistry, immunohistochemistry, RNA FISH, cloning.